Adaptive feedforward for reset control systems

Application in precision motion control

K. Brummelhuis

Master of Science Thesis

TU Delft Delft University of Technology

Delft Center for Systems and Control

Adaptive feedforward for reset control systems

Application in precision motion control

Master of Science Thesis

For the degree of Master of Science in Systems and Control at Delft University of Technology

K. Brummelhuis

August 16, 2019

Faculty of Mechanical, Maritime and Materials Engineering (3mE) · Delft University of Technology

Abstract

The constant demand for increasing performance in the precision industry and the fundamental limitations of PID control such as the waterbed effect and Bode's gain phase relationship, has led to a research focus on reset control. Reset control introduces extra phase which benefits the freedom of design, stability margins, and achievable bandwidth. Also, this is relatively easy in implementation since designing tools such as loop-shaping apply to the reset control framework.

The extra phase introduced by reset control increases the stability margins of a feedback controller. It has been shown that reset control increases disturbance rejection performance. However, reference tracking properties of a reset controller can be outperformed by linear PID control. Whenever a reset occurs, part of the controller memory is erased, which potentially creates the inability for a reset controller to accurately track a reference. Since disturbance rejection is improved, reset control is promising for research. Reference tracking can be improved by introducing other control strategies to the framework.

In this thesis, an adaptive feedforward controller is proposed. The algorithm is based on a parametrised model of the inverse of the plant. During operation, the feedforward adapts from the feedback controller to adjust the feedforward parameters. Accurate tracking is achieved as the feedforward parameters converge to the ideal value. Previously developed methods for reset control are mainly focussed on first-order reset elements and first-order plants, and therefore do not suffice in the requirement for precision industry, where all systems are second-order or above. Linear adaptive methods are not applicable as the non-linear nature of the feedback signal produced by the reset element can yield instability. The algorithm developed in this thesis introduces a parameter that leads to stable adaptation in the presence of the non-linearity introduced by reset.

The development of the adaptive feedforward algorithm has iteratively led to the method as is presented in this thesis. During the process, new insights were obtained and theories were developed. The final proposed algorithm is developed such that it applies to a wide class of reset control systems.

Convergence of the feedforward parameters by the adaptive algorithm is proven using a continuous Lyapunov function. This is validated with experiments on the Spider precision positioning stage. Different configurations for the feedback controller are subjected to the experiments. In all cases, the algorithm is able to converge the feedforward parameters and decrease the tracking error of the plant.

Preface and Acknowledgements

This thesis is performed as the final chapter of my master's degree for Systems and Control at Delft University of Technology. During a challenging period of completing all my courses, my interest in control engineering grew stronger. My main goal set for my master's thesis was the involvement of mechanical engineering. During the search for a master's thesis topic, Simone Baldi pointed out to me that I should look for an assignment at the Mechatronics department of Precision and Microsystems Engineering. Hassan HosseinNia proposed me this thesis assignment: Try to find a method in which reset control can be used for reference tracking of different frequencies. This assignment came with the instruction that the developed method should be validated on an experimental setup. Given the fact that I could carry out physical experiments, and Hassan's enthusiasm on reset control, convinced me to take the assignment.

During this thesis, I gained a lot of knowledge on mechatronic systems, PID control, feedforward control, reset control, and not to forget scientific research. The thesis process was very challenging and difficult, but also extremely informative. After the year of working on this thesis, I can conclude am very happy that I got the chance to take this challenging and interesting assignment.

For all the help and support provided to me during the last year I would like to thank the following people:

Niranjan Saikumar: As my daily supervisor you were always ready to help me out. I think I could not have been able to get a better daily supervisor for this thesis. Always being able to meet within one day and thinking along with deriving the algorithm, really helped me out. Even at the moment, I am writing these acknowledgements at 21:30, I see an incoming mail of your corrections to the thesis report, which is definitely some coincidental timing. I think this perfectly illustrates the great helpfulness.

Hassan HosseinNia: First of all thanks for the very interesting thesis subject. Next, to that, I also want to thank for the support you given through the entire thesis process. All the feedback and positive reactions to my work gave me positive energy to keep improving. It was also very nice that I was always welcome to ask you any sort of questions at your office.

Jan-Willem van Wingerden: Most credits go to the insights given to the way I conducted my research. If it were not for the clearing opinion during the meetings in the first stages of

my research, I might not have been able to complete the thesis as I did now. The clearing and informative feedback was very helpful.

Neel Nagda: You should also be on this list. As one of my fellow students working on a masters' thesis provided by Hassan, I would like to thank Neel for the nice times working together. As we were assigned to the same experimental setup, we faced the same 'major' struggles. If it was not for Neel I would have lost a lot of motivation. I am grateful that both of us are able to graduate on the same date.

Fellow people of the research group: The Monday morning meetings were very interesting and helpful. Even though I did not attend them very much, at the times I did, I could account for support. Also hearing other students' research, and helping them to find solutions or giving them some food for thought, was a nice way to spend a Monday morning. Next to that I also highly appreciate the meetings on every last Thursday of the month with the control students within the research group.

ps. Not to forget all the free coffee and as would say in Dutch: 'gezelligheid'.

Enjoy reading this thesis.

Karst Brummelhuis
Delft, August 2019

Table of Contents

List of Figures

Chapter 1

Introduction

In the automation industry, it is required that all motion is controlled within a certain error threshold. One within these applications which requires planned motions on a nanometre scale is wafer scanners. Wafer scanners are used for the production of high-performance microchips. All daily used electronic devices make use of these microchips. The extremely fast development in this industry would have not been possible without the development made in the high precision industry, for both hardware and software. Another example is high precision microscopy, which spans a wider range of interest than just the automation industry. An atomic force microscope can, for instance, be used to map any specimen on a nanometre scale. This makes it possible to gain more knowledge within the fields of biology and medicine, but also has application in the high precision industry.

As for the software, high precision motion control is necessary for these devices to meet their required specifications. The precision industry is constantly trying to push the limitations of control to improve its performance. These days, almost all of the industry still makes use of conventional PID control in their control loops. Out of all existing control strategies in the industry, more than 90% is PID control[1]. However, PID is limited by the rules of linear control established by years of research. These limitations can, for example, be expressed by the waterbed effect. In [1] it is fairly mentioned that too little effort is given to research in this form of control. The popularity of PID control is due to its simplicity, ease of implementation, and robustness and therefore desired in many applications. There exist control strategies that can overcome the limitations of linear PID control. Most other control strategies are either hard to implement, not robust or require exact knowledge of the device it is used on.

To answer the demand for improved control performance, and still maintain the robustness and simplicity of conventional PID control, reset elements can be included. This research focuses on reset control, which is one of many methods to mitigate the limitations of linear control. In [2] the first form of reset control appeared, introduced by J.C. Clegg. The so-called Clegg Integrator is capable of performing integral action with a phase advantage of 52°compared to a linear integrator. Unlike most novel methods, reset control comes with the same simplicity in implementation as PID control. Since reset control can be designed in the

frequency domain, it allows for design methods like loop-shaping.

Even though reset control is a promising candidate to improve PID control, it is accompanied by established disadvantages. The phase of a resetting integrator is estimated by analysing the describing function, which only approximates the first harmonic of the output signal. The information on the higher-order harmonics of the control signal is lost in this analysis. The higher-order harmonics do however affect the closed-loop response of the reset control system. Even though reset control favours the freedom of design and can increase phase margin or bandwidth, poor performance is sometimes achieved in terms of reference tracking. Some reset controllers are not capable of smooth reference tracking but rather show oscillatory behaviour. The goal of this thesis is to find a control strategy where reset control can be used to achieve accurate tracking while maintaining the desired non-linear properties.

Before tackling the tracking limitations of reset control, more background information is required on this subject. The first chapter of this thesis elaborates more on the fundamentals of reset control. Fundamental information is provided regarding dynamics, stability, and implementation in precision motion control. The advantage in disturbance rejection and disadvantage in reference tracking of a reset based PID controller compared to a linear PID controller is discussed, after which the goal of this thesis is presented. The second chapter presents the state of the art solutions obtained from different fields of research that are used to tackle similar problems. An analysis of these methods is also presented. The third chapter consists of a paper in which the main contribution of this thesis is presented and validated. In the final chapter conclusions and recommendations on further research are given.

Chapter 2

Reset control systems

There has been extensive research on reset control since its first appearance in literature. This chapter gives an overview of the established dynamics and different types of reset control since the introduction of the Clegg integrator. Reset control has seen a major improvement and has the potential to become industry standard for applications in, for example, the precision industry. An example in which reset control is used for disturbance rejection and reference tracking is given in the final section of this chapter, which leads to the research objective of this thesis.

2-1 Reset integrator

Current day reset control is based on the first research on resetting an integrator performed by J.C. Clegg [2]. The so-called Clegg integrator performs a resetting action whenever the integrator input equals zero. The dynamics of this resetting integrator can be described by the following differential inclusion, which is the common formulation used in reset control. Notation of the clegg integrator is shown in Figure 2-1, where the arrow indicates the presence of reset.

$$\begin{aligned} \dot{u}(t) &= e(t) \quad \text{if } e(t) \neq 0 \\ u(t^+) &= 0 \qquad \text{if } e(t) = 0 \end{aligned} \tag{2-1}$$

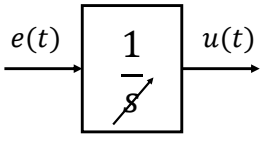

Figure 2-1: Common notation of the Clegg integrator

The signal produced by the Clegg integrator holds properties that show an advantage compared to the linear integrator. Direct analysis of the output signal is nontrivial. To analyse

this non-linear signal a linear approximation is suggested. Usage of the sinusoidal input describing function yields a linear representation of the Clegg integrator output. Figure 2-2a shows the response of both a linear integrator and a Clegg integrator to a sine input with an amplitude of 1 and a frequency of 1 rad/s.

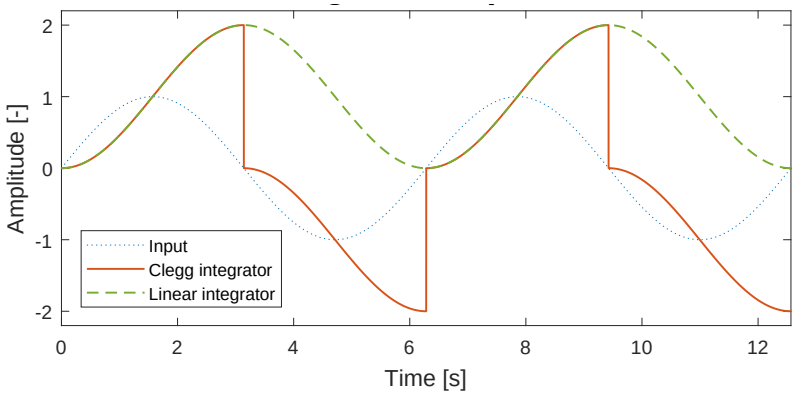

(a) Comparison of a linear integrator with a Clegg integrator

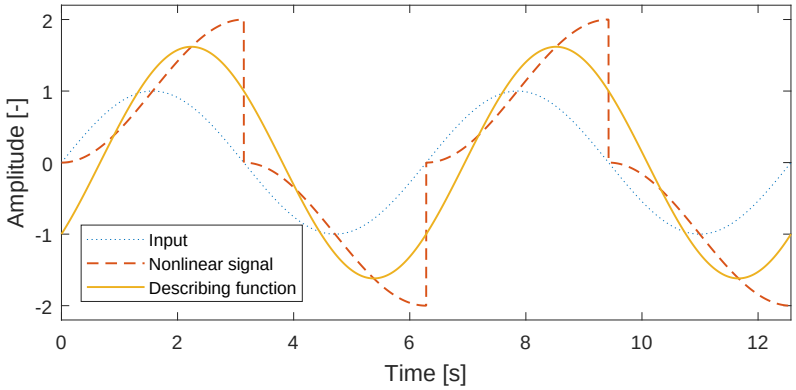

(b) Describing function of the Clegg integrator output

Figure 2-2: Analysis of the Clegg integrator response

The output of the Clegg integrator can be analysed through the sinusoidal describing function, as illustrated in Figure 2-2b. Since the first harmonic of the Clegg integrator output is dominant compared to the higher-order harmonics, this gives an accurate insight into the signal properties. Close observation of the linearised signal shows that the Clegg integrator overcomes part of the limitations in linear control. Whereas the linear integrator yields a phase lag of -90°, the Clegg integrator only yields a phase lag of -38°. Also, a slight increase in gain is observed. However, most importantly, the slope of gain remains the same. These properties make the Clegg integrator an interesting topic for control research, as the decrease in phase gives more freedom of design and benefits stability.

2-2 Definitions for reset control

There are multiple ways to include a resetting integrator in a control framework. The most basic form is the direct implementation of the Clegg integrator(CI). Research in reset control

has led to more advanced reset elements such as the First Order Reset Element(FORE) and the Second Order Reset Element(SORE). These forms of control are elaborated in Section 2-3. All these different forms can be analysed using the same dynamic framework.

2-2-1 Dynamics

General reset element dynamics are governed by the differential inclusion in Equation (2-2).

$$\begin{aligned} \dot{x}_r(t) &= A_r x_r(t) + B_r e(t) && \text{if } (x_r, e) \in \mathcal{F} \\ x_r(t^+) &= A_\rho x_r(t) && \text{if } (x_r, e) \in \mathcal{J} \\ u(t) &= C_r x_r(t) + D_r e(t) \end{aligned} \tag{2-2}$$

Where A_r, B_r, C_r, and D_r describe the state space of the reset element. The controller states propagate according to this state space system whenever $(x_r, e) \in \mathcal{F}$. If the reset conditions are met, given by $(x_r, e) \in \mathcal{J}$, a reset occurs. During reset, specified controller states are reset according to the reset matrix A_ρ.

$$A_\rho = \begin{bmatrix} I_m & 0_{m\times n} \\ 0_{n\times m} & 0_n \end{bmatrix} \tag{2-3}$$

Where m indicates the linear controller states and n the states which are being reset. Several different sets of reset conditions are presented in literature. Dominant reset conditions in literature are either based on zero crossings of the error[3], or based on the signs of the reset controller states and plant output[4]. The definition of the flow and jump set for both conditions are shown in Equation (2-4a) and (2-4b), respectively. This thesis focusses only on reset elements based on zero crossings of the error.

$$\mathcal{F} = \{x_r(t), e(t) \in \mathbb{R} : \ e(t) \neq 0\} \qquad \mathcal{J} = \{x_r(t), e(t) \in \mathbb{R} : \ e(t) = 0\} \tag{2-4a}$$

$$\mathcal{F} = \{x_r(t), e(t) \in \mathbb{R} : \ e(t)u(t) \geq 0\} \qquad \mathcal{J} = \{x_r(t), e(t) \in \mathbb{R} : \ e(t)u(t) \leq 0\} \tag{2-4b}$$

As mentioned, the matrix A_ρ determines which states of the controller are reset. At a reset instance, the values of the first m states of the controller are maintained at the same value. The other n states are reset to zero. The system which describes the linear evolution of the states, which would be the case for $A_\rho = I_{n+m}$, is called the base linear system.

Definition 1. *Base Linear system: The dynamical system which describes the evolution of the states of the reset controller, without including reset, is called the base-linear system. This means that the base linear system can also be defined by setting* $A_\rho = I_{(n+m)}$.

2-2-2 Closed loop

The graphical notation of a reset element in a closed loop system is given in Figure 2-3. The only exogenous signal considered here is the reference.

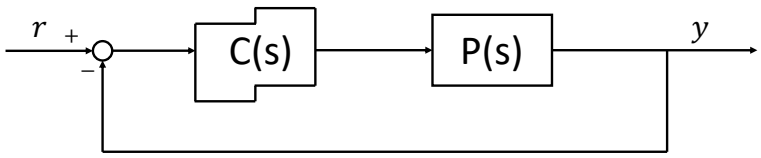

Figure 2-3: Closed loop configuration with a reset element

For stability and performance analysis purposes, dynamical equations of the closed-loop systems are required. The differential inclusion of this closed-loop system is given below in Equation (2-5).

$$\begin{aligned} \dot{x}_{cl}(t) &= A_{cl}x_{cl}(t) + B_{cl}r(t) \\ x_{cl}(t^+) &= A_{\mathrm{P}}x_{cl}(t) \\ y(t) &= C_{cl}x_{cl}(t) \end{aligned} \tag{2-5}$$

The individual matrices are defined in Equation (2-6) below.

$$\begin{aligned} x_{cl}(t) &= \begin{bmatrix} x_p(t) \\ x_r(t) \end{bmatrix} \quad A_{cl} = \begin{bmatrix} A_p - B_pD_rC_p & B_pC_r \\ -B_rC_p & A_r \end{bmatrix} \quad A_{\mathrm{P}} = \begin{bmatrix} I & 0 \\ 0 & A_\rho \end{bmatrix} \\ B_{cl} &= \begin{bmatrix} B_pD_r \\ B_r \end{bmatrix} \quad C_{cl} = \begin{bmatrix} C_p & 0 \end{bmatrix} \end{aligned} \tag{2-6}$$

Where the subscript r indicates the controller variables and p the plant variables. These equations hold for any type of reset controller.

2-3 Reset elements

There are multiple strategies available for including a resetting integrator in the control loop. For simple plants, only using a reset element in the control loop may suffice. For more complex plants, a reset element can be combined with any linear controller to increase performance in the overall control loop. This section briefly elaborates on the basic forms of the reset elements that can be applied for feedback control.

2-3-1 Clegg Integrator (CI)

The technique of resetting an integrator was first introduced by J.C. Clegg in [2]. The resetting integrator is now referred to as the Clegg integrator.

$$\frac{1}{s} \tag{2-7}$$

The definition of a Clegg integrator in state space notation is given in [5]. The relevant state space matrices are given below in Equation (2-8). Using a Clegg integrator yields an advantage in phase lag, which compared to a linear integrator is only 38° instead of 90°.

$$A_r = 0, \qquad B_r = 1, \qquad C_r = 1, \qquad D_r = 0, \qquad A_\rho = 0 \tag{2-8}$$

2-3-2 First order reset element (FORE)

The first order reset element is an extension on the dynamics of the Clegg integrator. This element is introduced in [6].

$$\frac{1}{\not{s+a}} \tag{2-9}$$

A basic state space notation for this element is given in Equation (2-10). Note that the base linear system is stable for a positive a.

$$A_r = -a, \qquad B_r = 1, \qquad C_r = 1, \qquad D_r = 0, \qquad A_\rho = 0 \tag{2-10}$$

Note that the advantage of the first order reset element is the ability to provide compensation at specific frequencies. The low-pass filter notation is given in Equation (2-11). The advantage of such a low-pass filter is integral action with a phase lag of only 38° after the cut-off frequency.

$$A_r = -\omega, \qquad B_r = \omega, \qquad C_r = 1, \qquad D_r = 0, \qquad A_\rho = 0 \tag{2-11}$$

Here ω defines the cut-off frequency.

2-3-3 Second order reset element (SORE)

A further extension is the second-order reset element. This reset element is introduced in [7].

$$\frac{\omega^2}{\not{s^2 + 2\beta\omega s + \omega^2}} \tag{2-12}$$

By increasing the order, it is possible to design resetting notch filters or second-order low-pass filters. The second-order reset element also provides the extra design variable β, which is the damping of the filter. The state space matrices of this filter are given in Equation (2-13).

$$A_r = \begin{bmatrix} 0 & 1 \\ -\omega^2 & -2\beta\omega \end{bmatrix}, \qquad B_r = \begin{bmatrix} 0 \\ \omega^2 \end{bmatrix} \qquad C_r = \begin{bmatrix} 1 & 0 \end{bmatrix} \qquad D_r = 0, \qquad A_\rho = \begin{bmatrix} 0 & 0 \\ 0 & 0 \end{bmatrix} \tag{2-13}$$

Here ω defines the cut-off frequency and β the relative damping coefficient.

2-3-4 Generalized reset elements

Generalized reset elements consist of standard reset elements as mentioned above. Instead of resetting to zero, the generalized reset elements only reset a fraction of the control action indicated by γ. The generalized first-order reset element is introduced in [8]. The generalized second-order reset element is introduced in [9]. For both cases, the only difference compared to the regular elements is the reset matrix A_ρ.

$$A_\rho = \begin{bmatrix} I_m & 0 & \dots & 0 \\ 0 & \gamma_1 & \dots & 0 \\ \vdots & \vdots & \ddots & \vdots \\ 0 & 0 & \dots & \gamma_n \end{bmatrix} \tag{2-14}$$

Where γ_i is a real number and is generally between 0 and 1.

2-3-5 Constant in gain lead in phase element

An extension of the GFORE and GSORE is introduced in [9] as the constant in gain-lead in phase element. This element is used to provide phase lead at a broad band of frequencies, whereas other reset elements only provide a reduction of phase lag. CgLp makes use of a reset lag filter in combination with a linear lead filter of the same order. By resetting the lag filter, the phase lead introduced by the lead filer is maintained to some extent over a wide range of frequencies. The resetting filters are stated below according to [9], respectively.

CgLp using GFORE

The transfer functions of the resetting lag filter and linear lead filter of CgLp using GFORE are given in Equation (2-15), respectively.

$$C(s) = \frac{1}{s/\omega_{r\alpha} + 1} \qquad \frac{s/\omega_r + 1}{s/\omega_f + 1} \tag{2-15}$$

The state space matrices of this transfer function are given in Equation (2-16).

$$\begin{aligned} A_r &= \begin{bmatrix} -\omega_{r\alpha} & 0 \\ \omega_f & -\omega_f \end{bmatrix} \qquad B_r = \begin{bmatrix} \omega_{r\alpha} \\ 0 \end{bmatrix} \quad A_\rho = \begin{bmatrix} \gamma & 0 \\ 0 & 1 \end{bmatrix} \\ C_r &= \begin{bmatrix} \dfrac{\omega_f}{\omega_r} & \left(1 - \dfrac{\omega_f}{\omega_r}\right) \end{bmatrix} \quad D_r = 0 \end{aligned} \tag{2-16}$$

CgLp using GSORE

The transfer functions of the resetting lag filter and linear lead filter of CgLp using GSORE are given in Equation (2-17), respectively.

$$C(s) = \frac{1}{(s/\omega_{r\alpha})^2 + (2s\beta_r/\omega_{r\alpha}) + 1} \qquad \frac{(s/\omega_r)^2 + (2s\beta_r/\omega_r) + 1}{(s/\omega_f)^2 + (2s/\omega_f) + 1} \tag{2-17}$$

The state space matrices of this transfer function are given in Equation (2-18).

$$\begin{aligned} A_r &= \begin{bmatrix} 0 & 1 & 0 & 0 \\ -\omega_{r\alpha}^2 & -2\beta_r\omega_{r\alpha} & 0 & 0 \\ 0 & 0 & 0 & 1 \\ 1 & 0 & -\omega_f^2 & -2\omega_f \end{bmatrix} \qquad B_r = \begin{bmatrix} 0 \\ \omega_{r\alpha}^2 \\ 0 \\ 0 \end{bmatrix} \quad A_\rho = \begin{bmatrix} \gamma & 0 & 0 & 0 \\ 0 & \gamma & 0 & 0 \\ 0 & 0 & 1 & 0 \\ 0 & 0 & 0 & 1 \end{bmatrix} \\ C_r &= \begin{bmatrix} \dfrac{\omega_f^2}{\omega_r^2} & 0 & \left(\omega_f^2 - \dfrac{\omega_f^4}{\omega_r^2}\right) & \left(\dfrac{2\beta_r\omega_f^2}{\omega_r} - \dfrac{2\omega_f^3}{\omega_r^2}\right) \end{bmatrix} \quad D_r = 0 \end{aligned} \tag{2-18}$$

Note that for both FORE and SORE based CgLp, the lag filter with ω_f is introduced to yield a proper non-resetting element. Therefore $\omega_f >> \omega_r$ is desired to neglect its dynamics at the lower frequencies of interest. To compensate for the shift in corner frequency introduced by reset, $\omega_{r\alpha}$ has to be shifted slightly. The amount of offset required is stated in [9].

2-4 Stability and performance of reset control systems

Proof of stability and performance analysis of a controlled system is important before implementing a control strategy on a real-time application. Multiple methods are available in literature to prove stability. The most common method for output feedback systems is an analysis in the frequency domain. Linear frequency domain analysis techniques for reset control are realized by the describing function of the reset controller. Another method of establishing stability proof is Lyapunov stability analysis.

2-4-1 Frequency domain analysis

The frequency domain is a very powerful design and analysis framework for linear control. The stability of output feedback control can be obtained through frequency domain analysis. Two powerful frequency domain methods are the Nyquist and Bode criteria[10]. However, the non-linearity of reset control systems creates a problem using these analysis tools. This is bypassed by approximating a linear system response using a sinusoidal input describing function. Since this is a linear approximation of the non-linear response, it is not entirely accurate, but it gives useful insights into the system dynamics.

Describing function

The sinusoidal input describing function for reset control systems is obtained from [8]. This frequency response function gives an accurate approximation of the non-linear response for linear analysis.

$$G(j\omega) = C_r \left(j\omega I - A_r\right)^{-1} \left(I + j\Theta_\rho(\omega)\right) B_r + D_r$$
$$\Theta_\rho = \frac{\pi}{2}\left(I + e^{\frac{\pi A_r}{\omega}}\right)\left(\frac{I - A_\rho}{I + A_\rho e^{\frac{\pi A_r}{\rho}}}\right)\left(\left(\frac{A_r}{\omega}\right)^2 + I\right)^{-1} \tag{2-19}$$

With this approximation, it is possible to use loop shaping techniques and provide stability analysis.

2-4-2 Lyapunov

The Lyapunov stability analysis of reset control systems is based on the analysis of hybrid systems. Different established stability criteria depend on the definitions of the flow set $\mathcal{F}$ and the jump set $\mathcal{J}$. As the main focus of this thesis lies on reset at zero crossings of the error, only methods involving these sets will be elaborated.

H_β-condition

Beker et al. developed the H_β-condition to provide necessary and sufficient conditions for proof of quadratic stability for reset control systems [3]. This condition is however conservative, as it requires the base linear system to be stable. The closed-loop state space of

Equation (2-5) is taken into account. The flow and jump set are defined as follows:

$$\begin{aligned}\mathcal{F} &= \{x_{cl}(t), e(t) \in \mathbb{R} : \ e(t) \neq 0\} \\ \mathcal{J} &= \{x_{cl}(t), e(t) \in \mathbb{R} : \ e(t) = 0, \ (I - A_{\mathrm{P}})x_{cl}(t) \neq 0\}\end{aligned} \tag{2-20}$$

With these set definitions, quadratic stability is guaranteed if the H_β-condition is satisfied.

Theorem 1. *The reset control system is quadratically stable if and only if there exists a $\beta \in \mathbb{R}^{l\times 1}$, where l is the amount of plant states, and a positive definite $P_\rho \in \mathbb{R}^{n\times n}$ such that $H_\beta(s)$ is strictly positive real.*

$$H_\beta(s) = \begin{bmatrix}\beta C_p & 0 & P_\rho\end{bmatrix} (sI - A_{cl})^{-1} \begin{bmatrix}0 \\ 0 \\ I_n\end{bmatrix} \tag{2-21}$$

This theorem is based on the following Lyapunov conditions, where the Lyapunov function $V(x)$ is positive definite, radially unbounded, and continuously differentiable.

$$\begin{aligned}\dot{V}(x) &< 0 \\ \Delta V(x) = V(A_{\mathrm{P}}x) - V(x) &\leq 0\end{aligned} \tag{2-22}$$

Although this theorem provides a stability proof for reset control systems, it is conservative. The Lyapunov stability requires the base linear system to be stable, which means that systems that are stabilized through reset are not accounted for. An example is given in [3] which refers to [11]. The following plant cannot be stabilized by a linear integrator. However, a Clegg integrator can stabilize the plant.

$$P(s) = \frac{3.1s + 1}{s^2 + 0.3322s - 0.1} \tag{2-23}$$

According to the H_β-condition this plant cannot be stabilized using a clegg integrator. The contradictory has been proven in [11]. This plant can be stabilized by a reset integrator.

L_n stability

Even stronger proof is given in [4]. The authors provide a wide variety of stability proofs. The stability criteria given prove Lyapunov based L_p stability of general reset systems containing a first-order reset element. The jump and flow set defined in this work are as defined in Equation (2-24). The reset condition is based on signs of the error and states, which is not used in this thesis, but closely resemble the same resetting behaviour.

$$\begin{aligned}\mathcal{F} &= \{x_{cl}(t) \in \mathbb{R}^n : x_{cl}^T(t)Mx_{cl}(t) + \epsilon x_{cl}^T(t)x_{cl}(t) \geq 0\} \\ \mathcal{J} &= \{x_{cl}(t) \in \mathbb{R}^n : x_{cl}^T(t)Mx_{cl}(t) + \epsilon x_{cl}^T(t)x_{cl}(t) \leq 0\}\end{aligned} \tag{2-24}$$

Since the stability proof given in [4] requires the definition of the sets given in Equation (2-24), this will not be further used in this thesis.

2-5 Application in motion control

This thesis focuses on the applications of reset control systems for motion control. As mentioned in the introduction, high precision motion control is required in applications like wafer scanners and atomic force microscopes. Most mechanical systems can be modeled as a single mass-spring-damper system, or a combination of multiple mass-spring-damper systems as stated in [12]. Every mechanical system has a mass and a limited stiffness. Even though damping terms could be very small, all mechanical systems are subjected to some amount of damping. The transfer function of a single mass-spring-damper system is given by the following equation.

$$P(s) = \frac{k\omega_n^2}{s^2 + 2\zeta\omega_n + \omega_n^2} \tag{2-25}$$

Here ω_n is natural resonance frequency, ζ the relative damping of the system, and k the overall gain. In general, the bandwidth is desired to be as high as possible, while stability criteria have to be met. Since this high bandwidth translates to the bandwidth being on the mass line, this can generally only be achieved by the use of a differentiator for phase lead at the bandwidth. The next two subsections discuss how this can be achieved by a standard linear PID and a class of reset controllers.

2-5-1 Industry standard PID

For precision motion control, a general industry standard series PID for loops-shaping can be defined as follows, obtained from [9].

$$PID(s) = k_p \left(\frac{s + \omega_i}{s}\right) \left(\frac{1 + \frac{s}{\omega_d}}{1 + \frac{s}{\omega_t}}\right) \left(\frac{1}{1 + \frac{s}{\omega_f}}\right) \tag{2-26}$$

With frequencies $\omega_i < \omega_d < \omega_t < \omega_f$.

- ω_i: The frequency at which the integrator action is stopped.
- ω_d: Starting frequency of differentiator action.
- ω_t: Taming frequency of differentiator action.
- ω_f: cut-off frequency of a low pass filter for noise attenuation at high frequency.

The integrator is required for good tracking and disturbance rejection at low frequencies. The differentiator, or lead-lag filter, is required to gain enough phase at the crossover frequency. The low pass filter is used to suppress higher frequencies for noise attenuation.

2-5-2 Reset control modification

Better performance can be achieved when incorporating a reset element in the PID controller. This can be achieved in multiple ways. A basic Clegg integrator based controller could take

the following form for example. The resetting action in this controller leads to a lower phase lag caused by the integrator.

$$C(s) = k_p \left(\frac{s + \omega_i}{\cancel{s}} \right) \left(\frac{1 + \frac{s}{\omega_d}}{1 + \frac{s}{\omega_t}} \right) \left(\frac{1}{1 + \frac{s}{\omega_f}} \right) \tag{2-27}$$

Another example of implementing reset control is by applying the FORE based CgLp. This controller is not resetting the integrator, which is required for tracking and disturbance rejections, but rather adds phase by introducing a new filter. This filter will add phase at the frequency ω_r. Note that the low pass filter acts as part of the linear filter of the CgLp element, as defined in Equation (2-16).

$$C(s) = k_p \left(\frac{\frac{s}{\omega_r} + 1}{\cancel{\frac{s}{\omega_r} + 1}} \right) \left(\frac{s + \omega_i}{s} \right) \left(\frac{1 + \frac{s}{\omega_d}}{1 + \frac{s}{\omega_t}} \right) \left(\frac{1}{1 + \frac{s}{\omega_f}} \right) \tag{2-28}$$

2-6 Performance

In this section, the performance of a CI-based PID controller is compared to a linear PID controller. Note that CI based PID is easily outperformed by more advanced forms of reset control. However, this type of reset control is able to clearly illustrate the goal of this thesis. Both controllers are applied in the framework of the industry-standard PID controller. The controlled plant in this example is the Spider stage, given in Appendix C. The dynamics of this plant can be represented by the following second-order transfer function.

$$P(s) = \frac{8760}{s^2 + 5.688s + 7443} \tag{2-29}$$

The plant has a natural frequency of approximately 13 Hz. To compare the performance of a Clegg Integrator based controller with its linear variant, both the CI based and linear PID are designed with the same gains according to the rules of thumb introduced in [12], at a bandwidth of 100 Hz. Since the CI based controller has a phase advantage of 58°, it is predicted that this controller has better performance in terms of stability margins.

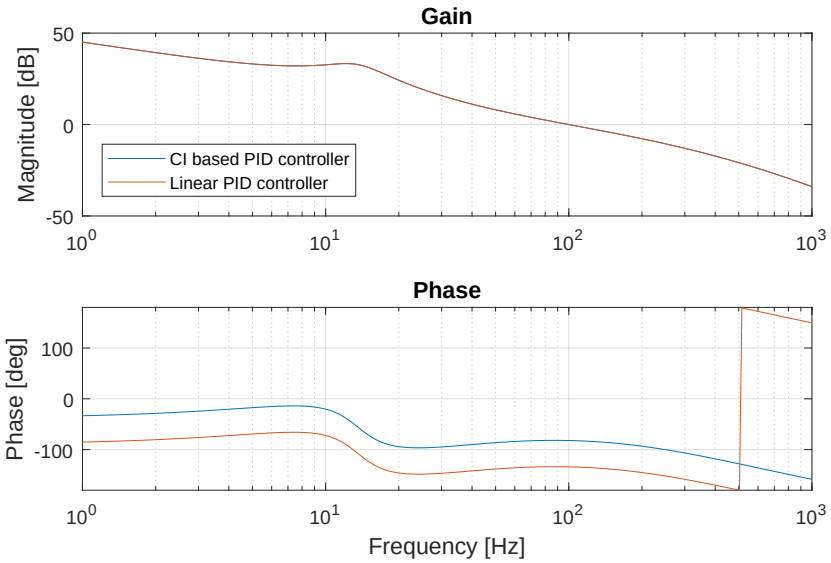

Figure 2-4: Bode plot of the linear PID controller compared with the CI based PID controller

A single reset integrator only suffers a phase lag of approximately -38°. The bode plot shows the phase advantage over the entire range of frequencies. This means that the use of reset favours stability when using an integrator in the control loop. A significantly higher phase margin or larger bandwidth can be achieved by using a resetting integrator.

2-6-1 Disturbance rejection

According to the theoretical controller analysis, reset control outperforms linear control due to this relative phase advantage. This holds for both disturbance rejection and noise suppression. As an example, a normalized sinusoidal input disturbance of 80 Hz is applied to the system. The error for zero reference is shown in Figure 2-5.

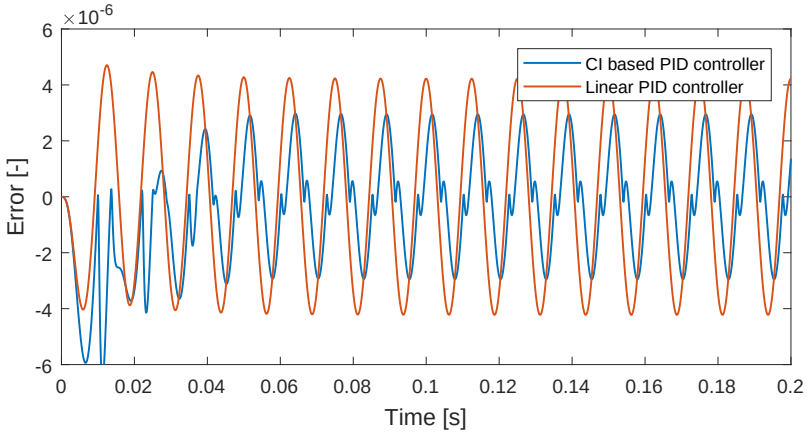

Figure 2-5: Disturbance rejection of a linear PID controller and a CI based PID controller

As expected from the theoretical analysis, the CI based PID controller outperforms the linear PID controller in terms of disturbance rejection at the applied frequency.

2-6-2 Reference tracking

The use of a reset element also has a major drawback. Resetting instances will show unwanted oscillations in the system response. This phenomenon is briefly discussed in [13],[14], and [15]. This behaviour is illustrated by using the same plant and controller. A normalized sine with a frequency of 10 Hz is given as a reference. The tracking error for the reset controller and the linear controller is shown in Figure 2-6.

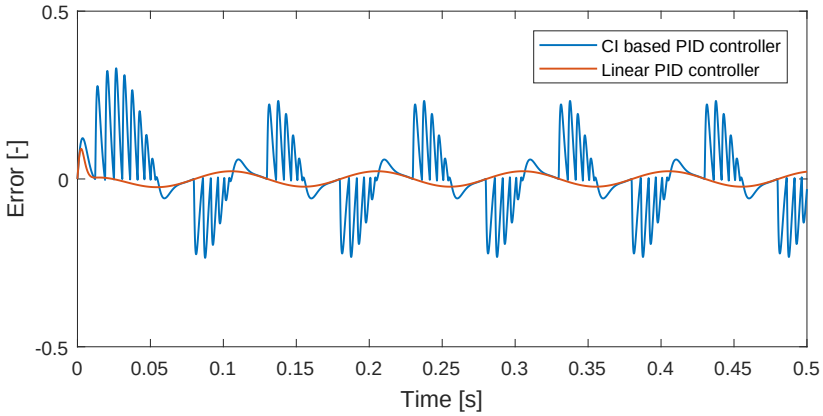

Figure 2-6: Reference tracking of a linear PID controller and a CI based PID controller

The CI based PID controller performs worse compared to the linear PID controller in terms of reference tracking. At resetting instances, relatively large spikes in the control input and the tracking error are observed. This behaviour can be explained by reasoning. Firstly, the controller dynamics are analysed by only taking the first harmonic of the non-linear controller into account. Higher harmonics are neglected in the theoretical analysis but are visible in the performance of a reset controller. Secondly, when resetting the control value to a non-ideal value for the given reference, the feedback controller will not be able to maintain the system at the desired reference since part of the memory of the controller is erased. The controller has to accumulate memory for the system to track the reference. Even in the case where reset is not directly used in the integrator, for example in CgLp, unwanted oscillations are still observed. Even though this is not observed as periodic limit cycles, the higher-order harmonics introduces unwanted dynamics when the after reset value is not optimal.

2-7 Thesis goal

Reference tracking properties of reset control can be outperformed by linear PID control, while linear analysis predicts improvement in other performance indices by introducing a resetting integrator. The advantage in phase obtained by resetting the integrator is however visible in disturbance rejection and noise rejection properties. During the development of reset

control in literature, an increase in performance of reset control is observed by exploring new reset elements such as CgLp [9]. A main advantage of reset control compared to other types of high-performance control is thanks to the ease of implementation through loop shaping techniques. In the future, reset control is expected to outperform linear PID control and overcome the limitations of linear control.

As the precision industry requires fast development of new, high-performance control strategies, reference tracking has to be improved now for reset control, for the utilization of real-time applications. The goal of this thesis is to develop a control strategy in which the advantageous properties of reset control are maintained, while accurate tracking of a reference is achieved. As real-time applications require a dynamic reference, such as a scanning motion, the control strategy should be able to cope with a reference containing multiple frequencies.

Developing a control strategy for accurate tracking of a reference containing multiple frequencies, for general reset control systems, while maintaining the desired properties of reset systems

Chapter 3

Feedforward state of the art

Since the describing function is only a linear approximation of a reset element, unmodelled dynamics caused by the resetting instances are causing unwanted behaviour. The advantage of reset control is thanks to the introduced non-linearities by the resetting actions, which in terms is likely to be accompanied by poor reference tracking. In this chapter, state of the art solutions on reset control itself and similar phenomena are discussed. There are several methods in literature such as PI+CI [16], Partial Reset [13], and reset band [17] which will partially solve for the unwanted behaviour but undesirably deduct part of the non-linearity. This means not only a reduction in tracking error but reduction even in the desired parts and hence mainly provides a trade-off and not relief from the undesired behaviour. Therefore these methods are undesired for this research and will not be discussed in this chapter.

3-1 Feedforward control

The lack of tracking performance of a reset feedback controller can be either compensated by introducing an additional control element or by adapting the characteristics of the reset controller. Adapting the characteristics of the reset controller is undesired as it will inherently change the favoured closed-loop properties introduced by reset. Introducing an extra controller can be either done with a feedback or feedforward element. Introducing an extra feedback element, for instance like in PI+CI control, introduces linearity to the reset controller. The control structure of PI+CI is presented in Figure 3-1. PI+CI control uses a parallel path with a linear integrator and a Clegg integrator to construct an output signal. The amount of non-linearity is determined by $\eta \in [0, 1]$.

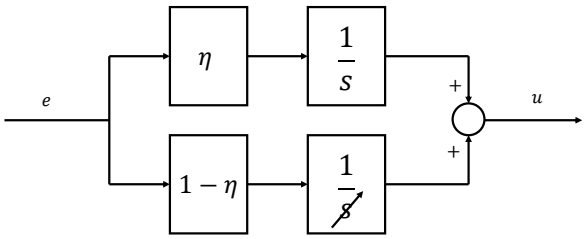

Figure 3-1: General concept of PI+CI control

Such a control structure requires a parallel linear controller in the feedback loop. Note that this structure is general for introducing parallel feedback elements, and therefore additional feedback is not desired. The choice of an additional feedforward element is substantiated by the fact that it does not diminish the introduced non-linearities. Also, whenever the plant is open-loop stable, it is impossible to make the system unstable using a stable feedforward controller. A typical two degree of freedom control structure involving a feedforward and feedback element is shown in Figure 3-2.

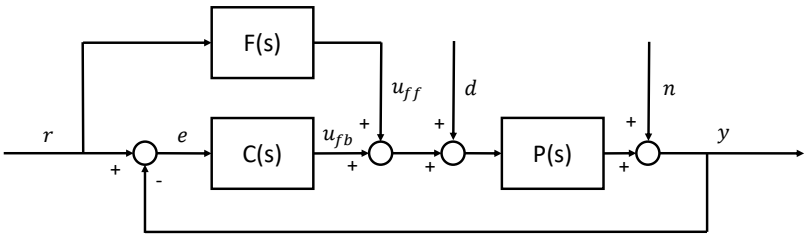

Figure 3-2: Block diagram of the two degree of freedom control structure

With the additional feedforward controller, the dynamics of the closed-loop system are governed by the following transfer functions.

$$y(s) = \frac{P(s)F(s) + P(s)C(s)}{1 + P(s)C(s)}r(s) + \frac{P(s)}{1 + P(s)C(s)}d(s) + \frac{1}{1 + P(s)C(s)}n(s) \tag{3-1}$$

It is also possible to exclude the reference from the feedforward element, yielding the following transfer function.

$$y(s) = \frac{P(s)C(s)}{1 + P(s)C(s)}r(s) + \frac{P(s)}{1 + P(s)C(s)}d(s) + \frac{1}{1 + P(s)C(s)}n(s) + P(s)u_{ff} \tag{3-2}$$

The dynamics illustrated in the transfer functions show why using a feedforward is particularly interesting in the case of applying a reset element in the feedback loop. The feedforward element is only affecting the dynamics of reference tracking, for reference r. The disturbance d and noise n are not influenced by the feedforward element. This inherently means that any feedforward can be used without degrading the increased performance of disturbance rejection and noise attenuation introduced by the reset element. There are multiple cases in which a feedforward controller can be used to improve the reset element.

Firstly, as used in Equation (3-1), by purely using the feedforward element for reference tracking and keep the feedback element for disturbance rejection and compensation of model mismatches of the feedforward. This means a model of the plant is required to generate the desired feedforward input u_{ff} based on r. In this case, the accuracy of a fixed feedforward is directly influenced by the quality of the identification of the system. The accuracy of a physical model approximation is influenced by environmental disturbances, non-linearities of the plant, model uncertainties, or time-varying parameters such as added mass.

Secondly, as used in Equation (3-2), a feedforward can be used to cancel unwanted dynamics introduced by exogenous signals d, or internal dynamics of the closed-loop. In this chapter, different control techniques will be discussed which have the potential to also cancel unwanted dynamics introduced by resetting actions. As there is no literature available on solving the unwanted behaviour in terms of reference tracking with a reset controller using this type of feedforward, other fields of research are explored.

3-2 Feedforward methods

For any feedforward controller, certain dynamic models are required to accurately produce the desired feedforward signal. For deriving these models, different fields of research are consulted. There are various types of systems for which it has been established that they suffer from unwanted oscillations. Although this research is on deriving methods for solving unwanted behaviour in reset controllers, other fields of research, showing similar undesired behaviour, give new insights for a solution in reset control. The following sections present different fields of research where unwanted oscillations occur, and their solutions found in literature. The explored research topics are:

- Reset control
- Non-linear friction
- Harmonic cancellation

Attention should be given to the fact that these limit cycles or unwanted oscillations have different natures. This means that most of the solutions are not similar to the ones occurring in reset controllers and therefore require minor or major adjustments. However, the insights and methods obtained from these fields of research give a great contribution to finding a solution for this research. The first section discusses the solutions for reset control systems in particular. The sections thereafter are dedicated to the other fields of research.

3-2-1 Adaptive feedforward in reset control

As mentioned in the introduction of this chapter, the main focus will be on additional feedforward to preserve the disturbance rejection properties of the feedback element. Several methods in literature explored the adaptation of the reset controller parameters during operation[15],[18]. These researches are not further elaborated since such methods will inherently change controller characteristics. This section only discusses available feedforward control methods to eliminate or suppress the unwanted behaviour of reset controllers, while maintaining reset controller properties.

Adaptive feedforward

A fixed feedforward could be used for reference tracking, while the reset element is used for only disturbance rejection and compensating for model mismatches. The model-based feedforward is based on the inverted plant dynamics, which theoretically yields perfect tracking.

$$y = \frac{P(s)F(s) + P(s)C(s)}{1 + P(s)C(s)}r \;\Rightarrow \frac{P(s)P^{-1}(s) + P(s)C(s)}{1 + P(s)C(s)}r = r \tag{3-3}$$

A proper model inverse feedforward can either be achieved by the availability of the derivatives of the reference signal or by introducing a stable filter $\Lambda(s)$, with at least the same amount of poles as the relative degree of $P^{-1}(s)$. As an example, a first-order plant as presented is [19] and [20], clearly illustrates the reasoning. Consider the following second-order system and its inverse.

$$P(s) = \frac{1}{as + b} \qquad P^{-1}(s) = as + b \tag{3-4}$$

Note that $P^{-1}(s)$ is improper, therefore it is not directly implementable. The two methods of using the inverse based feedforward is by directly using the derivatives of the reference, if available, or by introducing the stable filter $\Lambda(s)$.

$$F = \frac{as + b}{\Lambda(s)}r \quad \text{or} \qquad F = a\dot{r} + r \tag{3-5}$$

The accuracy of a fixed feedforward is proportionate to the accuracy of the identified model of the plant. The feedback element should compensate for any mismatch. It is self-evident that this will yield less accurate tracking than the case in which the feedforward controller is exact. In particular, reset feedback elements yield are deteriorating reference tracking accuracy. To compensate for the model mismatches and achieve more accurate tracking, adaptive laws can be applied.

In [19] and [20] an adaptive feedforward controller is designed for a first-order reset element. The system to be considered is a single input, single output first-order plant. As the reset element is used for fast and stable control, unwanted oscillations are solved with a feedforward element. The goal of the feedforward is to take over the control from the feedback element, while the FORE is only in charge of stabilizing the system for unwanted exogenous inputs. To modify the feedforward model, a linear parametrization of the function is constructed. In this parametrization, the feedforward parameters θ, can be separately analysed form parameters ϕ containing reference information.

$$u_{ff} = \theta^T\phi = \begin{bmatrix} b \\ a \end{bmatrix}^T \begin{bmatrix} \frac{s}{\Lambda(s)} \\ \frac{1}{\Lambda(s)} \end{bmatrix} r, \qquad \text{or} \begin{bmatrix} b \\ a \end{bmatrix}^T \begin{bmatrix} \dot{r} \\ r \end{bmatrix} \tag{3-6}$$

With the parameterized model, an adaptive update law is derived. The update law for the feedforward parameter given in [19], makes use of the feedback control input obtained from the reset controller.

$$\begin{cases} \dot{\theta} = 0 & x \in \mathcal{F} \\ \theta^+ = \theta + \gamma\dfrac{\phi}{\phi^T\phi}u_{fb} & x \in \mathcal{J} \end{cases} \Rightarrow \begin{cases} \dot{u}_{ff} = 0 & x \in \mathcal{F} \\ u_{ff}^+ = u_{ff} + \gamma u_{fb} & x \in \mathcal{J} \end{cases} \tag{3-7}$$

This controller is only used for set-point regulation. The work of [19] is extended in [20], where the adaptive feedforward element is applicable for a reference of more advanced dynamics. This work is also only focused on first order plants. the adaptation of θ is determined by the following adaptive law.

$$\begin{aligned} \dot{\theta} &= 0 && x \in \mathcal{F} \\ \theta^{+} &= \theta + \gamma \frac{\psi(\tau)}{\max(\eta, |\psi(\tau)|^2)} && x \in \mathcal{J} \end{aligned} \tag{3-8}$$

With

$$\psi(\tau) = \int_0^{\tau} C e^{A_f(\tau - s)} B_f ds$$

Where τ indicates the time after a reset. The derivation of this law is given in [20]. Experimental results show that with this control law, a reference containing multiple frequencies can be perfectly tracked. However, it takes a lot of time to converge to the desired values.

Discussion

The suggested adaptive feedforward control strategy eliminates the error in reference tracking. The use of an additional adaptive feedforward keeps the disturbance rejection properties of a reset controller intact. The feedforward in both cases is designed for, and only applicable for FORE feedback elements. Another main drawback of this strategy is the requirement of full state reset to zero of the feedback controller. The goal of this thesis is to find a control strategy that is applicable for general reset controllers, and therefore these methods will need adjustments.

3-2-2 Friction compensation

A reset controller shows unwanted behaviour caused by sudden changes in the control value. While the control value shows linear dynamics in-between reset instances, it suddenly changes whenever a reset occurs. The integrator is accumulating and storing memory of previous inputs, which is reset at zero crossings of the input. Similar behaviour can be observed in systems sensitive to stick-slip motion. Stick-slip motion can be characterized by sudden changes in friction force [21]. An example of a system subjected to stick-slip is shown in Figure 3-4. A constant force F_a is applied to the system. The friction force F_f will match the applied force F_a and will not allow motion. As F_a exceeds the maximum static friction force, the friction force is described by dynamic friction, which usually yields lower force at low velocity. This behaviour results in a similar resetting action.

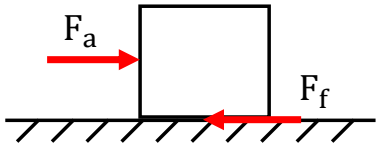

Figure 3-3: Example of a system being excited at with a constant force F. As the mass moves along the surface, stick-slip motion can be observed.

The changes in friction force during movement of the mass are compared to the control signal of a pure Clegg integrator controlling a simple first-order plant in closed-loop. The transfer function of the plant is given by $P(s) = 1/(s+1)$. A comparison of this open-loop stick-slip motion with a simple closed-loop reset control model suffices to illustrate the similarities. The comparison is shown in Figure 3-4, where the friction model is a simple piecewise linear approximation.

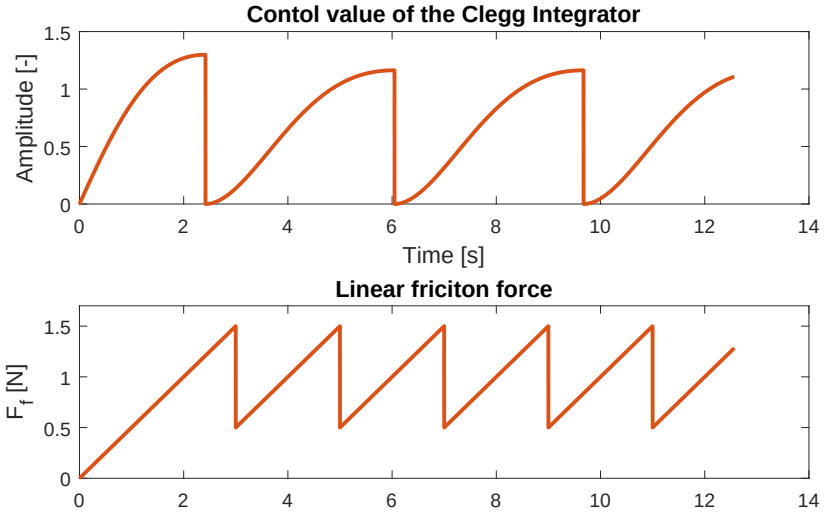

Figure 3-4: Clegg integrator control input compared with the approximated friction force during stick slip motion.

In [22] it is explained how mechanical systems can suffer from limit cycles caused by this non-linear friction. The most common form of limit cycling due to friction is the hunting limit cycle, caused by stick-slip motion. This can be easily illustrated by puling a mass with a spring at a constant velocity. It is shown that Coulomb friction, F_c, only depends on velocity, while static friction, F_s, is a system force at equilibrium. In this section, it is discussed how limit cycle cancellation is done for mechanical systems. As noted in the previous section, optimal feedforward is achieved with $F = P^{-1}$. Direct linear implementation of a model-based feedforward is sensitive to non-linear friction as it only accounts for linear parameters[23]. Note that the application of these methods yields small oscillations as it does not account for non-linear friction.

For a general system, the dynamic friction is accounted for through linearisation, while the static friction should be compensated by the feedback element which introduces a delay and causes oscillatory behaviour. Both model-based and model-free methods for non-linear friction compensation are suggested in literature. It should be noted that model-free friction compensation [24],[25], is not studied here as it requires additional feedback loops, which in terms does affect the reset controller properties.

Model-based techniques for compensating non-linear friction are all based on approximately the same friction function. The models are based on the same mapping of velocity to friction. Particularly interesting is the model proposed in [26]. A Lyapunov based adaptive controller

is designed for reference tracking and friction disturbance compensations. A friction model is introduced which consists only of hyperbolic tangent function and thus is continuously differentiable. Note that other friction models show the same dynamics [27],[28].

$$F_f(\dot{x}) = \gamma_1 \left(\tanh\left(\gamma_2 \dot{x}\right) - \tanh\left(\gamma_3 \dot{x}\right)\right) + \gamma_4 \tanh\left(\gamma_5 \dot{x}\right) + \gamma_6 \dot{x} \tag{3-9}$$

The model is used to compensate for the static friction at low frequencies. In reset control, similar models can be used to compensate for the lack of control input at reset instances. If this would be applied in reset control, the feedforward could be used to provide additional control input at reset instances.

Discussion

There is an important difference between control of non-linear friction force and reset control. Firstly, the friction is acting on the plant which can be modelled by non-linear dynamics. In reset control, the non-linear behaviour is introduced in the controller. The control input of the reset controller is dependent on the tracking error of the plant. A model similar to a friction compensation model could be used to account for sudden changes in control value. However, as this approach would only generate extra control effort near resets, the application of such an additional feedforward changes the behaviour of the reset controller in terms of tracking. Inserting additional control input at reset instances will directly influence control input of the reset controller as the error dynamics are affected and no control effort is stored in the feedforward controller. This method is not further discussed and researched as it requires a significant change of algorithm.

3-2-3 Harmonic cancellation

Reset control yields an increase in performance according to the linear analysis. A reset element is approximated by the describing function which only represents the first harmonic, illustrated in Figure 2-2. The higher-order harmonics yield less reliability of performance by linear analysis and introduce unwanted behaviour. Since there also exist higher-order harmonics, part of the dynamics are neglected.

Higher order harmonics

More accurate modelling of the Clegg Integrator output is achieved by also considering the higher-order harmonics. A more accurate representation of the Clegg integrator is illustrated in Figure 3-5. Note that only odd harmonics contribute to the output of the CI. By also considering higher-order harmonics, the resetting signal is more accurately approximated. Note that by describing function analysis only $F_1(t)$ exists. To illustrate the magnitude of higher-order harmonics of the Clegg Integrator, an input signal of $\sin(2\pi t)$ is considered. Figure 3-6 shows the magnitude of the first five harmonics of the output signal. The figure verifies the usage of the describing function when comparing the magnitude of the different harmonics. However, the higher-order harmonics clearly contribute to the output and therefore will show up in the system response. This section provides research to harmonic cancellation. If there exists a method to successfully cancel the higher-order harmonics in the output, the describing function output can be realized.

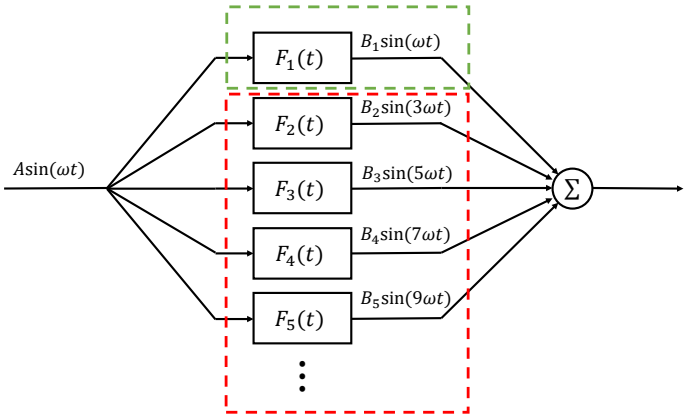

Figure 3-5: Schematic view of a reset integrator with sinusoidal input.

Force/torque ripple

Force ripple is a non-linear periodic disturbance, for example, present in linear motors[29]. Force ripple is characterized as a periodic disturbance moving along with the displacement of the motor. These force ripples will yield a problem in achieving smooth or accurate reference tracking by using only a linear feedback controller. While for the linear motor the harmonic disturbance is introduced in the plant itself, for the reset controller the disturbance is contained in the controller. As the controller output of a reset controller is modelled by a sum off odd harmonics, which can be classified as sinusoidal input disturbances, control techniques used to cancel force ripples form an interesting field of research. Existing control strategies solving the harmonic disturbances in linear motors involve simulating the force ripple as a sum of harmonics. Different researches have solved the force ripple problem through feedforward control[29],[30],[31],[32]. The different approaches suggest an additional feedforward element to account for the harmonic disturbance.

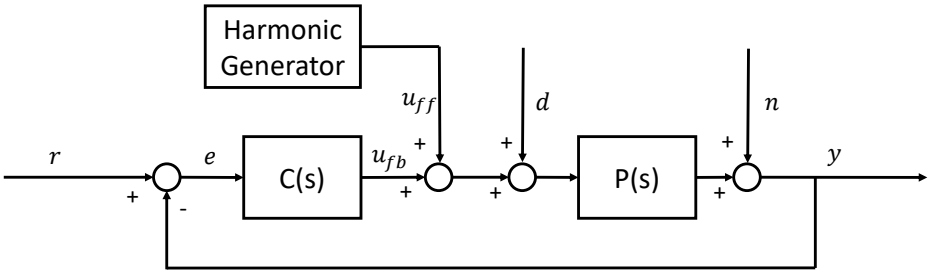

Figure 3-7: Control structure with a feedforward harmonic cancellation controller.

In reset control, only the first harmonic of the controller output is desired. In the configuration of Figure 3-7, the feedforward harmonic generator is used to cancel the higher-order harmonics. The following linear state space describes the dynamics with u_{ff} as the conjugate of the sum of harmonics introduced by the reset element.

$$\dot{x} = Ax + B\left(u + u_{ff}\right) \tag{3-10}$$

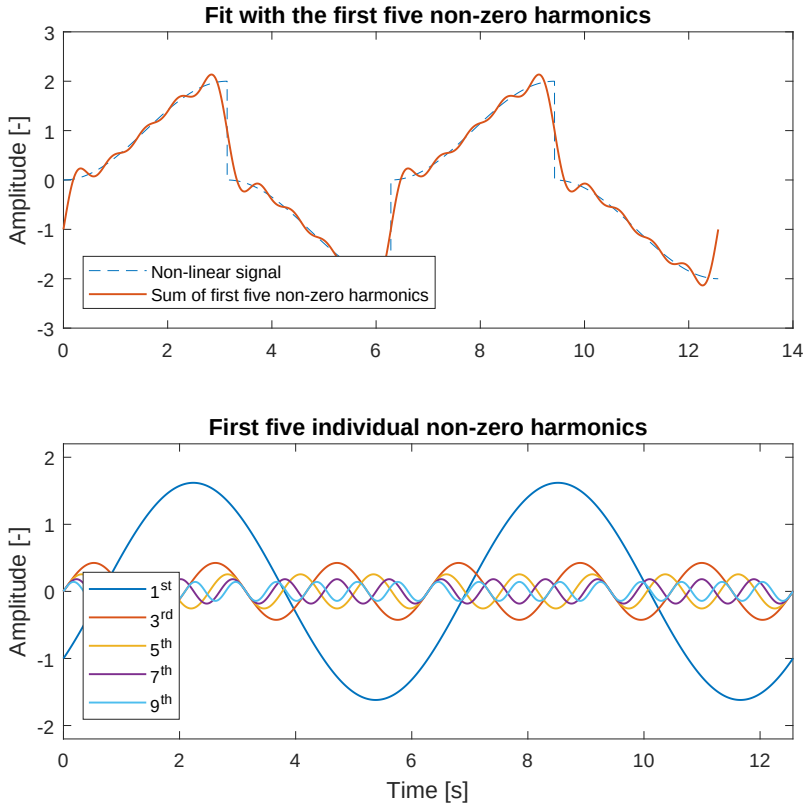

Figure 3-6: The first four odd harmonics of the Clegg Integrator output of 1 rad/s.

There are different models suggested for u_{ff}. In [29] the frequency of the periodic disturbance is estimated off-line using FFT analysis. In this research, only one harmonic is considered. The gains of the harmonics in the feedforward controller are updated according to a recursive least squares algorithm. The model for the feedforward given below can cancel a periodic disturbance with a known frequency. The same feedforward model is used in [30]. The adaptive law, however, is based on 'just in time learning' which yields faster convergence of the harmonic gains. An adaptive feedforward cancellation scheme based on a disturbance observer is suitable to eliminate unknown disturbances [31].

$$u_{ff} = -\sum_{k=1}^{N} A_k \sin(2\pi k\omega t) + B_k \cos(2\pi k\omega t) \tag{3-11}$$

A model based on the control voltage of the plant is suggested in [32]. As this model is proportional to the control voltage, it seems more suited for control use. The effect of the force ripple is reduced based on gradient calculation. The error profile is approximated based on a smooth polynomial in segments where the ripple is present.

$$u_{ff} = -u_{fb} \sum_{k=1}^{N} A_k \sin(2\pi k\omega t) + B_k \cos(2\pi k\omega t) \tag{3-12}$$

Note that these control techniques are based on knowledge of the harmonics' frequency. Therefore it is not possible to directly implement the control strategies for reset control. However, the higher-order harmonics are generated in the feedback controller with fully known dynamics. If the feedback controller is analysed carefully, the algorithms can be adjusted accordingly to cancel higher-order harmonics. If this is possible, a smooth integrator with less phase lag is realised.

Discussion

The open-loop signal of the Clegg integrator is exactly represented by a sum of harmonics when a sufficient amount of harmonics is modelled. This means that whenever an open-loop structure is used, the harmonic cancellation methods will be able to reproduce only the describing function as the output value of the controller. However, when used in closed-loop, this method is ambiguous as the signal is not represented by the same shape. Existing methods rely on knowledge of the frequency of the disturbance. For a varying reference, even the frequency of the harmonics will change, and thus this method is not applicable. Implementation of this method requires researching a system which exactly models the dynamics of the higher-order harmonics introduced by the resetting action.

Chapter 4

Adaptive Feedforward for Reset Control Systems

The main results of this thesis are documented as a paper posted in this chapter. The paper presented in this chapter concisely states the dynamics of the algorithm, the proof of stability and convergence, and experimental results. further elaboration of the algorithm can be found in Appendix A. The steps in the proof of convergence are presented in Appendix B. The experiments carried out to proof the concept are further elaborated in Appendix C.

Adaptive Feedforward For Reset Control Systems - Application in Precision Motion Control

Karst Brummelhuis

***Abstract*—This paper presents a novel adaptive feedforward controller designed for reset control systems. The combination of feedforward and reset feedback control promises high performance as the feedforward tracks the reference and the non-linear feedback element rejects disturbances. To overcome model mismatches, the feedforward controller adapts to increase precision in reference tracking. Where linear existing adaptive models are not able to converge in the presence of reset, this work presents adaptive law based on converging and diverging regions of adaptation to achieve convergence. Experimental results show that the adaptive feedforward controller adapts and converges well to provide improvement in precision tracking.**

***Index Terms*—adpative feedforward, reset control, mechatronics, nonlinear control, motion control**

I. Introduction

The precision industry continues to push the limits in terms of precision and throughput. Examples of precision applications are atomic force microscopes, used to achieve high-resolution imaging, and photo-lithography machines, used for the production of integrated circuits. The system limitations are both determined by hardware design, and just as important, the software. Optimization of the control loops is equally as important as developing new hardware. As the control precision and bandwidth contribute to the error margins of production and throughput of wafers, improved control strategies have a direct impact on increasing profit and production of smaller scale microchips.

As an industry-standard, PID control is still preferred in most applications, given the fact that more than 90% of all control loops are PID [1]. However, PID is fundamentally limited by its linearity. Limitations which can be expressed by e.g. the waterbed effect or Bode's gain phase relationship can be suppressed by introducing a resetting integrator. The idea of resetting was introduced in 1958 by J.C. Clegg [2]. Resetting the integrator whenever a zero crossing of the input occurs, yields a significant reduction in phase lag. This means that introducing non-linear reset control favours the freedom of design and improves the stability margins. Recent research on reset control can be found in [3], [4], [5], [6] [7], [8].

Since describing function analysis allows reset control to be used in the loop shaping framework, the usage of reset control is highly desired compared to other advanced methods such as sliding mode control, model predictive control, or advanced state feedback methods.

However, reset control is a non-linear control technique, which causes higher-order harmonics to be produced in the output of the controller. In the system response, these harmonics play a role by causing unwanted behaviour, which results in poor performance in terms of tracking. To achieve better tracking, control strategies are required to handle the higher-order harmonics. Strategies like PI+CI [9], reset band [10], partial reset [11], and adaptive reset controller [12] [13] partially solve this problem, but undesirably deduct part of the non-linearity introduced with reset, and hence only provide a trade-off.

Perfect reference tracking can be achieved with feedforward control [14]. With exact knowledge of the plant parameters, the feedforward element can be tuned such that output exactly follows the reference. In reality, exact knowledge of the plant is practically impossible due to non-linearities or uncertainties. As feedforward accounts for tracking, the main purpose of the feedback controller is disturbance rejection and compensation of plant uncertainties. Since reset control yields higher phase margin compared to linear control, a combination of feedforward with reset control promises high performance in both stability and tracking. However, as fixed feedforward is sensitive to model mismatches, a dynamic feedforward model is desired. Adaptive or iterative feedforward update laws are suggested to on-line adjust the feedforward to reduce the error induced by model mismatches. Non-linearities introduced by the reset feedback element exclude the direct implementation of linear adaptive or iterative laws.

Combinations of adaptive feedforward with reset control are explored in literature. Adaptive feedforward with first-order reset elements in the control loop is researched in [15] and [16]. The research which is done in [15] only accounts for set-point regulation. While this limitation is solved in [16], the method is only designed for first-order plants controlled by first-order reset elements. However, for application in precision motion control, in which general systems are represented by a mass-spring-damper system or a cascade of mass-spring-damper systems, none of the existing methods is applicable.

This work presents an adaptive feedforward controller for general reset control systems, applicable on plants of any order. The adaptive algorithm handles the non-linearities introduced by the reset element and adapts the feedforward parameters to achieve more accurate tracking. Different types of reset elements are accommodated within the framework. Section II provides preliminaries for reset control. Section III provides necessary information on feedforward in general, and how perfect tracking can be achieved. In Section IV the adaptive feedforward algorithm for general reset control systems is elaborated. The application in precision motion control is explored by implementing the control strategy on a precision positioning stage. These results are presented in

Section V. Conclusions and recommendations for further work are given in Section VI.

II. Reset Control

A. General Reset Control

General reset element dynamics are governed by the following differential inclusion.

$$\begin{aligned} \dot{x}_r(t) &= A_r x_r(t) + B_r e(t) \quad && (x_r, e) \in \mathcal{F} \\ x_r(t^+) &= A_\rho x_r(t) && (x_r, e) \in \mathcal{J} \\ u(t) &= C_r x_r(t) + D_r e(t) \end{aligned} \tag{1}$$

In this SISO system, the matrices A_r, B_r, C_r, and D_r describe the state space of the reset element. These linear dynamics are referred to as the base linear system. The controller states propagate according to the base linear system if $(x_r, e) \in \mathcal{F}$. Whenever the reset conditions are met, $(x_r, e) \in \mathcal{J}$, specified controller states are reset according to the reset matrix A_ρ. Several sets of reset conditions are presented in literature. Dominant reset conditions in literature are either based on zero crossings of the error [17], or based on the signs of the reset controller states and plant output [18]. This work focusses on reset elements based on zero crossings of the error.

$$\begin{aligned} \mathcal{F} &:= \{(x_r, e) \in \mathbb{R} : e \neq 0\} \\ \mathcal{J} &:= \{(x_r, e) \in \mathbb{R} : e = 0\} \end{aligned} \tag{2}$$

B. Reset elements

Different types of reset elements have been presented in literature. There are three main configurations for reset elements, the Clegg Integrator, first-order reset element, and second-order reset element. Adapted versions of the reset elements are researched to enhance the capabilities of reset control.

1) Clegg Integrator: The Clegg integrator (CI) was first introduced as a resetting technique in [2]. Using a Clegg integrator yields the advantage of 52° in reduced phase lag compared to a linear integrator. The definition of a Clegg integrator in state space notation is given in [19].

$$A_r = 0, \quad B_r = 1 \quad C_r = 1 \quad D_r = 0 \quad A_\rho = 0$$

In literature a resetting integrator is indicated by the arrow as shown in Equation (3) below.

$$C(s) = \frac{1}{\not{s}} \tag{3}$$

2) First Order Reset Element: The first extension of the CI is the First Order Reset Element (FORE) [20]. The advantage of FORE compared to CI is that phase lag reduction can be achieved for specific frequencies, as it can be implemented as a low pass filter. The base linear system of the FORE has a corner frequency of ω_r.

$$A_r = -\omega_r \quad B_r = \omega_r \quad C_r = 1 \quad D_r = 0 \quad A_\rho = 0$$

3) Second Order Reset Element: A further extension of the CI and FORE is the Second Order Reset Element (SORE) [21]. By increasing the order, the ability arises of designing resetting notch filters or second-order low-pass filters. The second-order reset element also provides the extra design variable β_r, which is the relative damping of the filter at the corner frequency ω_r.

$$A_r = \begin{bmatrix} 0 & 1 \\ -\omega_r^2 & -2\beta_r\omega_r \end{bmatrix} \quad B_r = \begin{bmatrix} 0 \\ \omega_r^2 \end{bmatrix}$$
$$C_r = \begin{bmatrix} 1 & 0 \end{bmatrix} \quad D_r = 0 \quad A_\rho = \begin{bmatrix} 0 & 0 \\ 0 & 0 \end{bmatrix}$$

4) Generalized FORE and SORE: Generalized reset elements are adapted versions of FORE or SORE. Instead of resetting to zero, the generalized reset element only reset the controller states to a fraction of their value according to the value of γ. The generalized first-order reset element(GFORE) is introduced in [22]. The generalized second-order reset element(GSORE) is introduced in [3]. The reset matrices, A_ρ, for the GFORE and GSORE are respectively,

$$A_\rho = \gamma \qquad A_\rho = \begin{bmatrix} \gamma & 0 \\ 0 & \gamma \end{bmatrix} \tag{4}$$

5) Constant in Gain Lead in Phase: The Constant in gain-lead in phase element(CgLp) is introduced in [3]. This element is used to provide phase lead over a broadband frequency range, whereas other reset elements only provide a reduction of phase lag. The element is either based on GFORE or GSORE. CgLp makes use of a reset lag filter in combination with a linear lead filter of the same order. In transfer function domain the GFORE based CgLp is given by the combination of reset filter and linear filter as given in Equation (5), with $\omega_r < \omega_{r\alpha} << \omega_f$. $\omega_{r\alpha}$ accounts for the shift in corner frequency introduced by the resetting action and the magnitude of shift determined by γ.

$$C(s) = \frac{1}{\not{s/\omega_{r\alpha} + 1}} \qquad \frac{s/\omega_r + 1}{s/\omega_f + 1} \tag{5}$$

C. Closed loop and stability

The closed-loop dynamics of a system controlled by a reset element are given in Equation (6). For ease of notation $x(t)$ is represented as x. The plant states and controller states are indicated by x_p and x_r, respectively. The considered plant is a SISO system.

$$\begin{aligned} \begin{bmatrix} \dot{x}_p \\ \dot{x}_r \end{bmatrix} &= \begin{bmatrix} A_p - B_p D_r C_p & B_p C_r \\ -B_r C_p & A_r \end{bmatrix} \begin{bmatrix} x_p \\ x_r \end{bmatrix} + \begin{bmatrix} B_p D_r \\ B_r \end{bmatrix} r \quad && (x, r) \in \mathcal{F} \\ \begin{bmatrix} x_p^+ \\ x_r^+ \end{bmatrix} &= \begin{bmatrix} I & 0 \\ 0 & A_\rho \end{bmatrix} \begin{bmatrix} x_p \\ x_r \end{bmatrix} && (x, r) \in \mathcal{J} \\ y &= \begin{bmatrix} C_p & 0 \end{bmatrix} \end{aligned} \tag{6}$$

To avoid Zeno solutions, the following assumption is made.

Assumption 1. *For the closed-loop reset control system, the states after reset are such that immediate successive reset is not possible.*

$$x \in \mathcal{J} \Rightarrow x^+ \in \mathcal{F} \tag{7}$$

Note that for discrete systems Zeno behaviour is excluded by definition, as resets can only occur at every sampling instance.

Lyapunov theorem can be used to prove the stability of the closed-loop system. A Lyapunov based stability criterion using a homogenous Lyapunov function is presented in [17]. The theorem obtained from this research is given by:

Theorem 1. *Let $V(x) : \mathbb{R}^n \to \mathbb{R}$ be a continuously differentiable, positive-definite, radially unbounded function such that:*

$$\begin{aligned} \dot{V}(x) &< 0 && x \in \mathcal{F} \\ \Delta V(x) = V(A_\rho x) - V(x) &\leq 0 && x \in \mathcal{J} \end{aligned} \tag{8}$$

If both conditions hold, the equilibrium $x = 0$ is globally asymptotically stable.

III. Feedforward Control

The general structure of a control scheme involving both feedforward and feedback control is given in the block diagram below of Section III. The dynamics of this system are governed

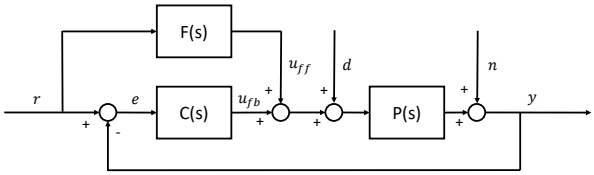

Fig. 1: Two degree of freedom closed loop structure

by the transfer function given in Equation (9).

$$y = \frac{PC + PF}{PC + 1} r + \frac{P}{PC + 1} d + \frac{1}{PC + 1} n \tag{9}$$

The feedforward controller only affects the reference tracking properties of the plant, hence disturbance rejection properties of the feedback controller are maintained for any arbitrary feedforward controller. Ideal feedforward is achieved by the inverse of the plant dynamics, as the mapping from the reference to the output becomes unity.

$$y = \frac{PC + PP^{-1}}{PC + 1} r = r \tag{10}$$

The accuracy of a fixed feedforward is directly influenced by the quality of the identification of the system. Accuracy of the physical model is influenced by environmental disturbances, non-linearities of the plant, model uncertainties, or time-varying parameters such as added mass. Adaptive or iterative feedforward models can estimate correct model parameters over time.

For reset control systems, existing linear adaptive or iterative feedforward controllers are not directly applicable for two reasons. As reset control consists of a flow state and a jump state, only the flow is considered in existing linear laws. Reset control can be implemented with an unstable base linear system. This means that linear laws based on a stable linear closed-loop, will not converge. Even in the case where the base linear system is stable, large spikes in control value can be observed at reset instances. Linear methods do not account for this behaviour, and therefore are unlikely to solve the adaptation problem.

IV. Adaptive Feedforward Algorithm

A. Important properties of the reset control loop

The time in the flow set $\mathcal{F}$ after a reset is defined by τ. At a reset instance, this time variable is reset to zero.

$$\dot{\tau}(t) = 1 \quad (x, r) \in \mathcal{F}, \qquad \tau(t^+) = 0 \quad (x, r) \in \mathcal{J}$$

Assumption 2. *The closed-loop with the reset feedback controller of Equation* (6)*, excluding the feedforward input, is asymptotically stable.*

Corollary 2.1. *Because of the asymptomatic stability of the closed-loop, when $x \in \mathcal{F}$ a reset will happen after a finite amount of time.*

Remark 1. Consider the case with a reset feedback controller, where the feedforward signal is not present. A reset controller can either have a stable or unstable base linear system. If unstable, the resetting action can stabilize the closed-loop [15], [16]. This resetting action introduces additional stability, which can be understood as bringing the controller states closer to the required value when the control input is diverging from the ideal value in the flow interval after some time $\overline{\tau}$. Due to the sharp nature of reset, the feedback control input will only enter the converging region after some amount of time $\underline{\tau}$. Hence it can be stated that in every flow interval, the control input to the plant is converging towards ideal control input u^* in the interval $[\underline{\tau}, \overline{\tau}]$. Note that for both a stable and unstable base linear system this interval exists.

Assumption 3. *In every flow set there exists a region with a lower bound $\underline{\tau}$ and an upper bound $\overline{\tau}$ in which u_{fb} converges to u^*:*

$$u_{fb}(\tau) \to u^*(\tau) \qquad \forall\ \underline{\tau} < \tau < \overline{\tau}$$

The overall control system consists of a feedforward and a feedback controller.

Corollary 3.1. *In the case of both feedforward and feedback, $u_{fb} + u_{ff}$ converges to u^* within the region lower bounded by $\underline{\tau}$ and upper bounded by $\overline{\tau}$:*

$$u_{fb}(\tau) + u_{ff}(\tau) \to u^*(\tau) \qquad \forall\ \underline{\tau} < \tau < \overline{\tau}$$

B. Parametrization

As the focus of this work is in precision positioning applications, plants without zeros are considered. However, in the case that the plant has zeros, this can be considered as plant uncertainties which are to be handled by the feedback

reset controller. For plants without zeros, the inverse is given by:

$$\tilde{P}^{-1}(s) = \theta_n s^{n-1} + \theta_{n-1} s^{n-2} + \ldots + \theta_1 \tag{11}$$

As a result, the feedforward control input is defined as $\tilde{P}^{-1}(s)r$. To define an update law, the feedforward signal is parametrised in linear form. The parametrization consists of a vector θ containing the individual gains, referred to as the feedforward parameters and a vector ϕ containing reference information. The size of θ is determined by the order of the plant.

$$\theta = \begin{bmatrix} \theta_1 & \theta_2 & \ldots & \theta_n \end{bmatrix}^T \tag{12}$$

Containing the same number of elements, ϕ consists of the reference and its first n derivatives:

$$\phi = \begin{bmatrix} r^{(n)} & r^{(n-1)} & \ldots & r \end{bmatrix}^T \tag{13}$$

With these two vectors, the feedforward signal is constructed in real-time as:

$$u_{ff} = \theta^T \phi \tag{14}$$

In the case where the reference is not completely known beforehand, Equation (15) can be used, where $\Lambda(s)$ is a stable filter of order n:

$$\phi = \begin{bmatrix} \frac{s^n}{\Lambda(s)} & \frac{s}{\Lambda(s)} & \ldots & \frac{1}{\Lambda(s)} \end{bmatrix}^T r \tag{15}$$

The update algorithm defined in the following section is based on this parametrization.

C. Update algorithm

The error on the feedforward control input is defined by:

$$\epsilon(t) = \theta^{*T}\phi(t) - \theta^T \phi(t) \tag{16}$$

Where $\theta^{*T}\phi = u^*$ is the ideal control input and θ^* is the vector of ideal feedforward parameters. Based on Corollary 3.1, $\theta^{*T}\phi$ is represented by the total control input. With the definition of

$$\epsilon(\tau) = u_{fb}(\tau) \qquad \forall\ \underline{\tau} < \tau < \overline{\tau} \tag{17}$$

a gradient descent based update law for θ is defined. This update algorithm is given as follows:

$$\begin{aligned} &\dot{\theta}(t) = \Gamma_F \psi(t) u_{fb}(t) \phi_n(t) && \\ &\dot{\theta}_J(t) = \psi(t) u_{fb}(t) \phi_n(t) && (x,r) \in \mathcal{F} \\ &\theta(t^+) = \theta(t) + \Gamma_J \left| J(t) \right| \theta_J(t) && \\ &\theta_J(t^+) = 0 && (x,r) \in \mathcal{J} \end{aligned} \tag{18}$$

where $\Gamma_F > 0$ and $\Gamma_J > 0$ are the adaptive gain matrices. These diagonal matrices can be tuned to determine the rate of adaptation of the feedforward parameters. $J(t) = u_{fb}(t^+) - u_{fb}(t)$ defines the jump in control value at reset. $\phi_n(t)$ is the normalized vector of the filtered input signals contained in $\phi(t)$. Normalization ensures the boundedness of the signal [23]. The normalization matrix $P \geq 0$ and $\zeta > 0$ can be set according to the reference properties.

$$\phi_n(t) = \frac{\phi(t)}{\phi(t)^T P \phi(t) + \zeta} \tag{19}$$

Let us define $\psi(t) \in \{0, 1\}$ as a variable which determines when the controller is in the converging region:

$$\psi(t) = \max\left(\beta, \xi(t)\right) \tag{20}$$

Here β is a design variable and $\xi(t)$ is the filtered absolute tracking error. With $\beta \in \{0, 1\}$ and $\xi(t) \in \{-1, 0, 1\}$. In the case that the base linear system is stable and the entire flow region belongs to the converging region, $\beta = 1$ can be selected. Else $\beta = 0$ is to be used in which case, $[\underline{\tau}, \overline{\tau}]$ is defined over part of the flow region.

$$\xi = \text{sign}\left(\frac{s}{s/\omega_e + 1} \left|e\right|\right) \tag{21}$$

For large values of the corner frequency ω_e, update is enabled for increasing error. Where ω_c is the bandwidth of the closed loop, values for $\omega_e >> \omega_c$ result in estimating the lower bound on the converging region to be $\underline{\tau} = 0$, which is generally not true. Also large values for ω_e will increase the influence of noise. Decreasing the value of ω_e results in increased phase lag, which creates a good estimate of the region $[\underline{\tau}, \overline{\tau}]$. A properly chosen value for ω_e ensures stable adaptation. Values for $\omega_e \in [\frac{\omega_c}{10}, \omega_c]$ are desirable.

D. Stability and convergence

The feedforward parameter is introduced as a state of the system. An augmented state space is adapted as presented in [15], with $x = (\tilde{x}, x_r)$ and the appended state $\tilde{\theta} = \theta^* - \theta$. The error on the states is defined as $\tilde{x} = \phi - x_p$, where ϕ inherently provides the reference value for the states and θ^* the ideal feedforward parameters. In [17], proof is given that if $\tilde{x}$ exists, and Equation (8) is satisfied, tracking with the feedback loop is achieved. Since the feedforward requires the reference to have at least n derivatives, $\tilde{x}$ can be defined. Following similar steps as in [15], and using Theorem 1:

Theorem 2. *The control system asymptotically tracks a given reference r and the feedforward parameters θ converge, if there exists a continuously differentiable, positive definite, radially unbounded function $W\left(x, \tilde{\theta}\right)$ which satisfies:*

$$\begin{aligned} \dot{W}\left(x, \tilde{\theta}\right) &< 0 \\ \Delta W\left(x, \tilde{\theta}\right) &\leq 0 \end{aligned} \tag{22}$$

Consider the following Lyapunov candidate function:

$$W\left(x, \tilde{\theta}\right) = V(x) + \tilde{\theta}^T \tilde{\theta} \tag{23}$$

Through Assumption 2, $V(x)$ satisfies the conditions of Theorem 2.

Flow set:

$$\begin{aligned} \dot{W}\left(x, \tilde{\theta}\right) &= \dot{V}(x) - 2\tilde{\theta}^T \Gamma_F \psi u_{fb} \phi \\ &\leq -2\tilde{\theta}^T \Gamma_F \psi u_{fb} \phi \end{aligned} \tag{24}$$

For $\tau \in [\underline{\tau}, \overline{\tau}]$ update is enabled by $\psi = 1$, and for $\tau \notin [\underline{\tau}, \overline{\tau}]$ update is disabled by $\psi = 0$. In the case were $\psi = 1$, ϵ is substituted for ψu_{fb}:

$$\begin{aligned}\dot{W}\left(x, \tilde{\theta}\right) &\leq -2\tilde{\theta}^T \Gamma_F \epsilon \phi \\ &\leq -\tilde{\theta}^T \Gamma_F \left(\tilde{\theta}^T \phi\right) \phi < 0\end{aligned} \tag{25}$$

And the case where $\psi = 0$, and thus $\tilde{\theta}^T \dot{\tilde{\theta}} = 0$:

$$\dot{W}\left(x, \tilde{\theta}\right) < 0 \tag{26}$$

Jump set:

$$\Delta W\left(x, \tilde{\theta}\right) = W\left(x^+, \tilde{\theta}^+\right) - W\left(x, \tilde{\theta}\right) \leq 0 \tag{27}$$

where $V(x^+) - V(x) \leq 0$ is satisfied and the after reset value $\tilde{\theta}^+$ is given by:

$$\tilde{\theta}^+ = \theta^* - (\theta + \Gamma_J J \theta_J) = \tilde{\theta} - \Gamma_J |J| \theta_J \tag{28}$$

Therefore:

$$\begin{aligned}\Delta W\left(x, \tilde{\theta}\right) &\leq \tilde{\theta}^T \tilde{\theta} - 2J\tilde{\theta}^T \Gamma_J \theta_J + J^2 \theta_J^T \Gamma_J^T \Gamma_J \theta_J - \tilde{\theta}^T \tilde{\theta} \\ &= -2J\tilde{\theta}^T \Gamma_J \theta_J + J^2 \theta_J^T \Gamma_J^T \Gamma_J \theta_J\end{aligned} \tag{29}$$

For guaranteeing $\Delta W\left(x, \tilde{\theta}\right) \leq 0$, the following must hold:

$$2J\tilde{\theta}^T \Gamma_J \theta_J \geq J^2 \theta_J^T \Gamma_J^T \Gamma_J \theta_J \tag{30}$$

As Γ_J is a positive definite diagonal matrix, and $|J|$ is a positive scalar, the inequality is defined by:

$$2\tilde{\theta}^T \theta_J \geq |J| \theta_J^T \Gamma_J \theta_J \tag{31}$$

The condition $\tilde{\theta}^T \theta_J \geq 0$ is sufficient to show $W(x, \tilde{\theta}) \leq 0$ for small enough Γ_J. The inequality holds for similar signs of the individual corresponding parameters in $\tilde{\theta}$ and θ_J.

$$\text{sign}\left(\tilde{\theta}\right) = \text{sign}\left(\theta_J\right) \tag{32}$$

Note that $\dot{\theta}_J = \Gamma_F^{-1} \dot{\theta}$ and $\theta_J^* = 0$.

$$\tilde{\theta}_J = \theta^* - \theta_J = -\theta_J \tag{33}$$

$$\dot{\tilde{\theta}}_J = -\dot{\theta}_J = -\Gamma_F^{-1} \dot{\theta} \tag{34}$$

Therefore:

$$\dot{\tilde{\theta}}_J = \Gamma_F^{-1} \dot{\tilde{\theta}} \tag{35}$$

It is assumed that during a flow set, $\text{sign}\left(\tilde{\theta}\right)$ remains constant. Update of θ and θ_J is only enabled in the region $[\underline{\tau}, \overline{\tau}]$. Note that $\tilde{\theta}(\underline{\tau}) \neq \tilde{\theta}_J(\underline{\tau})$.

$$\tilde{\theta}_J = -\int_{\underline{\tau}}^{\overline{\tau}} \left(\tilde{\theta}^T \phi\right) \phi \tag{36}$$

In $\mathcal{F}$, $\tilde{\theta}^T \dot{\tilde{\theta}} \leq 0$, and $\text{sign}\left(\tilde{\theta}\right)$ is preserved, therefore:

$$\text{sign}\left(\tilde{\theta}_J\right) \neq \text{sign}\left(\tilde{\theta}\right) \tag{37}$$

And since θ_J resets to zero at every jump:

$$\text{sign}\left(\tilde{\theta}_J\right) \neq \text{sign}\left(\theta_J\right) \tag{38}$$

Therefore from Equation (37) and (38) we have:

$$2\tilde{\theta}^T \theta_J \geq 0 \tag{39}$$

Hence, for small enough Γ_J the condition of Equation (32) is satisfied and thus:

$$\Delta W\left(x, \tilde{\theta}\right) \leq 0 \tag{40}$$

Hence, Equation (27) holds and Theorem 2 holds.

V. Application on Precision Positioning Stage

The adaptive algorithm is tested on a precision positioning stage. Performance of the algorithm can be tested and expressed in the convergence of the feedforward parameters, which should also result in a corresponding reduction in tracking error. In an ideal environment, the feedforward controller provides all the control action taking over from the feedback element. However, in practice plants are constrained to model mismatches and external disturbances, which requires a feedback element to provide part of the control action.

A. Setup

The control structure is validated on the planar precision motion stage named the Spider stage, shown in Figure 2. The Spider stage is equipped with voice coil actuators and linear encoders. Three masses (B) are actuated by individual voice coils (C). The masses are constrained to the base plate by leaf flexures. The position of the individual masses is measured by a linear encoder (D). By controlling the three individual masses, the centre mass (A), which is connected to the three individual masses by a leaf flexure, can be accurately positioned. For performance measurement of the feedforward algorithm, the stage is simplified as a SISO plant by only actuating and measuring one of the three masses. Only mass 1, indicated by the red square in Figure 2, is controlled.

The controls are implemented on FPGA using Labview programming. The control device used is the NI CompactRIO for obtaining a high sampling frequency for fast control. The encoder provides a resolution of 100nm

Identifying the system, its dynamics can be represented as that of a double mass-spring-damper system, governed by the following transfer function.

$$P(s) = \frac{8412s^2 + 1.366e4s + 5.851e7}{s^4 + 4.823s^3 + 1.414e4s^2 + 3.39e4s + 4.97e7} \tag{41}$$

However, to prove the effectiveness of the adaptive algorithm, an approximation as a single mass-spring-damper system suffices. This is possible since the double zero pair almost perfectly cancels the double pole pair. The transfer function of the second-order system is given below.

$$P(s) = \frac{8760}{s^2 + 5.886s + 7443} \tag{42}$$

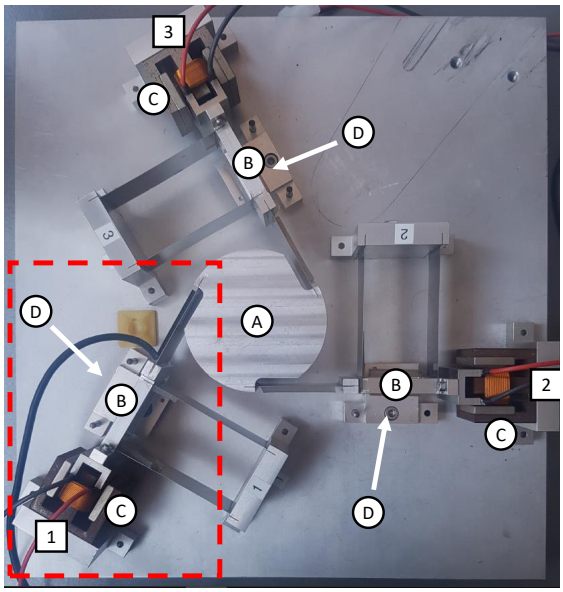

Fig. 2: Spider positioning stage

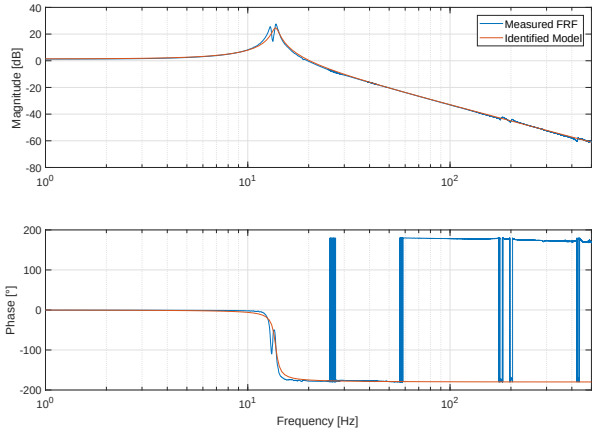

Fig. 3: Measured frequency response of the Spider stage fitted with the frequency response of the second-order estimated plant model for 1-500 Hz

The obtained frequency response is fitted with the frequency response of the second-order plant of Equation (42) as shown in Figure 3, with a resonance frequency of approximately 13.7 Hz. The frequency response is that of a linear system. Even though this is a good representation of the dynamics, the plant shows slight non-linear behaviour for the stiffness and damping terms.

B. Feedback Controller Configurations

All feedback controllers are designed for a bandwidth of $\omega_c = 100$ Hz, where the plant has a phase of -180°. Since the convergence of the feedforward parameters for different types of controllers is to be validated, the feedback controllers are not designed for performance comparison. Four different controllers are tested; linear PID, CI based PID, and two different CgLp based PID controllers.

1) PID: In industry, linear PID controllers are still widely used. As the update algorithm is designed for reset controllers, the effectiveness is also noticeable for application of linear PID controllers. For precision industry, a general series PID for loop-shaping is given by Equation (43). This linear controller is also the basis for the other reset controllers.

$$C(s) = k_p \left(\frac{s+\omega_i}{s}\right)\left(\frac{1+\frac{s}{\omega_d}}{1+\frac{s}{\omega_t}}\right)\left(\frac{1}{1+\frac{s}{\omega_f}}\right) \tag{43}$$

with $\omega_i < \omega_d < \omega_t < \omega_f$. The linear PID controller is designed for a phase margin of approximately 41°. The different frequencies are obtained from [14] as a rule of thumb.

$$\omega_i = \omega_c/10 \quad \omega_d = \omega_c/3 \quad \omega_t = 3\omega_c \quad \omega_f = 10\omega_c$$

2) CI based PID: The Clegg Integrator shows its advantage in reduction of phase lag. The modification on the industry-standard PID controller is the replacement of the linear integrator with the Clegg Integrator. In reset control, the CI based controller shows the most abrupt changes in control value which impairs convergence of the feedforward parameters.

$$C(s) = k_p \left(\frac{s+\omega_i}{\not{s}}\right)\left(\frac{1+\frac{s}{\omega_d}}{1+\frac{s}{\omega_t}}\right)\left(\frac{1}{1+\frac{s}{\omega_f}}\right) \tag{44}$$

A phase lead of 52° is provided after ω_i. The controller provides a phase margin of approximately 51° according to describing function analysis.

$$\omega_i = \omega_c/10 \quad \omega_d = \omega_c/1.2 \quad \omega_t = 1.2\omega_c \quad \omega_f = 10\omega_c$$

3) CgLp based PID 1: The Constant in Gain - Lead in phase element can be added to the controller to provide broadband phase compensation. The controller is designed as below for a phase margin of approximately 47°. The CgLp element, however, shows less abrupt changes in control value at reset instances compared to CI.

$$C(s) = k_p \left(\frac{\frac{s}{\omega_r}+1}{\frac{s}{\omega_{r\alpha}}+1}\right)\left(\frac{s+\omega_i}{s}\right)\left(\frac{1+\frac{s}{\omega_d}}{1+\frac{s}{\omega_t}}\right)\left(\frac{1}{1+\frac{s}{\omega_f}}\right) \tag{45}$$

$$\omega_i = \omega_c/10 \quad \omega_d = \omega_c/1.2 \quad \omega_t = 1.2\omega_c$$
$$\omega_f = 10\omega_c \quad \omega_r = \omega_c/4 \quad \omega_{r\alpha} = \omega_r/1.4$$

4) CgLp based PID 2: The amount of non-linearity is determined by either providing phase through the reset element or the lead filter. Comparison of convergence for two different CgLp configurations shows the effectiveness of the adaptive algorithm to different types of reset controllers. A second CgLp element with low non-linearity is validated in experiments. As the necessary phase is dominantly provided through the linear element, the converging region of the base linear system is larger. This control system has a phase margin of 52°.

$$\omega_i = \omega_c/10 \quad \omega_d = \omega_c/2.5 \quad \omega_t = 2.5\omega_c$$
$$\omega_f = 10\omega_c \quad \omega_r = \omega_c/1.1 \quad \omega_{r\alpha} = \omega_r/1.4$$

C. Experiments

The system is designed with a sampling rate of 10 kHz. All linear filters are discretized for the sampling rate using the bilinear Tustin approximation, this includes the feedback controllers and error filter ψ. Euler's approximation is used for updating the feedforward parameters.

$$\theta(k+1) = \theta(k) + T_s\dot{\theta}(k)$$

The jump update is discrete by definition, therefore this can be implemented as presented in Equation (18). Since the reference is known beforehand, direct derivatives are used for ϕ. The system can be modelled as a second-order plant, therefore a feedforward of only order two is used. This yields that feedforward parameters relatively represent the stiffness, damping, and mass.

$$\theta = \begin{bmatrix}\theta_k & \theta_c & \theta_m\end{bmatrix}^T \qquad \phi = \begin{bmatrix}r & \dot{r} & \ddot{r}\end{bmatrix}^T$$

Since the feedforward consists of three parameters, a multi-sine signal with the sum of at least two sinusoids suffices. Less periodicity is created by adding another sine of a frequency which is indivisible by the other two frequencies. The same reference with varying amplitude of A is used for all experiments.

$$r(t) = A\left(sin\left(2\pi t\right) + sin\left(10\pi t\right) + sin\left(28\pi t\right)\right)$$

The adaptive feedforward is tested for the four different feedback controller cases. Additional experiments have been done on the Cglp based PID 2 controller with artificially added sinusoidal disturbance.

$$d(t) = 15.3\sin\left(30\pi t\right)$$

The unit of this disturbance is in mV.

D. Results

For all configurations $\beta = 0$, this shows robust convergence of the adaptive algorithm even for linear controllers. Any initial values for θ should theoretically show convergence. Since it is only desired to prove convergence and hence reduction in tracking error, θ_0 is chosen as:

$$\begin{bmatrix}\theta_k & \theta_c & \theta_m\end{bmatrix}^T = \begin{bmatrix}0 & 0 & 0\end{bmatrix}^T$$

Since the same reference is applied in every case, it is straightforward to use the same normalization matrix P.

$$P = \text{diag}\left(1000, 1, 1\right)$$

As $\xi(t)$ determines the converging region, ω_e has to be set correctly. For all feedback controllers, approximately the same phase margin and the same bandwidth is used, therefore ω_e is kept constant through all experiments.

$$\omega_e = \omega_c/10$$

The adaptive gain matrices for the different controllers are listed in Table I. Note that the gains are more or less correlated with the relative difference of the second-order plant parameters. Experiments are run for 60 seconds to properly show convergence and steady-state behaviour of the feedforward parameters. The results for the four different controllers are shown in Figure 4.

TABLE I: Values of Γ_F and Γ_J for the different feedback controllers

controller	Γ_F	Γ_J
PID	diag $(150000, 5, 1)$	diag $(0, 0, 0)$
CI	diag $(40000, 2, 0.2)$	diag $(2, 0.0002, 0.00002)$
CgLp 1	diag $(100000, 3, 0.5)$	diag $(5, 0.0001, 0.00005)$
CgLp 2	diag $(150000, 4, 0.5)$	diag $(5, 0.00005, 0.00005)$

The time response θ_k, θ_c, and θ_m of all controller configurations are presented in one figure. As expected, in all cases θ_m converges to the same value as this represents the mass of the plant, which was constant during experiments. The damping value θ_c varies over time. As damping is a non-linear phenomenon modelled as linearity in the system, this behaviour is expected. The stiffness, represented by θ_k stays more constant but changes at the same rate as θ_c. The non-linearity of the stiffness is not observed very clearly as the deflection stays within a linear region due to the bounded reference.

The goal of the feedforward is taking over control action of the feedback controller to decrease the reference tracking error. For the CgLp base PID controller 1, the feedback control input u_{fb}, feedforward control input u_{ff}, and tracking error e, are shown in Figure 5. These three signals are similar for all feedback controllers since all show convergence of the feedforward parameters. The signals are only shown for the first 20 seconds as the feedforward parameters are converged within this time interval. It is observed that the feedback controller plays a significant role at the start of the experiment and decreases in value as the time increases. The value does not converge to zero, this can mainly be explained by the presence of noise and small disturbances. The reference tracking error is decreased by approximately 75% over time in this specific case. Comparison of tracking error for a control structure without feedforward and one with adapted feedforward is shown in Figure 6. In this case, a reduction in error of approximately 85% is observed, making the feedforward necessary for accurate tracking.

To test the algorithm for robustness to disturbance, a final test is done with added disturbance. A relatively high amplitude sinusoidal input disturbance is artificially added to the control signal. The same controller configuration of CgLp based PID 1 is used. The time response of θ is shown in Figure 7. It is observed that feedforward parameters converge as in the disturbance-free case. However, all θ oscillate at steady state. The disturbance is applied at a frequency which is nearly at resonance. To reject this disturbance, the feedback controller has to counteract with a high amplitude control signal, which inherently causes the feedforward parameters to slightly oscillate. However, the feedforward parameters oscillate around the ideal value and do not diverge. Figure 8 shows a decrease of the feedback control input and error as the feedforward control input increases. The tracking error

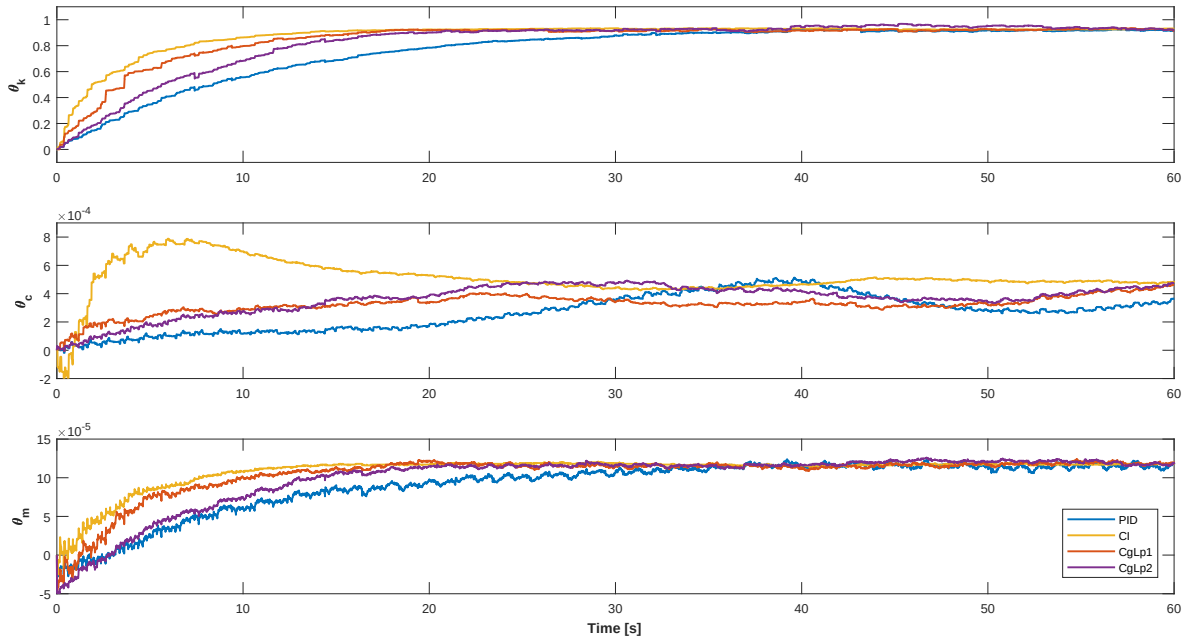

Fig. 4: Evolution of θ_k, θ_c, and θ_m for the different feedback controllers

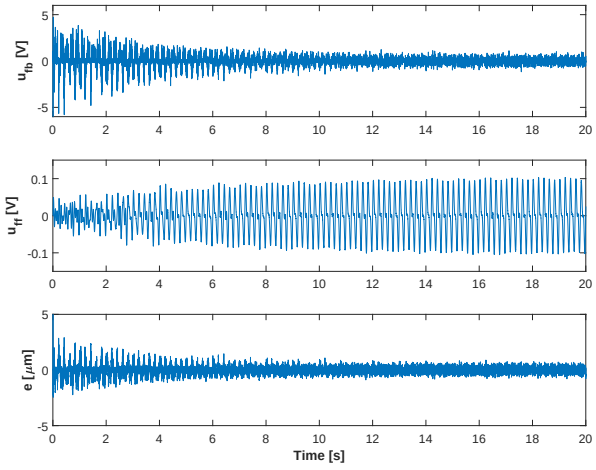

Fig. 5: Evolution of u_{fb}, u_{ff} and e for the first 20 seconds of the CgLp based PID controller 1

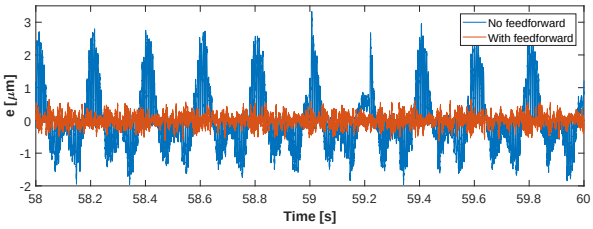

Fig. 6: Comparison of the reference tracking error e with and without the converged feedforward controller at steady state, using the CgLp based PID controller 1

for this case decreases by approximately 65% over time. Figure 9 shows the difference in tracking error for a case with and without feedforward. An error reduction of 65% is observed here. Note that error without additional feedforward is approximately the same as in the disturbance-free case of Figure 6. This shows the effectiveness in disturbance rejection of the reset controller.

VI. Conclusion

Reset controllers provide a good alternative for linear PID control because of an increase in stability margins and the ability to use loop shaping techniques. The reference tracking properties of a reset controller are not always good. Parallel feedforward control can be used to improve for accurate reference tracking. The accuracy of a fixed feedforward is directly dependent on the correctness of the identified plant. For increased precision, adaptive or iterative models can be used which estimate the parameters of the feedforward controller on-line. Existing linear update algorithms are not suited for reset control due to the non-linear nature of the control signal. In this research, an adaptive feedforward algorithm is proposed which can be applied with any type of reset feedback controller based on zero crossings of the tracking error. The scheme is based on linear parametrized plant inverse. The adaptive algorithm consists of both a flow update and a jump update

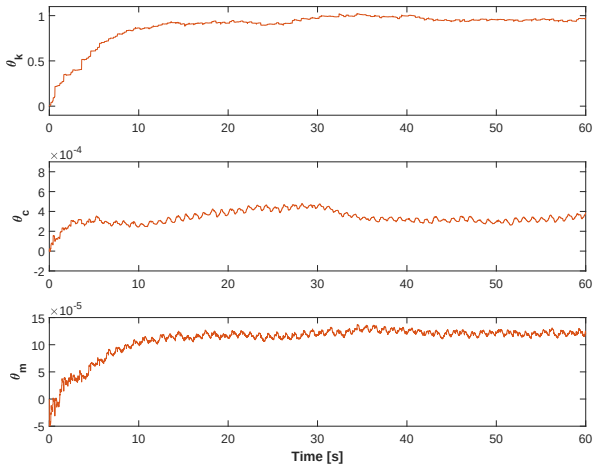

Fig. 7: Evolution of θ_k, θ_c, and θ_m of the CgLp based PID controller 1 with applied disturbance with an amplitude of 50 at 15 Hz

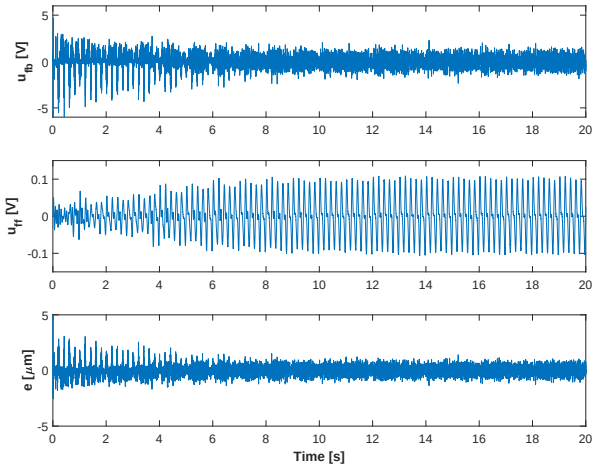

Fig. 8: Evolution of u_{fb}, u_{ff} and e for the first 20 seconds of the CgLp based PID controller 1 with applied disturbance with an amplitude of 15.2 mV at 15 Hz

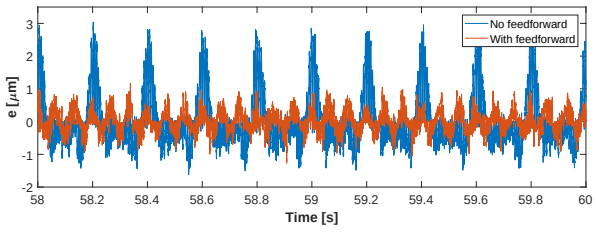

Fig. 9: Comparison of the reference tracking error e with and without the converged feedforward controller at steady state, using the CgLp based PID controller 1. With applied disturbance with an amplitude of 15.2 mV at 15 Hz

for increasing the rate of convergence. The convergence of the algorithm is proved with a continuous Lyapunov function. Experimental results have shown convergence of the feedforward parameters for a mass-spring-damper system, with a PID, CI based, and CgLp based controller in the feedback loop, as well with added disturbance.

References

[1] K. J. Åström and T. Hägglund, "The future of pid control," *Control engineering practice*, vol. 9, no. 11, pp. 1163–1175, 2001.

[2] J. Clegg, "A nonlinear integrator for servomechanisms," *Transactions of the American Institute of Electrical Engineers, Part II: Applications and Industry*, vol. 77, no. 1, pp. 41–42, 1958.

[3] N. Saikumar, R. K. Sinha, and S. H. HosseinNia, "'constant in gain lead in phase'element-application in precision motion control," *arXiv preprint arXiv:1805.12406*, 2018.

[4] Y. ISHINO, T. MIZUNO, M. TAKASAKI, and D. YAMAGUCHI, "Stabilization of magnetic suspension system by using first-order-reset element without derivative feedback," in *2019 12th Asian Control Conference (ASCC)*. IEEE, 2019, pp. 690–694.

[5] N. Saikumar, R. K. Sinha, and S. H. HosseinNia, "Resetting disturbance observers with application in compensation of bounded nonlinearities like hysteresis in piezo-actuators," *Control Engineering Practice*, vol. 82, pp. 36–49, 2019.

[6] L. Chen, N. Saikumar, and S. H. HosseinNia, "Development of robust fractional-order reset control," *IEEE Transactions on Control Systems Technology*, 2019.

[7] N. Saikumar, D. Valério, and S. H. HosseinNia, "Complex order control for improved loop-shaping in precision positioning," *arXiv preprint arXiv:1907.09249*, 2019.

[8] D. Valério, N. Saikumar, A. A. Dastjerdi, N. Karbasizadeh, and S. H. HosseinNia, "Reset control approximates complex order transfer functions," *Nonlinear Dynamics*, pp. 1–15, 2019.

[9] A. Baños and A. Vidal, "Definition and tuning of a pi+ ci reset controller," in *Control Conference (ECC), 2007 European*. IEEE, 2007, pp. 4792–4798.

[10] A. Barreiro, A. Baños, and S. Dormido, "Reset control systems with reset band: well-posedness and limit cycles analysis," in *Control & Automation (MED), 2011 19th Mediterranean Conference on*. IEEE, 2011, pp. 1343–1348.

[11] A. Baños and A. Barreiro, *Reset control systems*. Springer Science & Business Media, 2011.

[12] I. R. Scola, M. M. Quadros, and V. J. Leite, "Robust hybrid pi controller with a simple adaptation in the integrator reset state," *IFAC-PapersOnLine*, vol. 50, no. 1, pp. 1457–1462, 2017.

[13] S. H. HosseinNia, I. Tejado, B. M. Vinagre, and Y. Chen, "Iterative learning and fractional reset control," in *ASME 2015 International Design Engineering Technical Conferences and Computers and Information in Engineering Conference*. American Society of Mechanical Engineers, 2015, pp. V009T07A041–V009T07A041.

[14] R. M. Schmidt, G. Schitter, and A. Rankers, *The Design of High Performance Mechatronics-: High-Tech Functionality by Multidisciplinary System Integration*. Ios Press, 2014.

[15] F. S. Panni, H. Waschl, D. Alberer, and L. Zaccarian, "Position regulation of an egr valve using reset control with adaptive feedforward," *IEEE Transactions on Control Systems Technology*, vol. 22, no. 6, pp. 2424–2431, 2014.

[16] M. Cordioli, M. Mueller, F. Panizzolo, F. Biral, and L. Zaccarian, "An adaptive reset control scheme for valve current tracking in a power-split transmission system." in *ECC*, 2015, pp. 1884–1889.

[17] O. Beker, C. Hollot, Y. Chait, and H. Han, "Fundamental properties of reset control systems," *Automatica*, vol. 40, no. 6, pp. 905–915, 2004.

[18] D. Nešić, L. Zaccarian, and A. R. Teel, "Stability properties of reset systems," *Automatica*, vol. 44, no. 8, pp. 2019–2026, 2008.

[19] Y. Chait and C. Hollot, "On horowitz's contributions to reset control," *International Journal of Robust and Nonlinear Control: IFAC-Affiliated Journal*, vol. 12, no. 4, pp. 335–355, 2002.

[20] I. Horowitz and P. Rosenbaum, "Non-linear design for cost of feedback reduction in systems with large parameter uncertainty," *International Journal of Control*, vol. 21, no. 6, pp. 977–1001, 1975.

[21] L. Hazeleger, M. Heertjes, and H. Nijmeijer, "Second-order reset elements for stage control design," in *American Control Conference (ACC), 2016*. IEEE, 2016, pp. 2643–2648.
[22] Y. Guo, Y. Wang, and L. Xie, "Frequency-domain properties of reset systems with application in hard-disk-drive systems," *IEEE Transactions on Control Systems Technology*, vol. 17, no. 6, pp. 1446–1453, 2009.
[23] P. A. Ioannou and J. Sun, *Robust adaptive control*. Courier Corporation, 2012.

Chapter 5

Conclusions

Reset control can suffer from the inability to accurately track a reference signal. The goal of this thesis was to develop a control strategy which utilizes reset control and can accurately track a broad class of references while maintaining the desired non-linear properties of a reset controller. The method should apply to general reset control systems. In the process, different control strategies from other fields of research were explored. The developed algorithm consists of an adaptive feedforward which can converge the parameters to achieve accurate reference tracking using the output of the feedback controller.

The development of the adaptive feedforward controller for reset control systems is based on adaptation using the feedback control input. Different settings were explored and a converging and diverging region for the feedback control signal was established. The concluding algorithm is based on updating only in the converging region. This work introduces a design variable in the update algorithm which allows updating the feedforward parameters only in this defined region. This is not considered in existing linear update algorithms, and therefore these methods are not suitable to directly be implemented in combination with a reset controllers. The adaptive feedforward algorithm that is proposed can be applied with a general class of reset feedback controller. Since the algorithm consists of these two update parts, of which one is updating during the flow state, the proposed algorithm can also be applied with linear feedback controllers.

The convergence of the feedforward parameters is proven by analysis of a continuous Lyapunov function. The controller is also validated by experiments on the Spider precision positioning stage. Experimental results have shown that the algorithm converges the feedforward parameters of a mass-spring-damper system. The different controllers used in the feedback loop are a linear PID controller, CI based PID controller, and two different CgLp based PID controllers. The two different CgLp based controllers are designed with a different amount of non-linearity. One of the CgLp based controllers is tested for an artificially added disturbance close to the resonance frequency of the plant.

In conclusion, this thesis successfully solved the potential tracking problem of reset control. The feedforward controller can accurately track a reference while the non-linear properties of the feedback reset controller are not affected by the introduced control algorithm.

Chapter 6

Reflection and recommendations

6-1 Reflection on the process

After extensively reading literature, the decision was made to use feedforward utilizing the basis from the theories existing for reset control. Exploring all the different fields of research felt unnecessary at the end, although the idea of harmonic cancellation might be interesting if explored in a feedback framework.

The adaptive algorithm for reset control is updated using the feedback controller input. To get a full understanding of the update algorithm, a derivation from scratch was made. This was very helpful for deriving the algorithm as it is now since the basis is fully understood. The algorithm that was derived at first has the assumption that during the flow set, the control value continuously converges. Also, the assumptions made on the jump set were only true for very basic cases such as a CI and FORE. The assumptions were established using these controllers on a first-order plant.

Then by closely analysing the output signal for the basic reset controllers in closed-loop, a first condition on the converging and diverging regions was established. This is done by extensively comparing the ideal control input and the feedback controller input. For these full state reset controllers, the converging region was determined to be on the region where the error diverges. This was realized in the algorithm by only allowing to update in the region where the tracking error increases. As a direct derivative was not possible, a high pass filter for the absolute error was introduced. This filter had high taming frequency to accurately represent the derivative.

Whenever the controller becomes more complex and linear elements are introduced to the controller, propagation of the control signal during flow and the jump becomes less intuitive. After many simulations, it was established that updating in a small interval after reset was causing divergence. Also, the converging region could be slightly extended to reach further in the flow set. It was quickly realised that by lowering ω_e, extra phase lag was introduced, resulting in this shift in the flow region. This led to the algorithm as it is now.

The experiment part of this research was time-consuming. Switching from the Cedrat stage to the Spider stage was an excellent choice but felt like a waste of time. Using the Spider stage, which accurately represents the theoretical dynamics, was nice for testing the algorithm. Implementation of the algorithm in Labview is also quite time-consuming. It is highly inadvisable to use vector multiplication in FPGA as it will not function as expected, and therefore will waste a lot of time.

6-2 Recommendations for research

Stabilizing parameter ψ

The parameter which allows for adaptation in the stable region of the reset control output could be further explored. As of now, the stable region is based on increasing feedback tracking error. These bounds can be shifted by setting the frequency of the error filter ω to the proper value. Note that this introduces shifting of the region by introducing extra phase lag at operating frequencies of the error. Since this only shifts the error, the size of the region remains approximately the same. A suggesting is a law as defined below to give more freedom in defining the stable region.

$$\psi = \max\left(\beta, \text{sign}\left(F\left(\frac{s\,|e|}{s/\omega_{e1}+1}, \frac{s\,|e|}{s/\omega_{e2}+1}\right)\right)\right) \tag{6-1}$$

The function F could be a min function to narrow the bounds or a max function to broaden the bounds. It is expected that a min function will yield more robustness of the algorithm. It could also be explored to use ψ as float value instead of a boolean. This might however not work out properly since the parameter is introduced as a switch to define the stable update region.

Update in jump set

During the designing process of the algorithm, a lot of different update strategies were explored. As explained in Appendix A, another update law for the jump set was used in the first proposal for the algorithm. Since it is not established how the parameters, and thus the feedforward control input converges, this law can not directly be implemented. This is something to be explored. When applying the method for instance to a simple first-order model controlled by a Clegg integrator, adaptation is guaranteed. However, extending the complexity of the plant and the controller yields difficulties. The mathematical framework and assumptions of why the algorithm is implementable are already present. It may suffice to find a mathematical rule which approximates the value of σ.

Normalization law

The normalization law as used for the algorithm ensures boundedness of the exogenous signal. However, as can be observed from the experiments, the adaptive gains vary by large numbers. It is not explored, or no normalization law is found, which could be used to also normalize

the adaptive gains. The question arises if there are normalization laws which result in a normalized choice of adaptive gains. This would make it easier to implement the adaptive law for a varying class of systems.

Adaptive basis law

The current adaptive algorithm is based on gradient descent. This is essentially one of the most basic forms of adaptive control. Other forms of adaptive are recursive least squares, integral based update, and others. It is not explored in this thesis how these other algorithms affect the update rate or robustness. There is a high chance that the implementation of more advanced update algorithms will yield better results. Note that these algorithms should be only used as a basis for the developed update law.

Test for plant with non negligible zeroes, or extend the algorithm to handle this

The experiments of this thesis are done on a double mass-spring-damper system, which could be modelled as a second-order system due to its well-designed dynamics. It would be interesting to see how the algorithm converges for a system in which the zeroes have to be taken into account.

Stability

Stability is proven for the case where the base linear system of the reset controller is stable. This law is somewhat conservative. There exists no stability proof in literature yet for reset systems with zero crossings, which is more advanced. There might be the possibility to adapt another stability proof. Also, the assumption on the convergence of the total control input is used in the current stability proof. This holds for the proof but a stronger proof would yield a better argument.

Appendix A

Adaptive feedforward algorithm

A-1 Parametrization

The feedforward algorithm is based on feedback error learning. This is a learning feedforward method in which the feedforward parameters, learn from the feedback signal and update accordingly. As the feedback element consists of a reset controller, direct implementation of the linear algorithms is not possible.

Feedforward can be achieved in many ways such as on a polynomial basis or as a plant inverse model. The method used in this thesis is based on a plant inverse. The transfer function from reference to output, clearly shows why this theoretically should achieve perfect tracking.

$$\frac{y}{r} = \frac{PF + PC}{1 + PC} \tag{A-1}$$

Here F is the feedforward controller, C the feedback controller, and P the plant to be controlled. When the feedforward is modelled as $F = P^{-1}$, the transfer function becomes unity.

$$\frac{y}{r} = \frac{PF + PC}{1 + PC} = \frac{PP^{-1} + PC}{1 + PC} = \frac{1 + PC}{1 + PC} = 1 \tag{A-2}$$

All poles and zero's are cancelled in the transfer function, meaning the minimal realization of control system equals unity. Theoretically this can be achieved whenever the model of the plant is perfectly known. As an example for the explanation of the entire feedforward algorithm, a mass-spring-damper system is used, given by the following transfer function. Here, k is the stiffness, c the damping, and m the mass.

$$P = \frac{1}{ms^2 + cs + k} \tag{A-3}$$

Note that directly using the plant inverse is not possible since this would yield an improper transfer function. This can be solved by either introducing a stable filter with at least the

same amount of poles as the relative degree of the plant, or by directly applying the derivatives of the reference in case the reference is known beforehand.

$$F(s) = \frac{ms^2 + cs + k}{\Lambda(s)} \qquad \text{or} \qquad F = m\ddot{r} + c\dot{r} + kr \tag{A-4}$$

In the latter case, no extra design variables are introduced. In the case of introducing the stable filter, it is important to choose the poles such that zeroes are only tamed at frequencies well beyond the characterizing frequencies of the reference signal, only then does the plant inverse correctly approach the derivatives. For further analysis on the feedforward, the gains and time signals are parametrized.

$$\theta^T\phi = \begin{bmatrix} k \\ c \\ m \end{bmatrix}^T \begin{bmatrix} \frac{1}{\Lambda(s)} \\ \frac{s}{\Lambda(s)} \\ \frac{s^2}{\Lambda(s)} \end{bmatrix} \qquad \text{or} \qquad \theta^T\phi = \begin{bmatrix} k \\ c \\ m \end{bmatrix}^T \begin{bmatrix} r \\ \dot{r} \\ \ddot{r} \end{bmatrix} \tag{A-5}$$

This parametrization is an exact representation of the feedforward model. Since it is practically impossible to construct a perfect fixed feedforward from the available plant information, an adaptive law is introduced. With this adaptive law the feedforward parameters, or signal gains, θ are adapted on-line.

A-2 First proposition for the adaptive law

The adaptive law is based on the fact that whenever a stable controller is used, the feedback control input u_{fb} converges towards the ideal control input u^* in between resets up to a certain time $\bar{\tau}$ after a reset occurred. The ideal value for the feedforward parameters is given by θ^*. Then the error of the feedforward value can be determined by the following equation.

$$\epsilon = \theta^{*T}\phi - \theta^T\phi = u^* - \theta^T\phi \tag{A-6}$$

The law which is suggested in this section is only applicable to full state reset controllers.

A-2-1 Flow set

Now the following assumption is made, which always holds for full state reset elements.

Assumption 1. *Whenever a reset has occurred, the feedback element has to gain new control effort. While the controller is trying to push the system back to the desired reference position, the feedback control input u_{fb} converges towards the ideal control input u^* up to a certain point, from where it overshoots the ideal value and diverges.*

$$u_{fb} \to u^* \quad \forall\ \tau \in [0, \bar{\tau}] \tag{A-7}$$

Here τ is the time after a reset has occurred, and $\bar{\tau}$ the time up to which u_{fb} converges. All control inputs are a function of τ. For ease of notation this is not shown in the equations.

For now a second assumption is done based on Assumption 1 to properly construct the error ϵ and derive a law.

Assumption 2. *It is assumed that there is a law such that the feedforward input converges to the correct value such that:*

$$u(\tau) = u_{fb} + u_{ff} \to u^* \quad \forall\ \tau \in [0, \bar{\tau}] \tag{A-8}$$

This means that after every reset $u = u_{fb} + u_{ff}$ converges to u^*. With this assumption a definition for ϵ is established.

$$u - \theta^T \phi \to u^* - \theta^T \phi = \epsilon \quad \forall \tau \leq \bar{\tau} \tag{A-9}$$

Based on this error a cost function can be constructed. A simple cost function is the squared error.

$$J(\theta) = \frac{\epsilon^2}{2} = \frac{\left(u - \theta^T \phi\right)^2}{2} \tag{A-10}$$

The gradient of the cost function with respect to θ shows how θ effects the ϵ.

$$\nabla J(\theta) = -\left(u - \theta^T \phi\right) \phi \tag{A-11}$$

Note that $u_{ff} = \theta^T \phi$, yielding the following gradient.

$$\nabla J(\theta) = -u_{fb} \phi \tag{A-12}$$

As the goal is to minimize the value of $J(\theta)$, and thus minimize ϵ, a recursive law can be introduced. The gradient of the cost function shows the function for which the cost function increases, as it is a convex function. The minimizing direction of the gradient is the negative direction of the gradient. By introducing a recursive law, which utilizes the negative of the gradient, the value of the cost function will decrease over time.

$$\dot{\theta} = \Gamma_F u_{fb} \phi \tag{A-13}$$

The adaptive gain $\Gamma_F > 0$ determines the rate of adaptation. To ensure boundedness of the exogenous signal ϕ, a normalization is suggested.

$$\dot{\theta} = \Gamma_F u_{fb} \frac{\phi}{1 + \phi^T \phi} \tag{A-14}$$

Note that with this update law, updating is enables for all t. Since it is established that u only converges up to $\bar{\tau}$ in a flow set, it is required for

$$u(\tau) \qquad \forall \tau \in (\bar{\tau}, \tau_r] \tag{A-15}$$

where the subscript τ_r indicates the time of reset, to have less influence in updating then

$$u(\tau) \qquad \forall \tau \in (0, \bar{\tau}_i] \tag{A-16}$$

A-2-2 Jump set

A feedback controller is considered in which the controller output is always reset to zero at a zero crossing of the error, for which Assumption 1 must hold. The feedback controller value u_{fb} converges to u^* up to $\overline{\tau}$ and diverges afterwards. After a reset instance occurred, $u_{fb} = 0$. Since the controller output is reset to zero, u^* must be in between the before and after reset value of u_{fb}.

$$u^* = u_{fb}^- - \sigma \left(u_{fb}^- - u_{fb}^+ \right) \tag{A-17}$$

Where it is obvious that $\sigma \in (0, 1)$. If Assumption 2 holds, there are three situations which can occur, that influence the range of values for σ. As the before and after reset instances are at an infinitely small time interval, it is assumed that $u_{ff}^+ \approx u_{ff}^- = u_{ff}$. For the total control input u, the following equation is used to determine the relationship to u^*.

$$u^* = u^- - \sigma \left(u^- - u^+ \right) \tag{A-18}$$

The three different conditions for σ are defined in a, b, and c below.

a. Overshoot

The flow update yields an update rate for θ such that at reset u_{ff} has an overshoot on u^*; $|u_{ff}(\tau_r)| > |u^*(\tau_r)|$. If this is the case, the first assumption of σ does not hold for the total control value u since after the reset, the total control value will exceed u^*.

$$\left| u_{fb}^- + u_{ff} \right| > |u^*| \rightarrow \left| u_{fb}^+ + u_{ff} \right| = |u_{ff}| > |u^*| \tag{A-19}$$

For this case $\sigma > 1$

b. Undershoot

The flow update yields an update rate for θ such that u_{ff} does not overshoot u^*; $|u_{ff}(\tau_r)| < |u^*(\tau_r)|$. In this case the first assumption of σ does hold for the total control value.

$$\left| u_{fb}^- + u_{ff} \right| > |u^*| \rightarrow \left| u_{fb}^+ + u_{ff} \right| = |u_{ff}| < |u^*| \tag{A-20}$$

For this case $\sigma \in (0, 1)$

c. Equality

The flow update yields an update rate for θ such that u_{ff} is equal to u^* at reset; $u_{ff}(\tau_r) = u(\tau_r)^*$. Note that when the feedforward is fully converged, this is the case at any reset instance. The chance at which this occurs without a fully converged feedforward is small, and therefore this case is neglected. It is obvious that for this case $\sigma = 0$.

The definition of the error in the jump set can now be defined.

$$\epsilon^+ = u^- - \sigma \left(u^- - u^+ \right) - \theta^T \phi \tag{A-21}$$

Based on this error a cost function can be generated. A squared error based cost function also suffices for the jump set.

$$J^+(\theta) = \frac{\epsilon^2}{2} = \frac{\left(u^- - \sigma\left(u^- - u^+\right) - \theta^T\phi\right)^2}{2} \tag{A-22}$$

The gradient of the cost function with respect to θ is gives as follows.

$$\nabla J^+(\theta) = -\left(u^- - \sigma\left(u^- - u^+\right) - \theta^T\phi\right)\phi \tag{A-23}$$

Now by using the fact that the feedforward value is approximately constant at the reset instance $u_{ff}^+ \approx u_{ff}^-$, $u_{ff} = \theta^T\phi$, and that the feedback control value is reset to zero $u_{fb}^+ = 0$, the gradient becomes as follows.

$$\nabla J^+(\theta) = -\left(u_{fb}^- - \sigma u_{fb}^-\right)\phi = u_{fb}\left(\sigma - 1\right)\phi \tag{A-24}$$

Now it immediately becomes clear that it is important to know if there is overshoot of the feedforward during reset, since case a. and case b. both yield a different sign for the gradient. Leaving this problem unsolved and keeping σ a design parameter, an update law for the jump set can be defined as follows.

$$\theta^+ = \theta + \Gamma_J u_{fb}\left(1 - \sigma\right)\phi \tag{A-25}$$

Again to ensure boundedness of the exogenous signal, normalization is applied.

$$\theta^+ = \theta + \Gamma_J u_{fb}\left(1 - \sigma\right)\frac{\phi}{1 + \phi^T\phi} \tag{A-26}$$

For small enough Γ_F, this can be used with some certainty of convergence for $\sigma \in [0, 1]$.

A-2-3 Summarized

The total update law is given by:

$$\begin{aligned} \dot{\theta} &= \Gamma_F u_{fb}\phi_n & x \in \mathcal{F} \\ \theta^+ &= \theta + \Gamma_J u_{fb}\left(1 - \sigma\right)\phi_n & x \in \mathcal{J} \end{aligned} \tag{A-27}$$

With ϕ_n as the normalized vector of the exogenous signals. The adaptive gains $\Gamma_F > 0$ and $\Gamma_J > 0$ determine the rate of adaptation. The value of $\sigma > 0$ is not straightforward to determine. As is established, slow adaptation in the flow set requires $\sigma \in (0, 1)$, while fast adaptation in the flow set requires $\sigma > 1$. This means that in the first case the jump update stimulates the rate of adaptation, and in the second case the jump update acts as a correction. This update law works for pure reset controllers in the feedback loop. More advanced controllers, such as presented in Chapter 2 are not suitable for this adaptive law.

A-3 Second proposition for the adaptive law

Even though the first proposition for the adaptive law is not always applicable, it is the basis for the final adaptive law developed in this thesis. Tests in simulations have shown that Assumption 1 holds for both simple and advanced forms of reset controllers. Both the adaptive law for the flow set and jump set have been adjusted.

A-3-1 Flow set

The reason why the first flow set update does not work in all cases is that it is allowed to update in any region of the flow set. As mentioned, only for some time after a reset has occurred, u_{fb} converges toward u^* up to $overline\tau$. In the first proposition, it is only considered if u_{fb} converges but still is allowed to update in any region even though it is clear that there exists a region in which θ should be updated. The region in which θ should be updated is no referred to as the converging region, whereas the opposite is referred to as the diverging region. For more advanced reset controllers, this region is both upper-bounded and lower bounded.

Assumption 3. *It is assumed that there is a law such that the feedforward input converges to the correct value such that:*

$$u \to u^* \quad \forall \tau \in [\underline{\tau}, \bar{\tau}] \tag{A-28}$$

This means that ideally θ is only updated in this converging region of the flow set. However, the bounds of this region can not be directly determined and implemented. Some observations can be used to determine the approximation of this region. The first observation is partly done in Assumption 1, which states that the stable update region exists for $\tau \leq \bar{\tau}$. An approximation for this region is described by the divergence of the feedback error.

$$u \to u^* \quad \forall \ |\dot{e}| > 0 \tag{A-29}$$

To realize this derivative and implement it in the algorithm, a new parameter is introduced in the update law which is either equal to 0 or 1, according to the change in e. The variable ψ is given by the following equation.

$$\psi = \max\left(0, \text{sign}\left(\frac{s\,|e|}{s/\omega_e + 1}\right)\right) \tag{A-30}$$

Whenever the taming frequency ω_e is chosen high enough, the filter represents the derivative of the absolute error.

However, as determined in Assumption 3, the converging region is also lower bounded, in which $|\dot{e}| > 0$ does not always describe this region. A second observation is that whenever a reset instance occurs, the controller states are reset such that for a short instance of time u_{fb} is in the diverging region. Since the feedback controller must be stable, the control input is forced to the converging region. Note that for large values ω_e, the phase lead of the filter is equal to 90°. By lowering the value of ω_e, phase lag is introduced, which shift the region is which $\psi = 1$. This means setting ω_e to a lower value lets ψ describe the converging region. Also, a new variable $\beta \in \{0, 1\}$ is introduced to allow for update over the entire region, in case a linear controller is used.

$$\psi = \max\left(\beta, \text{sign}\left(\frac{s\,|e|}{s/\omega_e + 1}\right)\right) \tag{A-31}$$

The final proposition for the flow update law is given below.

$$\dot{\theta} = \Gamma_F \psi u_{fb} \phi_n \tag{A-32}$$

A-3-2 Jump set

The jump update law of the first proposition is very unreliable, as the value of σ can vary over time for higher order feedback controllers involving reset elements. It is established that the new flow update law updates in the stable region, therefore this information can be used for a jump update. The jump update is used to speed up convergence of θ. A new dynamic variable is introduced, having the same properties as the flow update of θ.

$$\dot{\theta}_J = \psi u_{fb} \phi_n \tag{A-33}$$

Since it is established that this law yields stable updates in the flow set, the value of θ_J can be used at reset to determine the amount of change in θ. The value of θ_J has to be reset to zero at every resetting instance. By using the absolute value of the jump in control value, update in the correct direction is established.

$$\begin{aligned} \dot{\theta}_J &= \psi u_{fb} \phi_n && x \in \mathcal{F} \\ \theta^+ &= \theta + \Gamma_J \left| u_{fb}^- - u_{fb}^+ \right| \theta_J && x \in \mathcal{J} \\ \theta_J^+ &= 0 \end{aligned} \tag{A-34}$$

This law can be implemented along with the flow set law to boost up convergence.

A-3-3 Summarized

The total update law can be summarized by the following differential inclusion. This is finalized update law used in this thesis.

$$\begin{aligned} \dot{\theta} &= \Gamma_F \psi u_{fb} \phi_n \\ \dot{\theta}_J &= \psi u_{fb} \phi_n && x \in \mathcal{F} \\ \theta^+ &= \theta + \Gamma_J \left| u_{fb}^- - u_{fb}^+ \right| \theta_J \\ \theta_J^+ &= 0 && x \in \mathcal{J} \end{aligned} \tag{A-35}$$

A-4 Discrete implementation

For validation on the experimental setup, as described in Appendix C, a discrete version of the adaptive algorithm is required. Since the algorithms is designed in continuous time, direct implementation is not possible. The continuous variables used in the algorithm are u_{fb}, e, and ϕ. First of all, implementation of the update of θ can be easily realized by using Euler's numerical integration law.

$$\theta(k+1) = \theta(k) + T_s \dot{\theta}(k) \tag{A-36}$$

Where T_s is the sampling time of the control system. $\dot{\theta}$ is obtained by using sampled instances of u_{fb} and ϕ. The only remaining continuous signal is ψ. To maintain properties of the error filter, Tustin's approximation is used.

Appendix B

Stability

B-1 Reset control

B-1-1 Preliminaries

Strict positive realness

Strict positive realness is a property of transfer functions. The transfer function $G(s) = \frac{n(s)}{d(s)}$ is said to be strictly positive real when in satisfies the following conditions.

- All poles of $G(s)$ are negative.
- For any ω, $\mathrm{Re}\{G(j\omega)\} \geq 0$.
- Either $G(\infty) > 0$ or $G(\infty) = 0$ and $\lim_{\omega \to \infty} \omega \mathrm{Re}\{G(\omega)\} > 0$.

B-1-2 H_β-condition

The results of this section are obtained from [3]. For considering the stability conditions of a closed-loop system with a reset feedback element, the following closed-loop state space matrices are used.

$$\begin{aligned} A_{cl} &= \begin{bmatrix} A_p - B_p D_r C_p & B_p C_r \\ -B_r C_p & A_r \end{bmatrix} & B_{cl} &= \begin{bmatrix} B_r D_r \\ B_c \end{bmatrix} \\ A_{\mathrm{P}} &= \begin{bmatrix} I & 0 \\ 0 & A_\rho \end{bmatrix} & C_{cl} &= \begin{bmatrix} C_p & 0 \end{bmatrix} \end{aligned} \tag{B-1}$$

Then the state evolution of the reset control system can be described by the following equations, with $\mathcal{M}$ being the reset surface. The system states are $x = \begin{bmatrix} x_p & x_r \end{bmatrix}^T$.

$$\begin{aligned} \dot{x}(t) &= A_{cl}x(t) + B_{cl}r(t) \quad x(t) \in \mathcal{M} \\ x(t^+) &= A_{\mathrm{P}}x(t) \qquad\qquad\quad x(t) \notin \mathcal{M} \end{aligned} \tag{B-2}$$

The reset surface is defined as follows.

$$\mathcal{M} = \{x \in \mathbb{R}^{n_p+n_c} : C_{cl}x = 0, (I - A_{\mathrm{P}})\, x\} \tag{B-3}$$

A general Lyapunov statement regarding stability of reset control systems is given by the following theorem. This theorem does not require assumptions on the reset times.

Theorem 2. *Let $V(x) : \mathbb{R}^n \to \mathbb{R}$ be a continuously differentiable, positive-definite, radially unbounded function such that*

$$\begin{aligned} \dot{V}(x) &= \frac{\partial V}{\partial x}\dot{x} < 0 \qquad\qquad x \neq 0 \\ \Delta V(x) &= V(A_{\mathrm{P}}x) - V(x) \leq 0 \quad x \in \mathcal{M} \end{aligned} \tag{B-4}$$

If both these condition hold, two conclusions can be drawn, namely:

- *there exists a left-continuous function x(t) satisfying Equation* (B-2) *for all $t \geq 0$.*
- *The equilibrium $x = 0$ is globally asymptotically stable.*

There is a more general condition which proofs different types of stability of a reset control system. A reset control system satisfies the H_β-conditions if there exists a $\beta \in \mathbb{R}^{n\times 1}$ and a positive definite $P_\rho \in \mathbb{R}^{n\times n}$ such that the transfer function of Equation (B-5) is strictly positive real.

$$H_\beta(s) = \begin{bmatrix} \beta C_p & 0_{n\times m} & P_\rho \end{bmatrix} (sI - A_{cl})^{-1} \begin{bmatrix} 0_{l\times n} \\ 0_{m\times n} \\ I_{n_\rho} \end{bmatrix} \tag{B-5}$$

Where l is the amount of plant states, m the non resetting controller states, and n the resetting controller states. There are different conditions for the the H_β-condition, where this method can be used to check either quadratic stability, uniformly bounded input bounded state stability, and steady state performance.

Quadratic stability

The system is said to be quadratically stable if the conditions from Theorem 2 hold. This means there exists a positive-definite P for Lyapunov candidate $V(x) = x^T Px$ such that the following is true.

$$\begin{aligned} x^T \left(A_{cl}^T P + PA_{cl}\right) x < 0 \quad x \neq 0 \\ x^T \left(A_{\mathrm{P}}^T P A_{\mathrm{P}} + P\right) x \leq 0 \quad x \in \mathcal{M} \end{aligned} \tag{B-6}$$

The quadratic stability result regarding the H_β-condition then becomes as follows.

Theorem 3. *The reset control system Equation* (B-2) *is quadratically stable if and only if the system satisfies the H_β-condition.*

B-2 Adaptive Algorithm

B-2-1 Gradient descent

For a basic gradient descent adaptive algorithm, the following Lyapunov approach proves convergence of the adaptive parameters. There exists an ideal value for the parameters θ^*, which defines the error:

$$\epsilon = \theta^{*T}\phi - \theta^T\phi = \tilde{\theta}^T\phi \tag{B-7}$$

For proof of convergence $\tilde{\theta} = \theta^* - \theta$ is considered as a state. If it is proven that $\tilde{\theta}$ is asymptotically stable in the origin, the values of θ converge to θ^*. The time derivative of $\tilde{\theta}$ is given by the following equation. Note that the ideal value θ^* is does not change over time.

$$\dot{\tilde{\theta}} = \dot{\theta}^{*T} - \dot{\theta}^T = -\dot{\theta}^T = -\Gamma\left(\tilde{\theta}^T\phi\right)\phi \tag{B-8}$$

Now define the following Lyapunov function.

$$V(\tilde{\theta}) = \frac{1}{2}\tilde{\theta}^T\Gamma^{-1}\tilde{\theta} \tag{B-9}$$

Yielding the following time derivative.

$$\begin{aligned}
\dot{V}(\tilde{\theta}) &= \tilde{\theta}^T\Gamma^{-1}\dot{\tilde{\theta}} && \text{(B-10)}\\
&= \tilde{\theta}^T\Gamma^{-1}\left(-\Gamma\epsilon\phi\right) && \text{(B-11)}\\
&= \tilde{\theta}^T\Gamma^{-1}\left(-\Gamma\left(\tilde{\theta}^T\phi\right)\phi\right) && \text{(B-12)}\\
&= -\tilde{\theta}^T\left(\tilde{\theta}^T\phi\right)\phi = -\left(\tilde{\theta}^T\phi\right)^2 \leq 0 && \text{(B-13)}
\end{aligned}$$

This shows that $\dot{V}(\tilde{\theta}) \leq 0$, proving of convergence for θ.

B-2-2 Convergence and stability of the closed loop

Theorem 2 can be used to establish convergence in the the closed loop with a reset controller. Therefore the states are augmented. The assumption is made that the reference exists of the same modes as the state space of the plant. Therefore an augmented state can be introduces which represents the error of plant state with respect to the reference states. Note that ϕ represents these states as the feedforward requires these states to exist.

$$\tilde{x}_p = x_p - \phi \tag{B-14}$$

The controller states do not have to be augmented. If the feedforward converges, the controller states converged to zero. The error of the feedforward parameters $\tilde{\theta}$ is appended for the stability proof.

$$\tilde{\theta} = \theta^* - \theta \tag{B-15}$$

The new states which are being used are:

$$\begin{bmatrix} x \\ \tilde{\theta} \end{bmatrix}, \qquad \text{with } x = \begin{bmatrix} \tilde{x}_p \\ x_r \end{bmatrix} \tag{B-16}$$

The time derivative of x is given by:

$$\dot{x} = Ax + B\tilde{u}_{ff} = Ax + B\tilde{\theta}^T\phi \tag{B-17}$$

With matrices

$$A = \begin{bmatrix} A_p - B_p D_r C_p & B_p C_r \\ -B_r C_p & A_r \end{bmatrix} B = \begin{bmatrix} B_p \\ 0 \end{bmatrix} \tag{B-18}$$

Now a Lyapunov function can be defined which satisfies Theorem 2.

$$V(x, \tilde{\theta}) = V_1(x) + V_2(\tilde{\theta}) \tag{B-19}$$

B-2-3 Flow set

For the flow set, the following condition of the time derivative of the Lyapunov function must hold:

$$\dot{V}(x, \tilde{\theta}) \leq 0 \tag{B-20}$$

The time derivative of $V(x, \tilde{\theta})$ is given by:

$$\dot{V}_1(x) = \frac{\partial V_1(x)}{\partial x}\left(Ax + B\tilde{\theta}^T\phi\right) \tag{B-21}$$

Note that the feedback loop is assumed to be stable. Therefore, there exists a $V_1(x) > 0$ which satisfies $\dot{V}_1(x) \leq 0$.

Now a function for $V_2(\tilde{\theta})$ is required, to prove convergence. The time the derivative for $\tilde{\theta}$ with respect to the Lyapunov function is:

$$\dot{V}_2(\tilde{\theta}) = \frac{\partial V_2(\tilde{\theta})}{\partial \tilde{\theta}}\left(-\Gamma_F \psi u_{fb} \phi\right) \tag{B-22}$$

The following Lyapunov function will be used for the stability proof of the algorithm.

$$V_2(\tilde{\theta}) = \tilde{\theta}^T\tilde{\theta} \tag{B-23}$$

According to Assumption 2, in the stable update region $[\underline{\tau}, \overline{\tau}]$, the ideal control value u^* is approached by the total feedback control value $u_{fb} + u_{ff}$:

$$u_{fb} + u_{ff} \Rightarrow u^* \qquad \tau \in [\underline{\tau}, \overline{\tau}] \tag{B-24}$$

This region is approached by introducing the variable ψ. Now consider the case where ψ is determined for $\beta = 0$, meaning either $\psi = 1$ or $\psi = 0$. In the case where $\beta = 1$, it is assumed that the whole flow set belongs to the converging region.

$\psi = 1$:

If $\psi = 1$, the feedback control input u_{fb} is in the converging region, where Equation (B-24) holds. This makes the following equation hold for the flow region where $\psi = 1$.

$$\epsilon = u * -\theta^T \phi = u_{fb} + u_{ff} - \theta^T \phi = u_{fb} \tag{B-25}$$

Therefore $\dot{V}_2(\tilde{\theta})$ is represented by:

$$\dot{V}_2(\tilde{\theta}) = \frac{\partial V_2(\tilde{\theta})}{\partial \tilde{\theta}} \left(-\Gamma_F \epsilon \phi\right) \tag{B-26}$$

As the ideal control input is represented by $u^* = \theta^{*T}\phi$, the following holds:

$$\epsilon = \theta^{*T}\phi - \theta^T \phi = \tilde{\theta}^T \phi \tag{B-27}$$

Yielding the following time derivative. Note that Γ_F is a positive definite diagonal matrix.

$$\begin{aligned} \dot{V}_2(\tilde{\theta}) &= 2\tilde{\theta}^T \dot{\tilde{\theta}} \\ &= 2\tilde{\theta}^T \left(-\Gamma_F \epsilon \phi\right) \\ &= 2\tilde{\theta}^T \left(-\Gamma_F \left(\tilde{\theta}^T \phi\right) \phi\right) \\ &= -2\tilde{\theta}^T \Gamma_F \left(\tilde{\theta}^T \phi\right) \phi = -2 \left(\tilde{\theta}^T \phi\right) \tilde{\theta}^T \Gamma_F \phi \leq 0 \end{aligned} \tag{B-28}$$

$\psi = 0$:

Whenever $\psi = 0$, the time derivative of the Lyapunov function simply becomes:

$$\dot{V}_2(\tilde{\theta}) = 0 \tag{B-29}$$

Full flow set

The value for $\psi \in [0, 1]$ acts as a switch for updating θ. This yields the following two cases for $\dot{V}(\tilde{\theta})$.

$$V_2(\tilde{\theta}) \leq 0 \quad \text{if } \psi = 1 \tag{B-30}$$

$$V_2(\tilde{\theta}) = 0 \quad \text{if } \psi = 0 \tag{B-31}$$

The closed loop is required to be stable. Also the reference is assumed to be bounded. Whenever this is the case there is always a region in every individual flow set where there is an increase and a decrease in error. This means there always exists $\psi > 0$ in the flow set as long as there is a tracking error, therefore $V_2(\tilde{\theta})$ proves asymptotic stability in $\mathcal{F}$.

B-2-4 Jump set

For the jump set, the following conditions on the Lyapunov function must hold:

$$\Delta V(x,\tilde{\theta}) = V(x^+,\tilde{\theta}^+) - V(x,\tilde{\theta}) \leq 0 \tag{B-32}$$

For a quadratic Lyapunov function on x it is obvious that this holds for $V_1(x)$. Since the states are reset according to a value $\gamma \leq 1$, the value of the states decreases for the states which are being reset. $\Delta V_1(x)$, relatively decreases by γ^2 for these specific states.

The after reset value of $\tilde{\theta}$ is defined as follows.

$$\begin{aligned}\tilde{\theta}^+ &= \theta^* - (\theta + \Gamma_J J\theta_J) = \tilde{\theta} - \Gamma_J J\theta_J \\ &= \tilde{\theta} - \Gamma_J J \int_{T_i}^{T_{i+1}} (\psi u_{fb}\phi)\end{aligned} \tag{B-33}$$

With $J = \left|u_{fb}^+ - u_{fb}\right|$ where u_{fb} is the feedback controller value before reset. The time in the flow state is determined by the time instances of two consecutive resets on T_i and T_{i+1}. The first line in the above equation leads to the following condition on the Lyapunov equation to be true.

$$\Delta V_2(\tilde{\theta}) = V_2(\tilde{\theta} - \Gamma_J J\theta_J) - V_2(\tilde{\theta}) \leq 0 \tag{B-34}$$

Considering the quadratic Lyapunov function in Equation (B-23), this yields:

$$\begin{aligned}\Delta V_2(\tilde{\theta}) &= \tilde{\theta}^T\tilde{\theta} - J\tilde{\theta}^T\Gamma_J\theta_J - J\theta_J^T\Gamma_J^T\tilde{\theta} + J^2\theta_J^T\Gamma_J^T\Gamma_J\theta_J - \tilde{\theta}^T\tilde{\theta} \\ &= -2J\tilde{\theta}^T\Gamma_J\theta_J + J^2\theta_J^T\Gamma_J^T\Gamma_J\theta_J\end{aligned} \tag{B-35}$$

The value for $\Delta V_2(\tilde{\theta})$ is always negative or equal to zero if the following holds since $J^2\theta_J^T\Gamma_J^T\Gamma_J\theta_J \geq 0$:

$$2J\tilde{\theta}^T\Gamma_J\theta_J \geq J^2\theta_J^T\Gamma_J^T\Gamma_J\theta_J \tag{B-36}$$

As the Γ_J is a diagonal matrix, and is present in both sides of the equation, it can be replaced with an identity matrix. The matrix is diagonal, which means $\Gamma_J = \Gamma_J^T$. The jump value J is a positive scalar, and thus will cancel out on both sides of the equation.

$$2\tilde{\theta}^T\theta_J \geq J\theta_J^T\Gamma_J\theta_J \tag{B-37}$$

Since Γ_J can be manually chosen, it only has to be proven that $\tilde{\theta}^T\theta_J \geq 0$. Also $\tilde{\theta}^T\theta_J = 0$ yields $J\theta_J^T\Gamma_J\theta_J = 0$. This always holds since θ_J appears on both sides of the equation. The following equality has to be proven to show convergence in the jump set.

$$\text{sign}\left(\tilde{\theta}\right) = \text{sign}\left(\theta_J\right) \tag{B-38}$$

Note that the sign function indicates the sign of the individual components in the vector. When the equality holds, it is obvious that the jump update is stable as $V_2(\tilde{\theta}) \leq 0$ for small enough Γ_J.

The results on the flow set show constant decrease or equality on $V_2(\tilde{\theta})$. The ideal value for the jump variable is $\theta_J = 0$ since this indicates full convergence. Also note that $\dot{\theta}_J = \Gamma_F^{-1}\dot{\theta}$.

$$\tilde{\theta}_J = 0 - \theta_J \tag{B-39}$$

$$\dot{\tilde{\theta}}_J = -\dot{\theta}_J = -\Gamma_F^{-1}\dot{\theta} \tag{B-40}$$

This means that following also holds

$$\dot{\tilde{\theta}}_J = \Gamma_F^{-1}\dot{\tilde{\theta}} \tag{B-41}$$

It is assumed that during a flow set, overall the signs of the individual parameters of $\tilde{\theta}$ remains constant, $\text{sign}\left(\tilde{\theta}(T_i)\right) = \text{sign}\left(\tilde{\theta}(T_{i+1})\right)$.. This means that from in the region $[T_i, T_{i+1}]$, $\text{sign}\left(\tilde{\theta}\right)$ remains the same. Note that the only effective update happens in the converging region $[\underline{\tau}, \overline{\tau}]$ when $\psi = 1$, and thus $\psi u_{fb} = \epsilon$. The initial conditions on a flow set are different $\tilde{\theta}(T_i) \neq \tilde{\theta}_J(T_i)$.

$$\tilde{\theta}_J = 0 - \int_{\underline{\tau}}^{\overline{\tau}} \left(\tilde{\theta}^T\phi\right)\phi \tag{B-42}$$

In the same region the following holds for $\tilde{\theta}$

$$\tilde{\theta} = \tilde{\theta}(T_i) - \int_{\underline{\tau}}^{\overline{\tau}} \Gamma_F\left(\tilde{\theta}^T\phi\right)\phi \tag{B-43}$$

As it is proven that in every flow set the error $\tilde{\theta}$ decreases, the assumption that the sign of $\tilde{\theta}$ remains the same during the flow set, and the fact that Γ_F is a positive definite diagonal matrix,the following holds.

$$\text{sign}\left(\tilde{\theta}_J\right) \neq \text{sign}\left(\tilde{\theta}\right) \tag{B-44}$$

And also because θ_J resets to zero at every jump:

$$\text{sign}\left(\tilde{\theta}_J\right) = \text{sign}\left(0 - \theta_J\right) = -\text{sign}\left(\theta_J\right) \tag{B-45}$$

Therefore

$$2\tilde{\theta}^T\theta_J \geq 0 \tag{B-46}$$

This means that for small enough Γ_J:

$$\Delta V_2(\tilde{\theta}) = -2J\tilde{\theta}^T\Gamma_J\theta_J + J^2\theta_J^T\Gamma_J^T\Gamma_J\theta_J \leq 0 \tag{B-47}$$

This proves convergence of the jump update for the given Lyapunov conditions.

Appendix C

Experiments

The adaptive feedforward algorithm suggested in this thesis, is validated on an experimental setup, the Spider stage. This chapter explains more about the setup and implementation of the controller in the Labview environment.

C-1 Setup

The used setup is the Spider stage, shown in Figure C-1. As mentioned in the paper, his stage is equipped with voice coil actuators and linear encoders. Three masses (B) are actuated by individual voice coils (C). The masses are constrained to the base by leaf flexures. The position of the individual masses is measured by the linear encoder (D). By controlling the three individual masses, the centre mass (A), which is connected to the three individual masses by a leaf flexure, can be accurately positioned. Only mass 1 is actuated and measured for the experiments. Since the feedforward algorithm is developed for a SISO system, MIMO control is not explored in this thesis. Only the mass indicated in the red square is controlled. The devices used to correctly measure the position of the mass and actuate the voice coil are all based on the NI CompactRIO-9309.

For actuating the voice coil the NI 9264 analogue output module is used. This module has a 16-bit resolution which outputs a voltage in the range of -10V to 10V. A linear amplifier is used to provide the current required by the voice coil. No specifications on this amplifier are available. The amplifier is powered by a +/- 15V, 1A, stabilized power supply, labelled as THD LAB WO& TT.

The position of the mass is measured with a linear encoder. The encoder strip has a resolution of 100 nm. The used encoder is the Mercury 2000 SS-200c, which sends counts to the digital input module. The encoder is powered by a stable power supply which suppresses the 50 Hz of the power net. The input NI 9401 digital input/output module is used as the digital input module to measure the counts sent by the encoder.

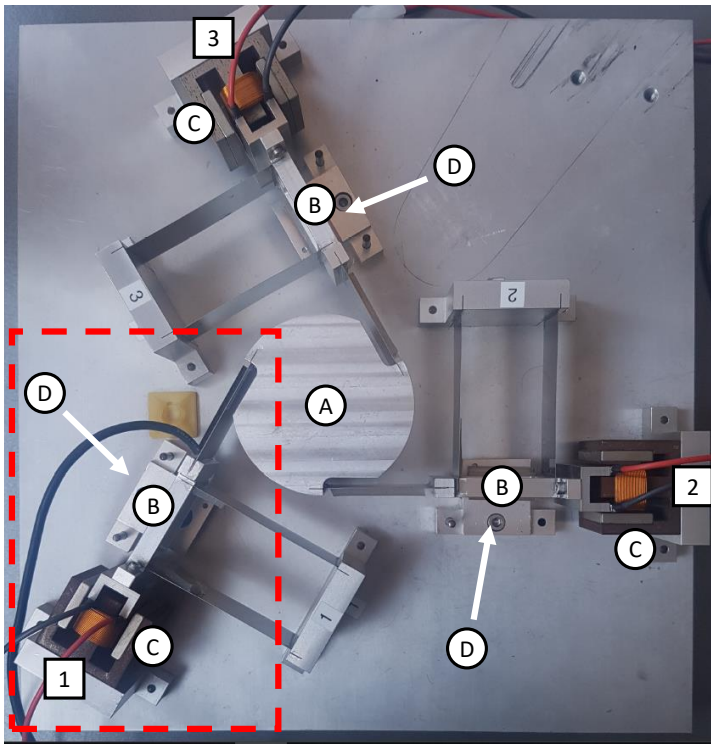

Figure C-1: Spider stage

The dynamics of one of the single mass are governed by a fourth-order differential equation. Essentially it almost exactly represents the dynamics of a double mass-spring-damper system.

C-1-1 Identification

To get a proper understanding of the Spider stage, it is identified for frequencies of 1-500 Hz. The system is identified using a chirp signal of 0.1-1000 Hz. The chirp signal is manually build using Labview. The chirp signal is defined as follows by $u = A\sin(\omega t)$. At every 50 ms, the frequency is increased to 1.03ω. To also capture proper amounts of frequency information at high frequencies, and achieve high Coherence of the entire frequency range, the frequency is increased to $\omega + 1$ from the point at which $1.03\omega > \omega + 1$. Since at high frequency the amplitude of the output is significantly reduced, higher input amplitude is required at increasing frequency. The following scheme is used over the range of 0.1-1000 Hz. The following definition for amplitude is used: $A = 30000/b$.

$$\begin{aligned} b &= 20 \quad \text{for} \quad 0.1 \leq \omega < 20 \\ b &= 10 \quad \text{for} \quad 20 \leq \omega < 30 \\ b &= 3 \quad \text{for} \quad 30 \leq \omega < 50 \\ b &= 1 \quad \text{for} \quad 50 \leq \omega \end{aligned}$$

The sampling time for the identification is set to 10000 Hz. This means the applied frequencies stay well below the Nyquist frequency. Note that the sampling frequency of the applied controllers should be the same.

The frequency response of the system is obtained using Matlab. The frequency data is calculated by simply implementing the tfestimate function. The build-in function makes use of the power spectral density of the input and output data.

$$H(f) = \frac{P_{yx}(f)}{P_{xx}(f)}$$

The cross power spectral density P_{yx} the power spectral density P_{xx} are obtained using Welch′s power spectral density estimate. The coherence of the data is determined using mscohere. This function uses the same power spectral density functions.

$$C_{xy}(f) = \frac{|P_{xy}|^2}{P_{xx}(f)P_{yy}(f)} \tag{C-1}$$

By using the obtained frequency data, the corresponding transfer function is found using the tfest function. The Matlab documentation can be consulted for more information as it clearly elaborates the algorithm. As mentioned, the system can be modelled as a double mass-spring-damper-system. This system consist of two poles and four zeros. The identified transfer function is given in Equation (C-2).

$$P(s) = \frac{8412s^2 + 1.366e4s + 5.851e7}{s^4 + 4.823s^3 + 1.141e4s^2 + 3.39e4s + 4.974e7} \tag{C-2}$$

The frequency response data obtained from the setup is shown in Figure C-2 in blue. The frequency data of the identified transfer function is plotted in the same figure in orange.

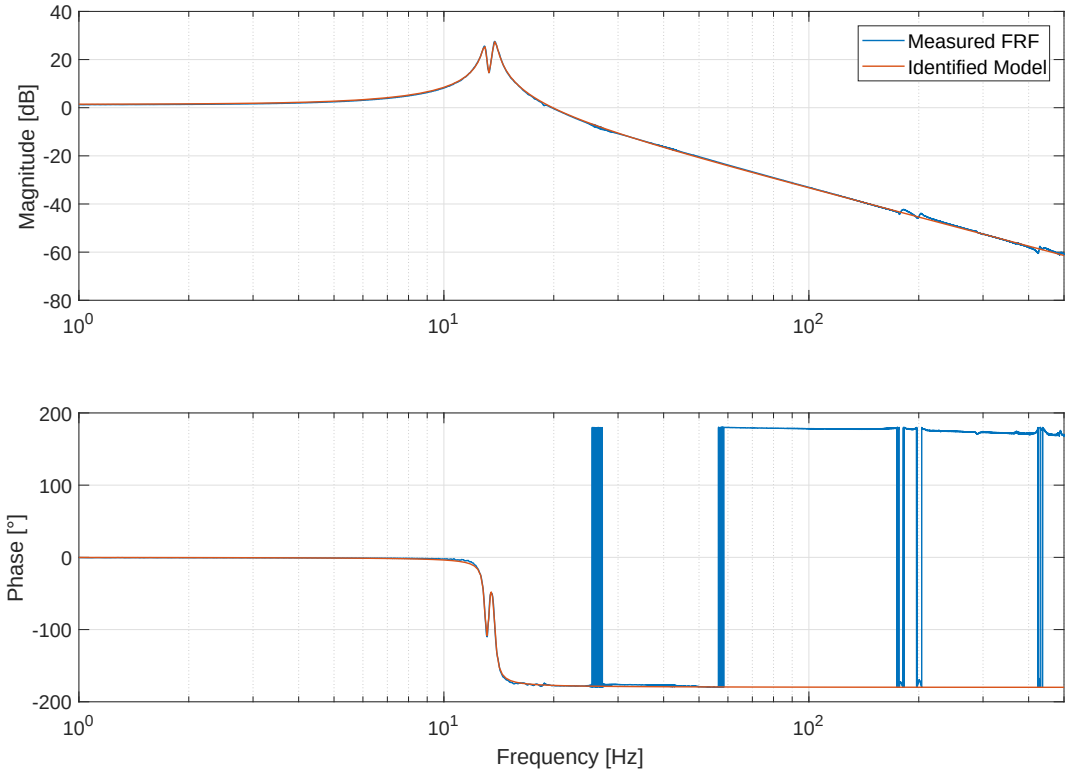

Figure C-2: Frequency response of the Spider stage, fitted with the fourth-order model

The fit of the transfer function is nearly exact, which indicates that except for small high-frequency modes, the system behaves as the linear model. It can also be observed that frequency response is almost similar to that of a single mass-spring-damper system. The pole pair and zero pair nearly cancel each other. Since the frequency response is close to that of a second-order plant, the system is estimated that way for the research of this thesis. Another identification for the transfer function is done, consisting of two poles and no zeros. The second-order transfer function is shown in Equation (C-3).

$$P(s) = \frac{8760}{s^2 + 5.886s + 7443} \tag{C-3}$$

The frequency response data obtained from the setup is also shown in Figure C-3 in blue. The frequency data of the identified second-order transfer function is plotted in the same figure in orange. The fit of the transfer function is nearly exact. However, close to resonance, the two resonance peaks an anti-resonance are smoothed. In open-loop configuration this may yield slightly different behaviour. The frequency response is required for feedback controller design by loop-shaping, therefore the model suffices.

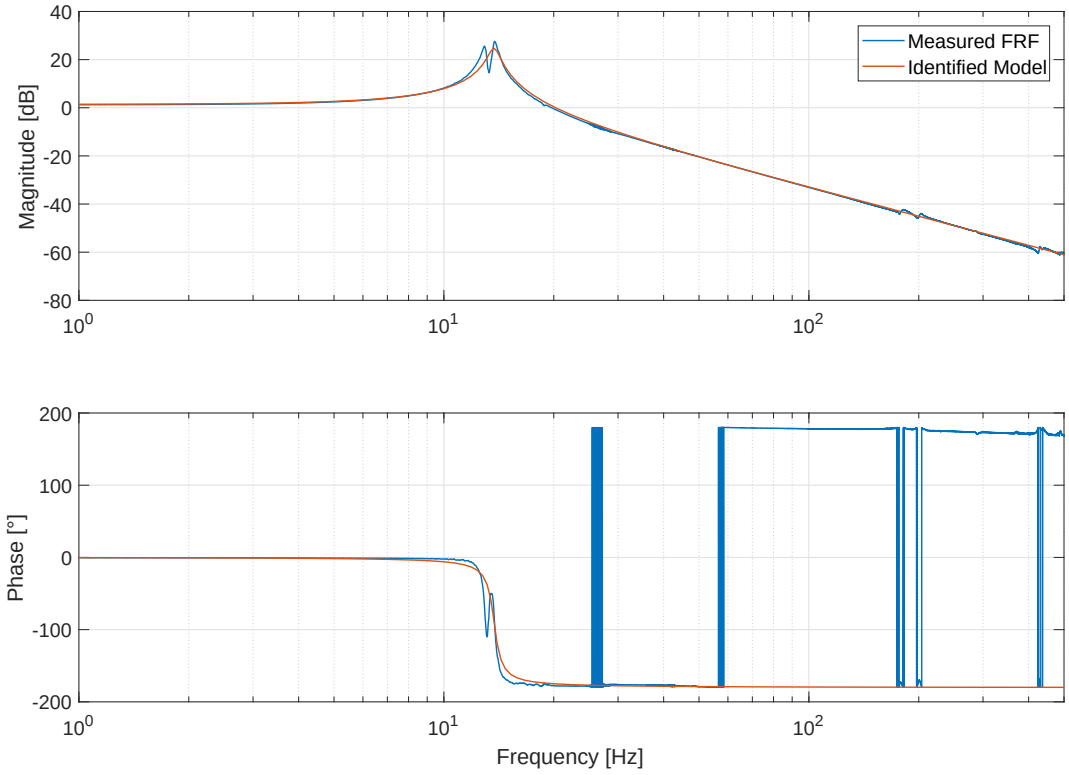

Figure C-3: Frequency response of the Spider stage, fitted with the second order model

C-2 Experimental results

For a clearer view on the performance of the adaptive algorithm, the results of the experiments shown in the paper, are also presented in this section. Both the convergence plots of the feedforward parameters as the evolution of the feedback control signals and the error are

given. An equal reference signal is used for all experiments. Implementation in Labview is defined in ticks given as amplitude, yielding the following reference signal.

$$r(t) = 300\left(\sin\left(2\pi t\right) + \sin\left(10\pi t\right) + \sin\left(28\pi t\right)\right) \tag{C-4}$$

Note that 1 tick translates to 100 nm in the application. The physical reference is given in the equation below, with the amplitude in μm. The same reference is shown in Figure C-4 for the first 3 seconds.

$$r(t) = 30\left(\sin\left(2\pi t\right) + \sin\left(10\pi t\right) + \sin\left(28\pi t\right)\right) \tag{C-5}$$

A sinusoidal disturbance of 50 ticks at 15 Hz is applied at the input of the plant for the final

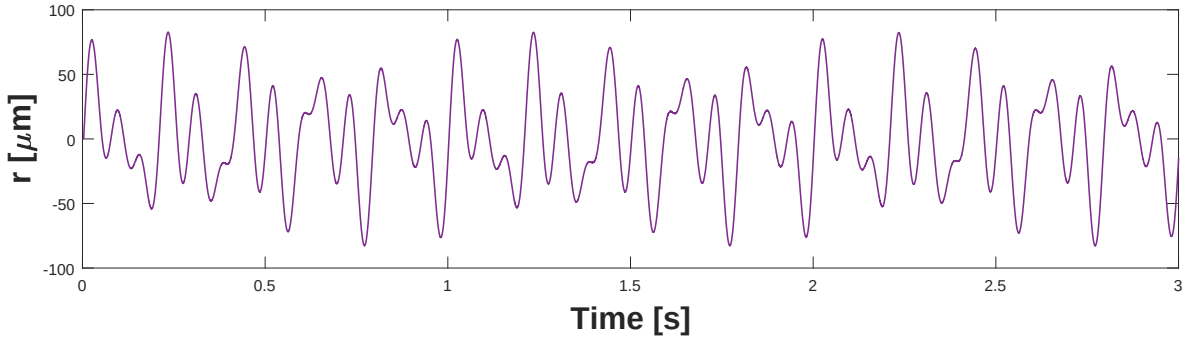

Figure C-4: Reference used for the experiments. The reference consists of a sum of sinusoids at 1 Hz, 5 Hz, and 14 Hz, with an amplitude of 30μm.

experiment. This disturbance approximately 10% of the amplitude of the control input at steady state.

$$d(t) = 50\sin\left(30\pi t\right) \tag{C-6}$$

In the input, 1 tick translates to $\frac{10}{32676}$ V. This yields the following physical disturbance in mV, shown in Figure C-5.

$$d(t) = 15.26\sin\left(30\pi t\right) \tag{C-7}$$

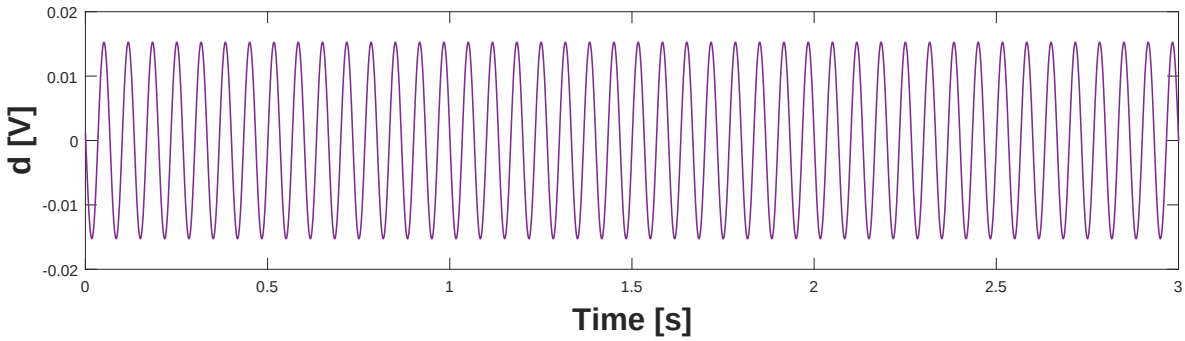

Figure C-5: Added sinusoidal input disturbance at 15 Hz with an amplitude of 0.015V

The experimental results for all different controllers are given in the next sections. The transfer function of the controller is given along with all design parameters.

C-2-1 PID

$$C(S) = k_p \left(\frac{s + \omega_i}{s} \right) \left(\frac{1 + \frac{s}{\omega_d}}{1 + \frac{s}{\omega_t}} \right) \left(\frac{1}{1 + \frac{s}{\omega_t}} \right) \tag{C-8}$$

k_p	ω_i	ω_f	ω_d	ω_t
16.2	10π	1000π	33.3π	300π

Γ_F	Γ_J	P	ω_e	β
$\begin{bmatrix} 150000 & 0 & 0 \\ 0 & 5 & 0 \\ 0 & 0 & 1 \end{bmatrix}$	$\begin{bmatrix} 0 & 0 & 0 \\ 0 & 0 & 0 \\ 0 & 0 & 0 \end{bmatrix}$	$\begin{bmatrix} 1000 & 0 & 0 \\ 0 & 1 & 0 \\ 0 & 0 & 1 \end{bmatrix}$	10π	0

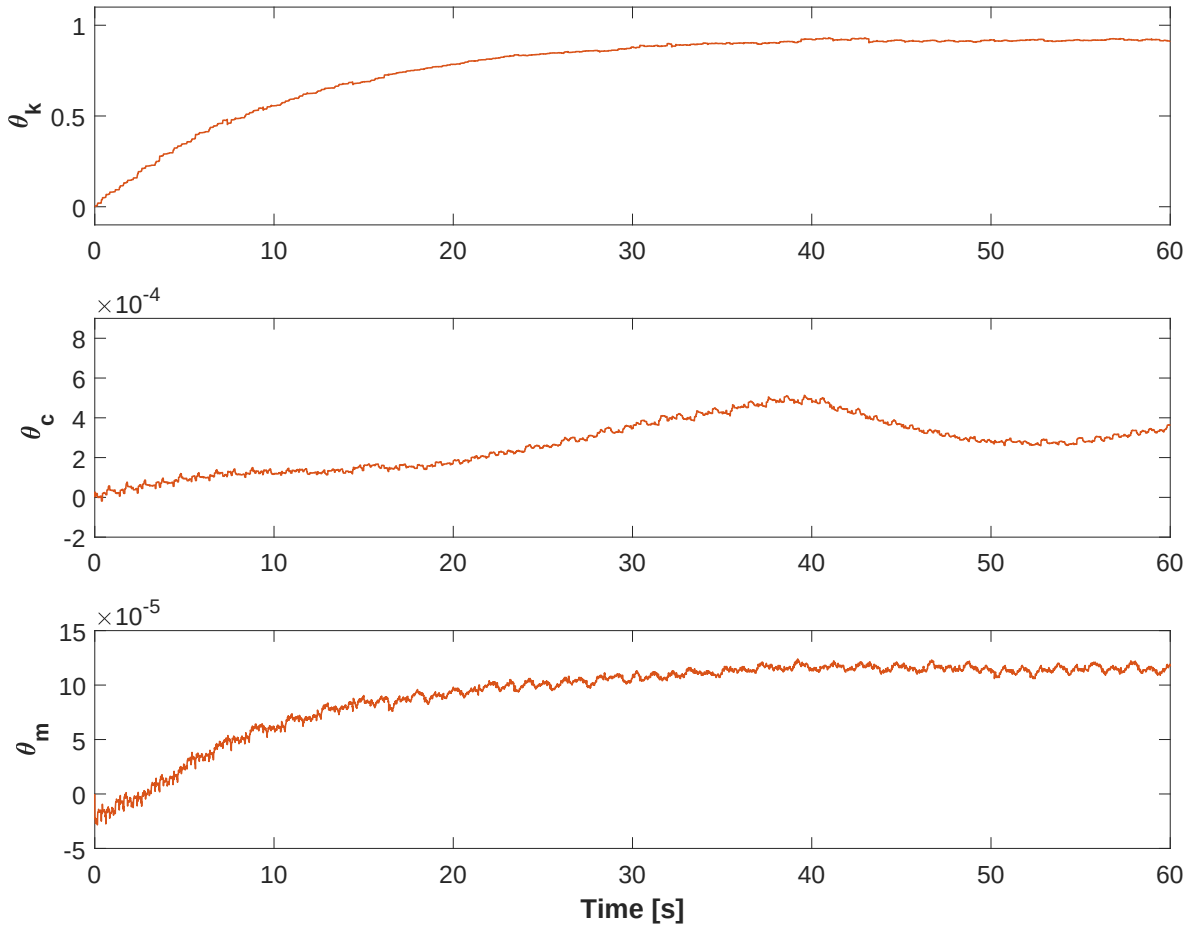

Figure C-6: Evolution of θ over time for a linear PID controller

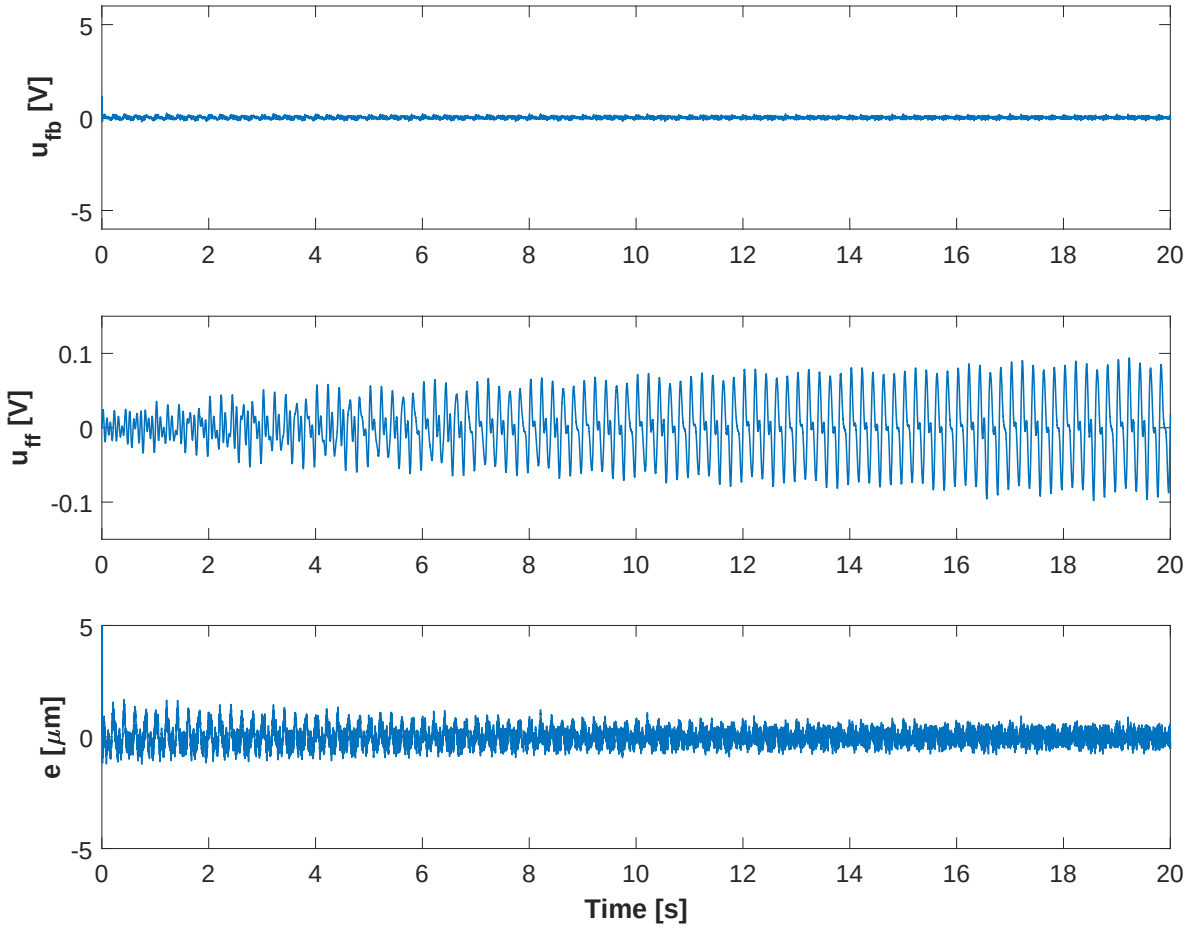

Figure C-7: Evolution of u_{fb}, u_{ff}, and e over time for a linear PID controller

C-2-2 CI based PID

$$C(S) = k_p \left(\frac{s + \omega_i}{\cancel{s}} \right) \left(\frac{1 + \frac{s}{\omega_d}}{1 + \frac{s}{\omega_t}} \right) \left(\frac{1}{1 + \frac{s}{\omega_t}} \right) \tag{C-9}$$

k_p	ω_i	ω_f	ω_d	ω_t
25.1	10π	1000π	83.3π	120π

Γ_F	Γ_J	P	ω_e	β
$\begin{bmatrix} 40000 & 0 & 0 \\ 0 & 2 & 0 \\ 0 & 0 & 0.2 \end{bmatrix}$	$\begin{bmatrix} 2 & 0 & 0 \\ 0 & 0.0002 & 0 \\ 0 & 0 & 0.00002 \end{bmatrix}$	$\begin{bmatrix} 1000 & 0 & 0 \\ 0 & 1 & 0 \\ 0 & 0 & 1 \end{bmatrix}$	10π	0

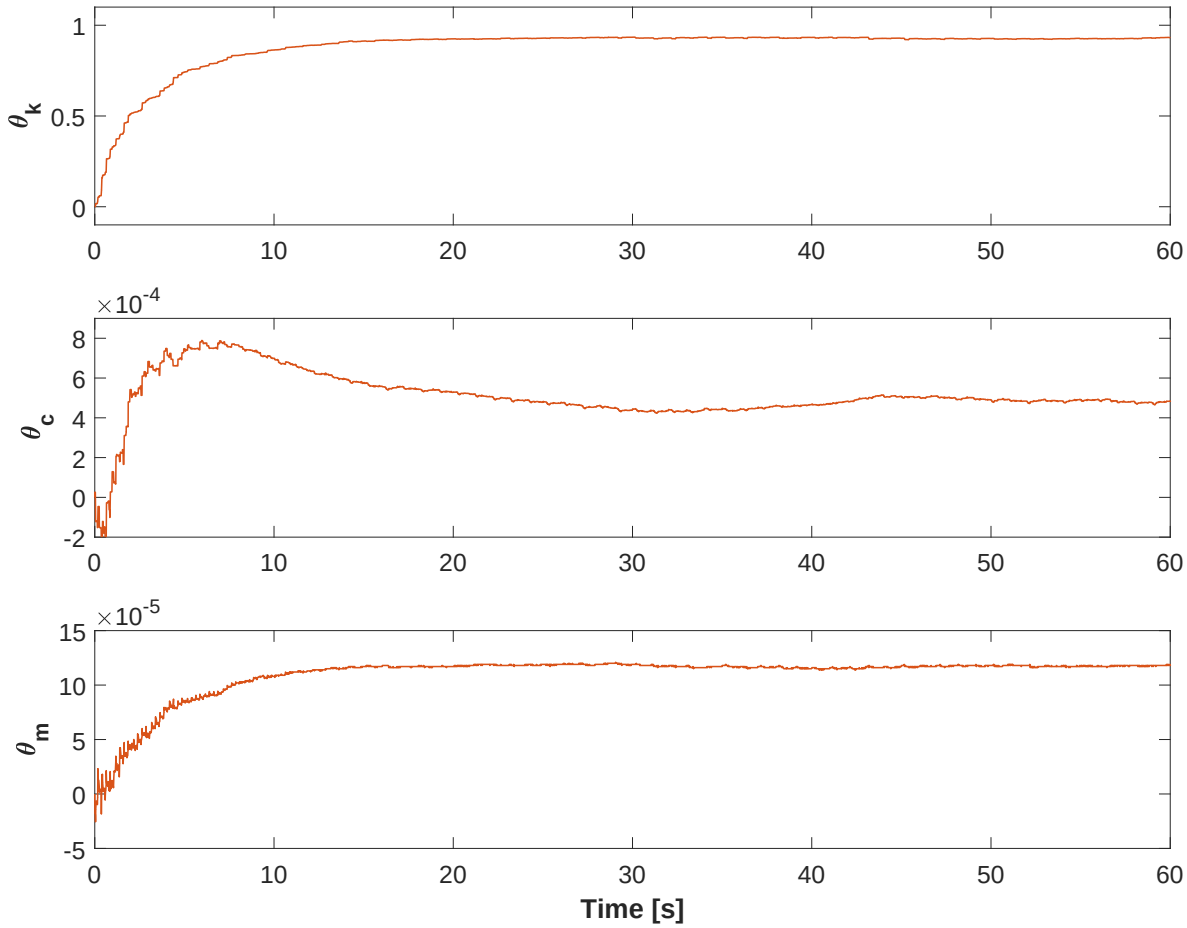

Figure C-8: Evolution of θ over time for a CI based PID controller

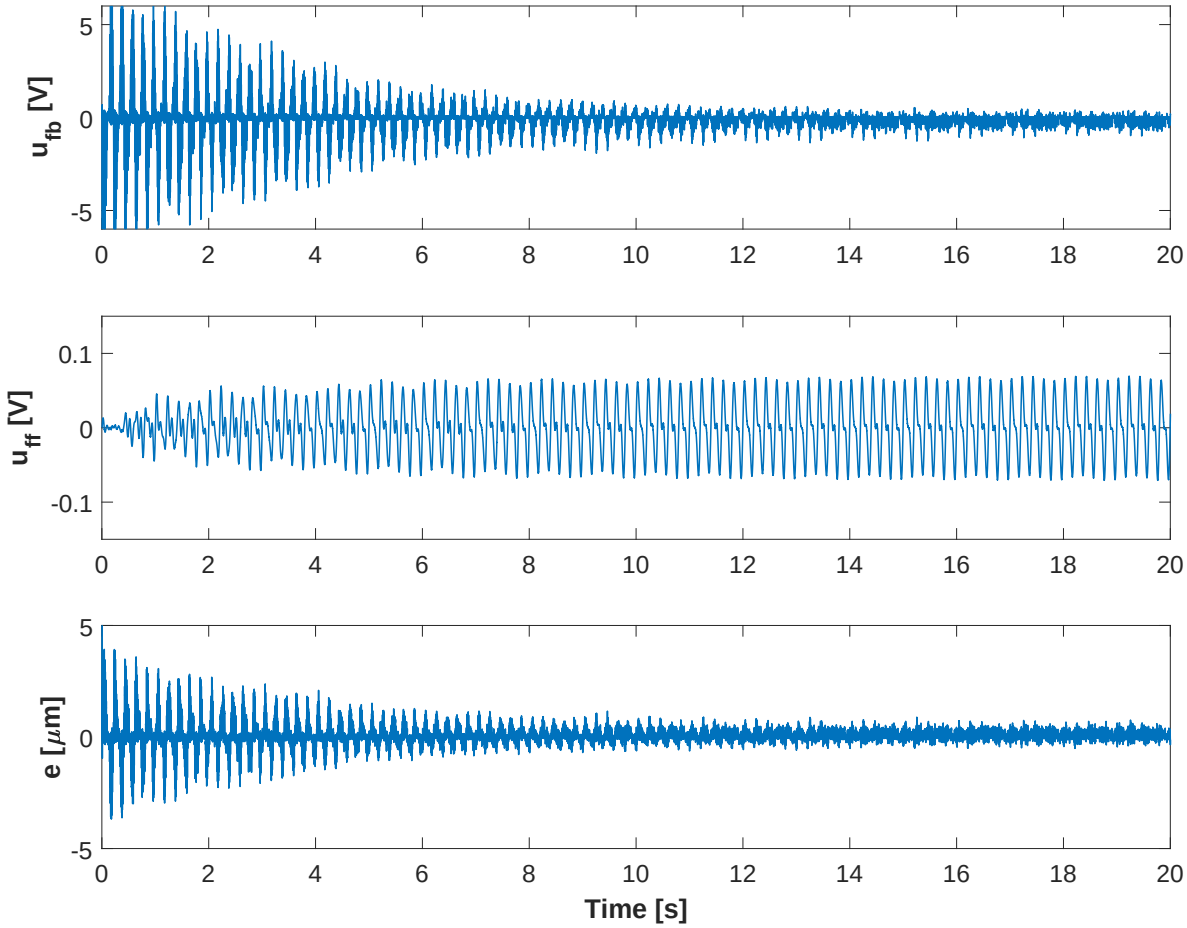

Figure C-9: Evolution of u_{fb}, u_{ff}, and e over time for a linear CI based controller

C-2-3 CgLp based PID1

$$C(S) = k_p \left(\frac{1 + \frac{s}{\omega_r}}{1 + \frac{1.4s}{\omega_{r\alpha}}} \right) \left(\frac{s + \omega_i}{s} \right) \left(\frac{1 + \frac{s}{\omega_d}}{1 + \frac{s}{\omega_t}} \right) \left(\frac{1}{1 + \frac{s}{\omega_t}} \right) \tag{C-10}$$

k_p	ω_i	ω_f	ω_d	ω_t	ω_r	$\omega_{r\alpha}$
34.5	10π	1000π	71.4π	140π	25π	35π
Γ_F	Γ_J	P	ω_e	β	-	-
$\begin{bmatrix} 100000 & 0 & 0 \\ 0 & 3 & 0 \\ 0 & 0 & 0.5 \end{bmatrix}$	$\begin{bmatrix} 5 & 0 & 0 \\ 0 & 0.0001 & 0 \\ 0 & 0 & 0.00005 \end{bmatrix}$	$\begin{bmatrix} 1000 & 0 & 0 \\ 0 & 1 & 0 \\ 0 & 0 & 1 \end{bmatrix}$	10π	0	-	-

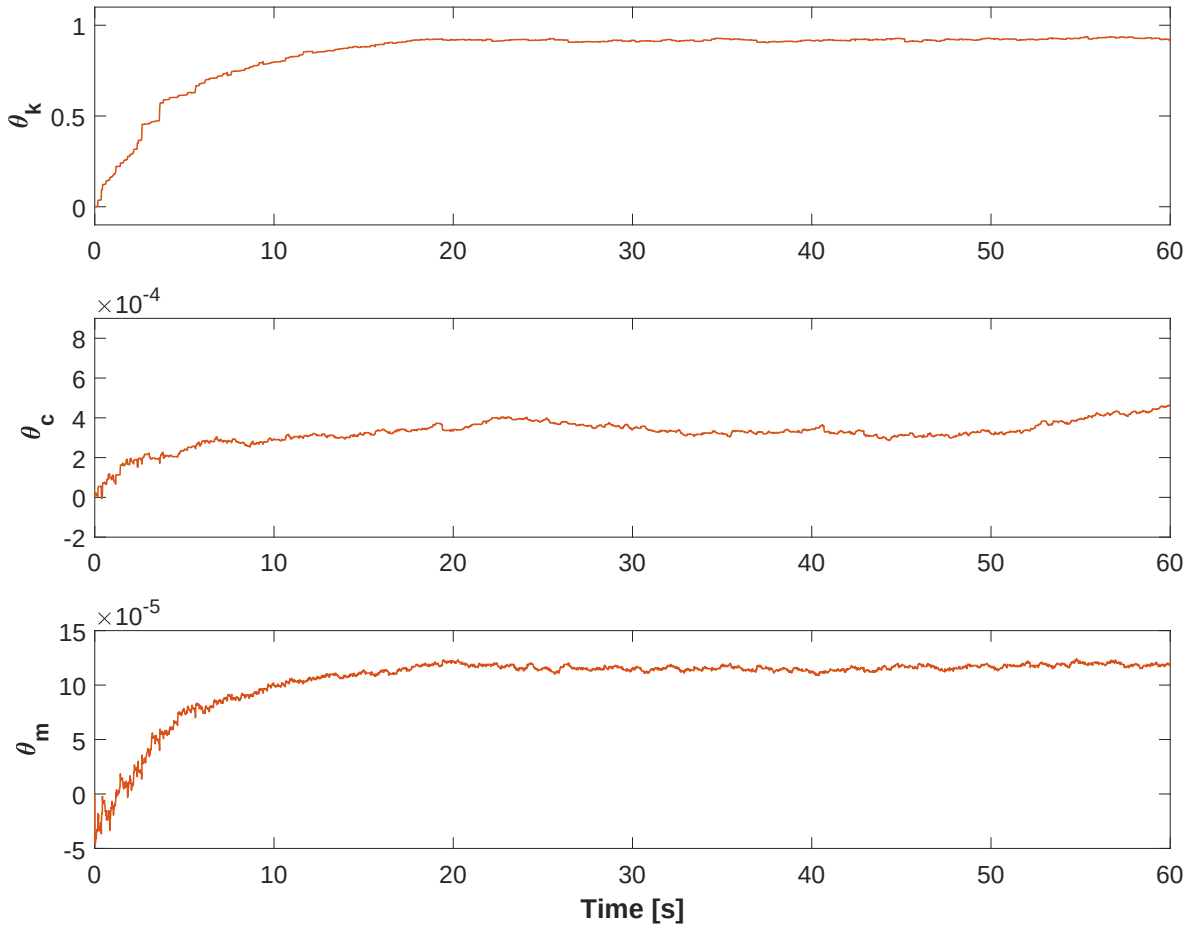

Figure C-10: Evolution of θ over time for the CgLp based PID controller 1

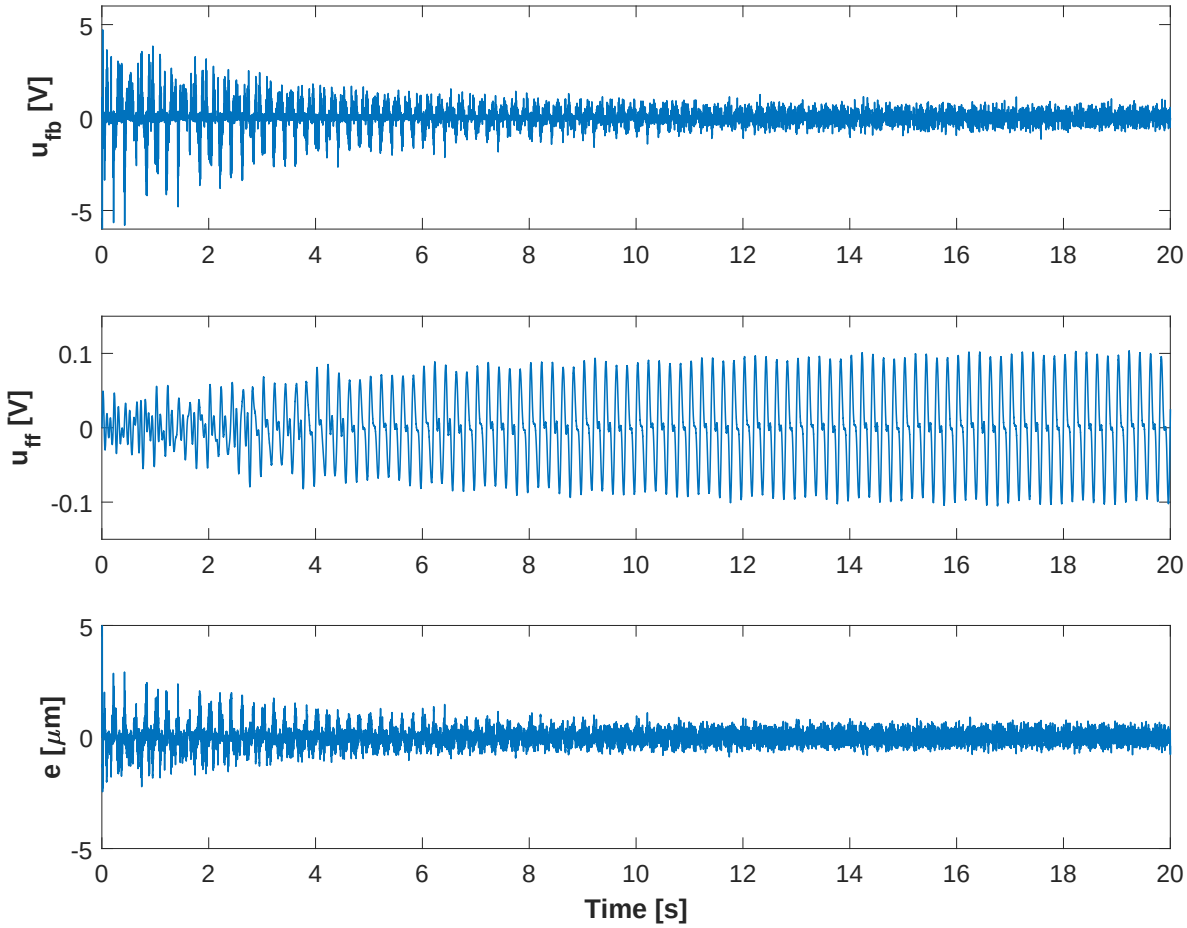

Figure C-11: Evolution of u_{fb}, u_{ff}, and e over time for the CgLp based PID controller 1

C-2-4 CgLp based PID2

$$C(S) = k_p \left(\frac{1 + \frac{s}{\omega_r}}{1 + \frac{1.4s}{\omega_{r\alpha}}} \right) \left(\frac{s + \omega_i}{s} \right) \left(\frac{1 + \frac{s}{\omega_d}}{1 + \frac{s}{\omega_t}} \right) \left(\frac{1}{1 + \frac{s}{\omega_t}} \right) \tag{C-11}$$

k_p	ω_i	ω_f	ω_d	ω_t	ω_r	$\omega_{r\alpha}$
21.5	10π	1000π	40π	250π	110π	127.3π

Γ_F	Γ_J	P	ω_e	β	-	-
$\begin{bmatrix} 150000 & 0 & 0 \\ 0 & 4 & 0 \\ 0 & 0 & 0.5 \end{bmatrix}$	$\begin{bmatrix} 5 & 0 & 0 \\ 0 & 0.00005 & 0 \\ 0 & 0 & 0.00005 \end{bmatrix}$	$\begin{bmatrix} 1000 & 0 & 0 \\ 0 & 1 & 0 \\ 0 & 0 & 1 \end{bmatrix}$	10π	0	-	-

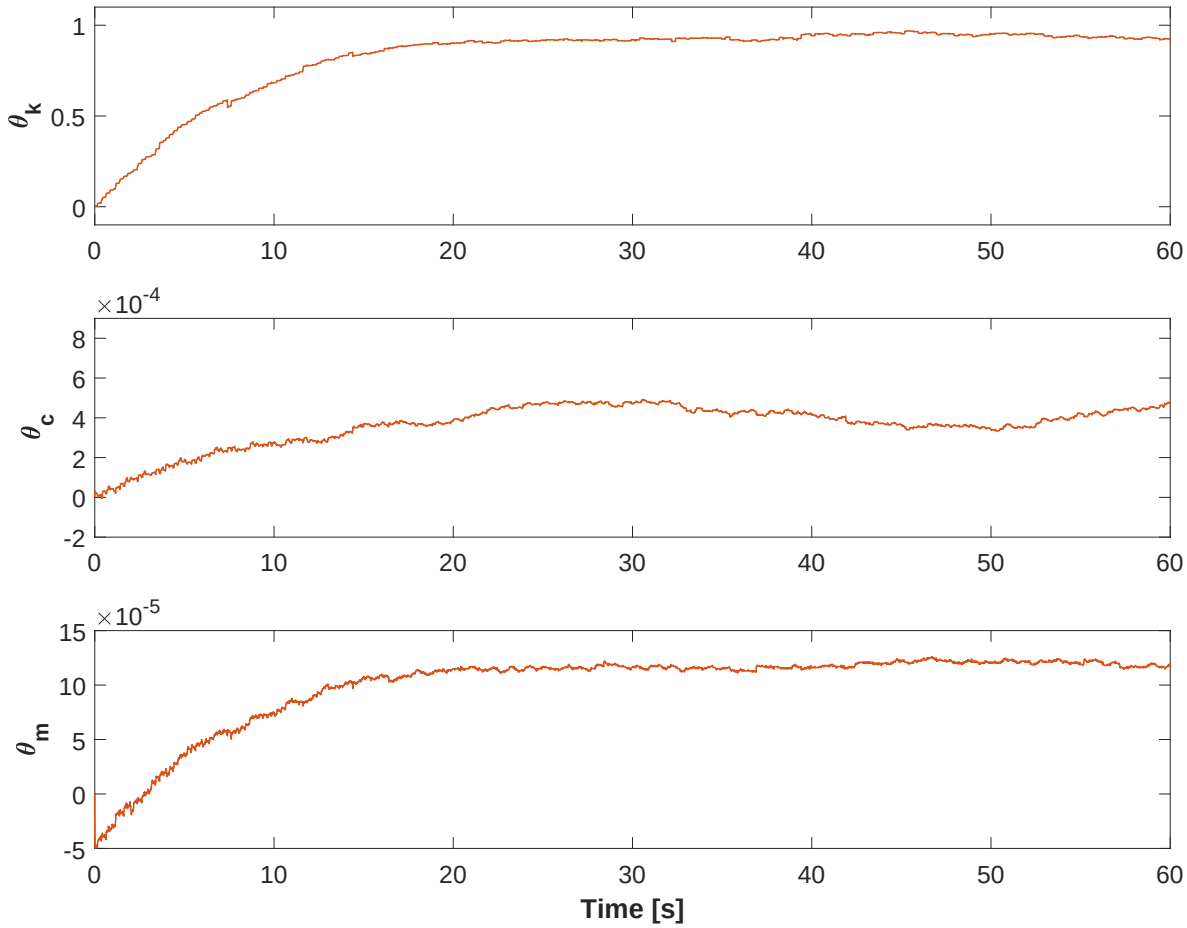

Figure C-12: Evolution of θ over time for the CgLp based PID controller 2

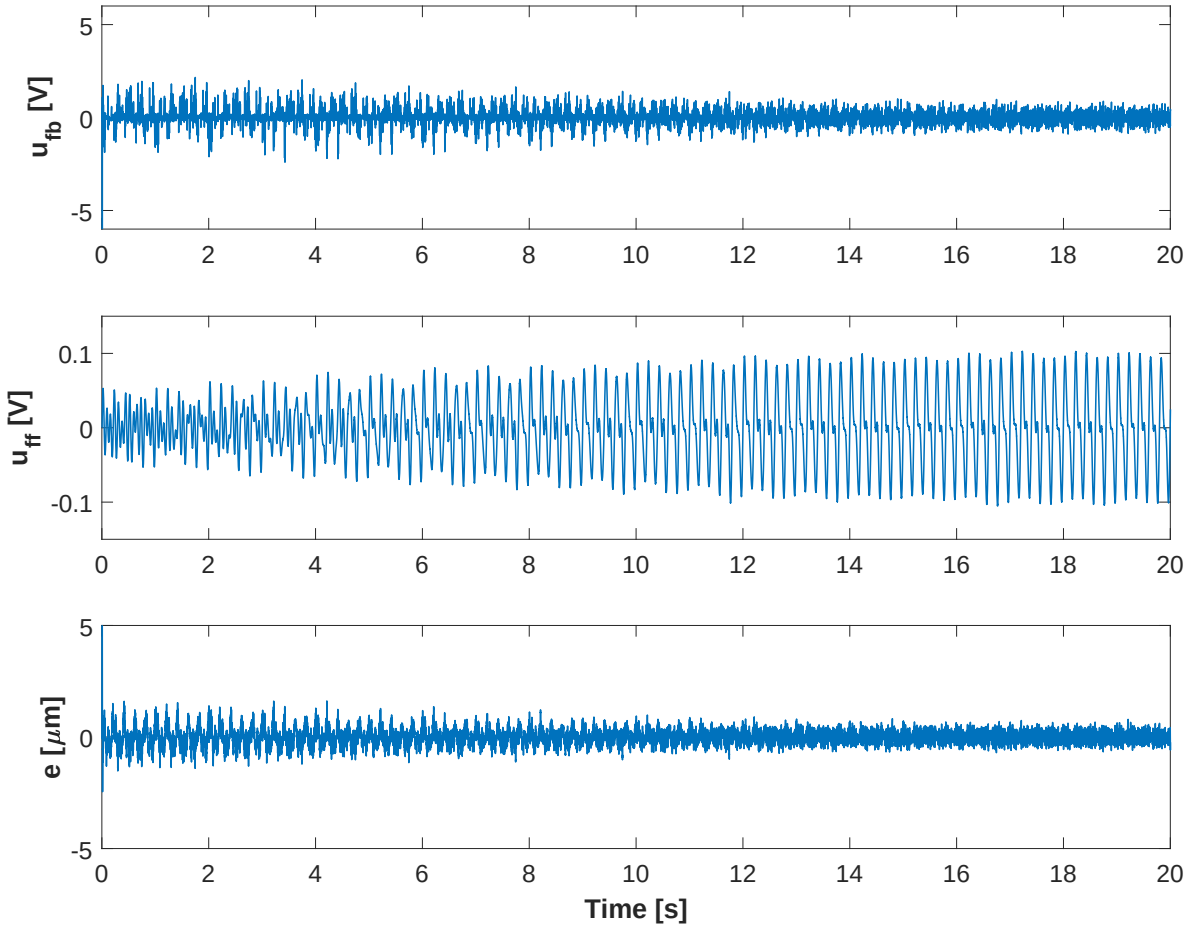

Figure C-13: Evolution of u_{fb}, u_{ff}, and e over time for the CgLp based PID controller 2

C-2-5 CgLp based PID1 with disturbance

$$C(S) = k_p \left(\frac{1 + \frac{s}{\omega_r}}{1 + \frac{s}{\omega_{r\alpha}}} \right) \left(\frac{s + \omega_i}{s} \right) \left(\frac{1 + \frac{s}{\omega_d}}{1 + \frac{s}{\omega_t}} \right) \left(\frac{1}{1 + \frac{s}{\omega_t}} \right) \tag{C-12}$$

k_p	ω_i	ω_f	ω_d	ω_t	ω_r	$\omega_{r\alpha}$
34.5	10π	1000π	71.4π	140π	25π	35π
Γ_F	Γ_J	P	ω_e	β	-	-
$\begin{bmatrix} 100000 & 0 & 0 \\ 0 & 3 & 0 \\ 0 & 0 & 0.5 \end{bmatrix}$	$\begin{bmatrix} 5 & 0 & 0 \\ 0 & 0.0001 & 0 \\ 0 & 0 & 0.00005 \end{bmatrix}$	$\begin{bmatrix} 1000 & 0 & 0 \\ 0 & 1 & 0 \\ 0 & 0 & 1 \end{bmatrix}$	10π	0	-	-

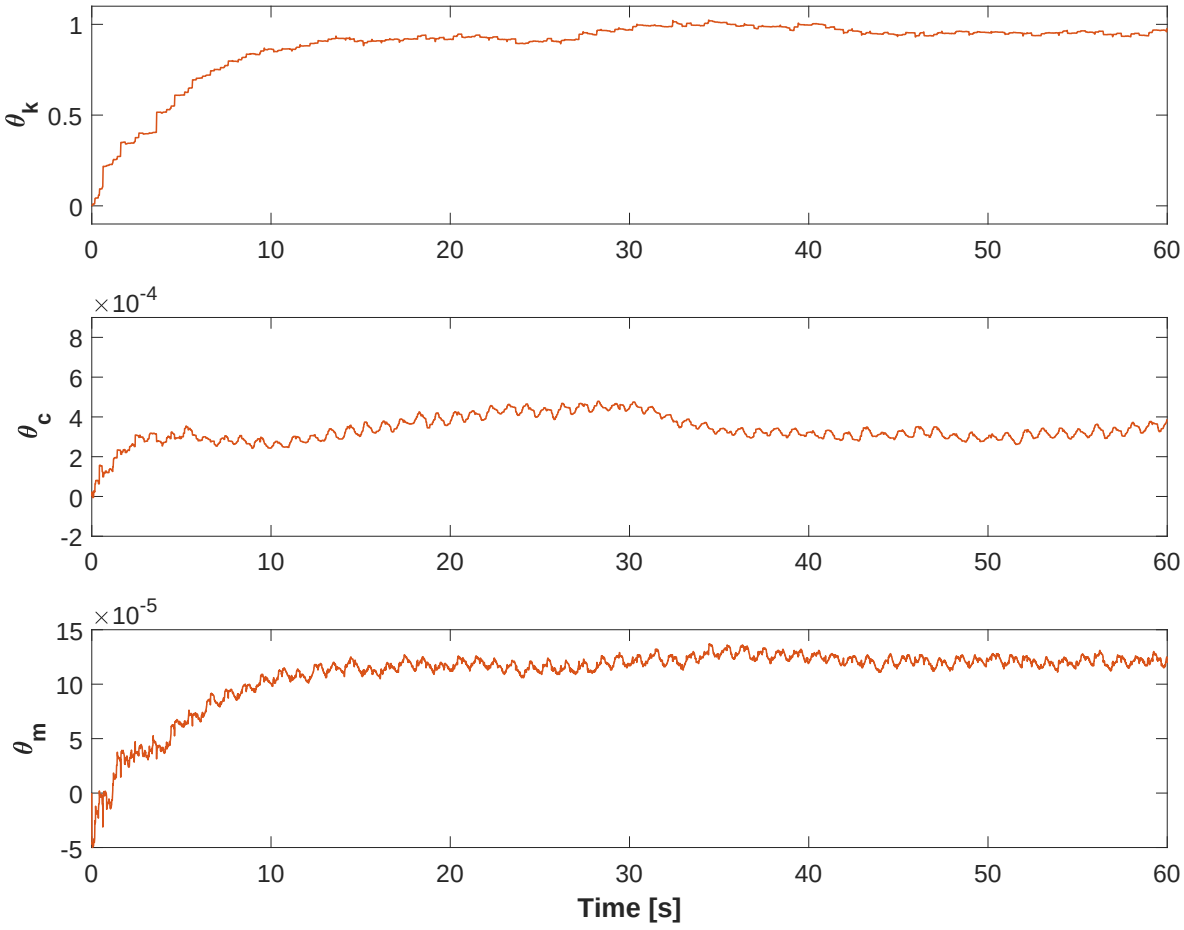

Figure C-14: Evolution of θ over time for the CgLp based PID controller 1 with added sinusoidal disturbance

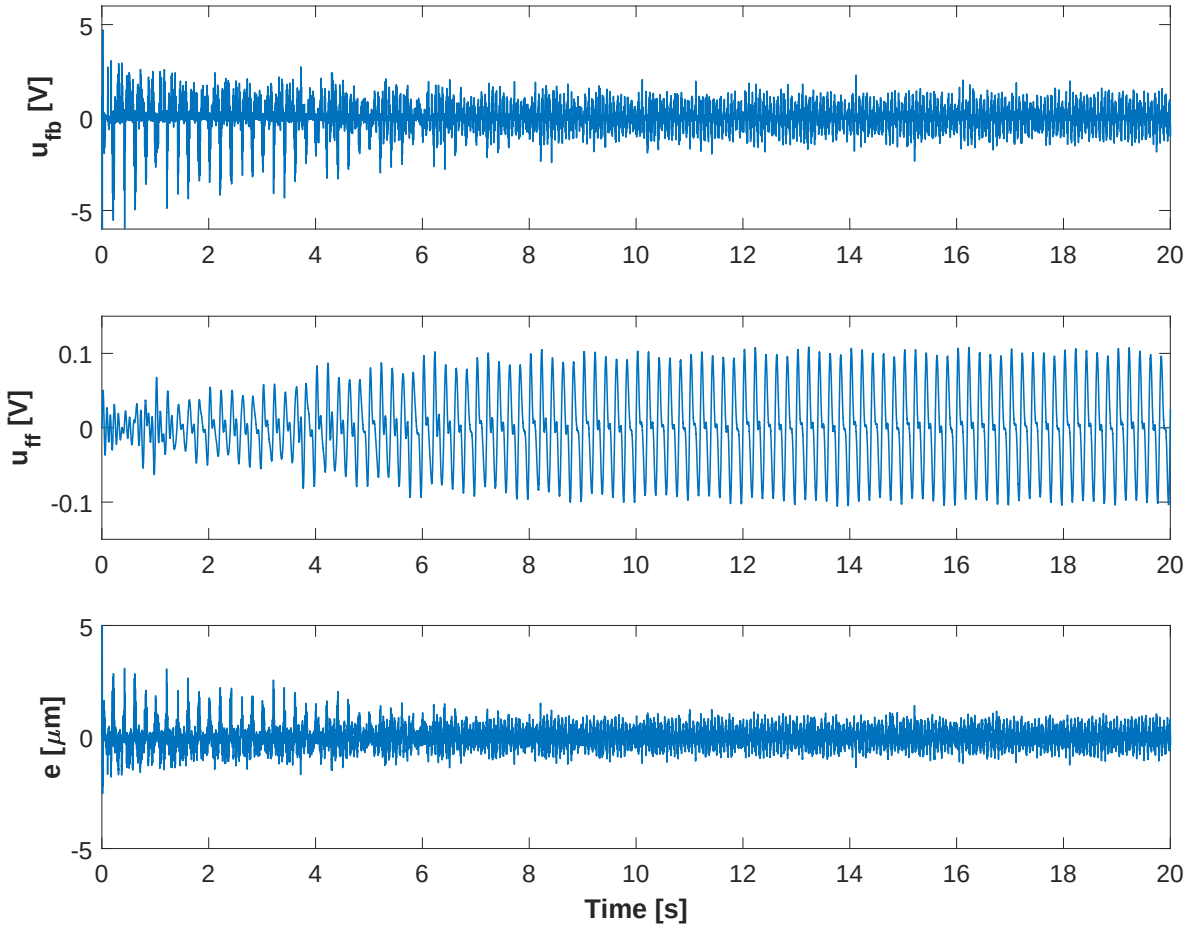

Figure C-15: Evolution of u_{fb}, u_{ff}, and e over time for the CgLp based PID controller 1 with added sinusoidal disturbance

Bibliography

[1] K. J. Åström and T. Hägglund, "The future of pid control," *Control engineering practice*, vol. 9, no. 11, pp. 1163–1175, 2001.

[2] J. Clegg, "A nonlinear integrator for servomechanisms," *Transactions of the American Institute of Electrical Engineers, Part II: Applications and Industry*, vol. 77, no. 1, pp. 41–42, 1958.

[3] O. Beker, C. Hollot, Y. Chait, and H. Han, "Fundamental properties of reset control systems," *Automatica*, vol. 40, no. 6, pp. 905–915, 2004.

[4] D. Nešić, L. Zaccarian, and A. R. Teel, "Stability properties of reset systems," *Automatica*, vol. 44, no. 8, pp. 2019–2026, 2008.

[5] Y. Chait and C. Hollot, "On horowitz's contributions to reset control," *International Journal of Robust and Nonlinear Control: IFAC-Affiliated Journal*, vol. 12, no. 4, pp. 335–355, 2002.

[6] I. Horowitz and P. Rosenbaum, "Non-linear design for cost of feedback reduction in systems with large parameter uncertainty," *International Journal of Control*, vol. 21, no. 6, pp. 977–1001, 1975.

[7] L. Hazeleger, M. Heertjes, and H. Nijmeijer, "Second-order reset elements for stage control design," in *American Control Conference (ACC), 2016*, pp. 2643–2648, IEEE, 2016.

[8] Y. Guo, Y. Wang, and L. Xie, "Frequency-domain properties of reset systems with application in hard-disk-drive systems," *IEEE Transactions on Control Systems Technology*, vol. 17, no. 6, pp. 1446–1453, 2009.

[9] N. Saikumar, R. K. Sinha, and S. H. HosseinNia, "'constant in gain lead in phase'element-application in precision motion control," *arXiv preprint arXiv:1805.12406*, 2018.

[10] K. J. Aström and R. M. Murray, *Feedback systems: an introduction for scientists and engineers*. Princeton university press, 2010.

[11] H. Hu, Y. Zheng, C. V. Hollot, and Y. Chait, "On the stability of control systems having clegg integrators," in *Topics in Control and its Applications*, pp. 107–115, Springer, 1999.

[12] R. M. Schmidt, G. Schitter, and A. Rankers, *The Design of High Performance Mechatronics-: High-Tech Functionality by Multidisciplinary System Integration.* Ios Press, 2014.

[13] A. Baños and A. Barreiro, *Reset control systems.* Springer Science & Business Media, 2011.

[14] J. Zheng, Y. Guo, M. Fu, Y. Wang, and L. Xie, "Improved reset control design for a pzt positioning stage," in *Control Applications, 2007. CCA 2007. IEEE International Conference on*, pp. 1272–1277, IEEE, 2007.

[15] S. H. HosseinNia, I. Tejado, B. M. Vinagre, and Y. Chen, "Iterative learning and fractional reset control," in *ASME 2015 International Design Engineering Technical Conferences and Computers and Information in Engineering Conference*, pp. V009T07A041–V009T07A041, American Society of Mechanical Engineers, 2015.

[16] A. Baños and A. Vidal, "Definition and tuning of a pi+ ci reset controller," in *Control Conference (ECC), 2007 European*, pp. 4792–4798, IEEE, 2007.

[17] A. Barreiro, A. Baños, and S. Dormido, "Reset control systems with reset band: well-posedness and limit cycles analysis," in *Control & Automation (MED), 2011 19th Mediterranean Conference on*, pp. 1343–1348, IEEE, 2011.

[18] I. R. Scola, M. M. Quadros, and V. J. Leite, "Robust hybrid pi controller with a simple adaptation in the integrator reset state," *IFAC-PapersOnLine*, vol. 50, no. 1, pp. 1457–1462, 2017.

[19] F. S. Panni, H. Waschl, D. Alberer, and L. Zaccarian, "Position regulation of an egr valve using reset control with adaptive feedforward," *IEEE Transactions on Control Systems Technology*, vol. 22, no. 6, pp. 2424–2431, 2014.

[20] M. Cordioli, M. Mueller, F. Panizzolo, F. Biral, and L. Zaccarian, "An adaptive reset control scheme for valve current tracking in a power-split transmission system.," in *ECC*, pp. 1884–1889, 2015.

[21] A. D. Berman, W. A. Ducker, and J. N. Israelachvili, "Origin and characterization of different stick- slip friction mechanisms," *Langmuir*, vol. 12, no. 19, pp. 4559–4563, 1996.

[22] H. Olsson and K. J. Astrom, "Friction generated limit cycles," *IEEE Transactions on Control Systems Technology*, vol. 9, no. 4, pp. 629–636, 2001.

[23] V. Van Geffen, "A study of friction models and friction compensation," *DCT*, vol. 118, p. 24, 2009.

[24] M. Sun, Z. Wang, Y. Wang, and Z. Chen, "On low-velocity compensation of brushless dc servo in the absence of friction model," *IEEE Transactions on Industrial Electronics*, vol. 60, no. 9, pp. 3897–3905, 2013.

[25] B. Arifin, C. J. Munaro, M. S. Choudhury, and S. L. Shah, "A model free approach for online stiction compensation," *IFAC Proceedings Volumes*, vol. 47, no. 3, pp. 5957–5962, 2014.

[26] C. Makkar, G. Hu, W. G. Sawyer, and W. E. Dixon, "Lyapunov-based tracking control in the presence of uncertain nonlinear parameterizable friction," *IEEE Transactions on Automatic Control*, vol. 52, no. 10, pp. 1988–1994, 2007.

[27] Y. Zhu and P. R. Pagilla, "Static and dynamic friction compensation in trajectory tracking control of robots," in *ICRA*, pp. 2644–2649, 2002.

[28] T. H. Lee, K. K. Tan, and S. Huang, "Adaptive friction compensation with a dynamical friction model," *IEEE/ASME transactions on mechatronics*, vol. 16, no. 1, pp. 133–140, 2011.

[29] S. Zhao and K. Tan, "Adaptive feedforward compensation of force ripples in linear motors," *Control Engineering Practice*, vol. 13, no. 9, pp. 1081–1092, 2005.

[30] S. Lu, X. Tang, B. Song, S. Zheng, and F. Zhou, "Identification and compensation of force ripple in pmslm using a jitl technique," *Asian Journal of Control*, vol. 17, no. 5, pp. 1559–1568, 2015.

[31] Y.-S. Lu and S.-M. Lin, "Disturbance-observer-based adaptive feedforward cancellation of torque ripples in harmonic drive systems," *Electrical Engineering*, vol. 90, no. 2, pp. 95–106, 2007.

[32] H. Stearns, S. Mishra, and M. Tomizuka, "Iterative tuning of feedforward controller with force ripple compensation for wafer stage," in *Advanced Motion Control, 2008. AMC'08. 10th IEEE International Workshop on*, pp. 234–239, IEEE, 2008.